CRWMS/M&O

Design Analysis Cover Sheet

Complete only applicable items.

(1.) QA: L

Page: 1 Of: 90

2. DESIGN ANALYSIS TITLE			
Geochemical Analysis of Degradation Modes of HEU SNF in a Codisposal Waste Package with HLW Canisters			
3. DOCUMENT IDENTIFIER (Including Rev. No.) BBA000000-01717-0200-00059 REV00 plc 3/6/98			4. TOTAL PAGES 90
5. TOTAL ATTACHMENTS 7	6. ATTACHMENT NUMBERS - NO. OF PAGES IN EACH I-4, II-9, III-19, IV-8, V-7, VI-1, VII-1		
	Printed Name	Signature	Date
7. Originator	Paul L. Cloke Peter Gottlieb	Paul F. Cloke Peter Gottlieb	12/15/97 12/15/97
8. Checker	David H. Lester Emilio Fuenties	Hugh A. Benton for DAVID H. LESTER & EMILIO FUENTES	12/15/97
9. Lead Design Engineer	Peter Gottlieb	Peter Gottlieb	12/15/97
10. Department Manager	Hugh A. Benton	Hugh A. Benton	12/15/97

11. REMARKS

Sections 7.4 and 8, and Attachments II and V, were prepared by Peter Gottlieb. The remainder of the document was prepared by Paul Cloke.

Flushing routine and cutout routine checked by Emilio Fuenties. Remainder of document checked by David H. Lester.

Initial Issue

Editorial Corrections in Block 6 plc 3/6/98 HAB 3/6/98

2. DESIGN ANALYSIS TITLE
Geochemical Analysis of Degradation Modes of HEU SNF in a Codisposal Waste Package with HLW Canisters
3. DOCUMENT IDENTIFIER (Including Rev. No.)
BBA000000-01717-0200-00059 REV 00

4. Revision No.	5. Description of Revision
00	Initial Issue

Table of Contents

1. Purpose

This analysis is prepared by the Mined Geologic Disposal System (MGDS) Waste Package Operations of the Civilian Radioactive Waste Management System Management & Operating (CRWMS M&O) contractor to provide input to the design of a waste package (WP) for the disposal of US Department of Energy spent nuclear fuel (DOE SNF) from the Massachusetts Institute of Technology (MIT) and Oak Ridge Research (ORR) reactors. This SNF is currently stored at the Savannah River Site (SRS). The specific objectives are to determine the geochemical conditions under which:

1) the criticality control material which has been suggested for this design will remain in the degraded waste package after the corrosion/dissolution of its initial form (so that it can be effective in preventing criticality), and

2) the fissile uranium will be carried out of the degraded waste package by infiltrating water (so that internal criticality is no longer possible, but the possibility of external criticality may be enhanced).

The results will be used to determine the nominal chemical composition for the criticality evaluations of the waste package design, and to suggest the range of parametric variations for additional evaluations. These chemical compositions (and consequent criticality evaluations) are determined for time periods up to 100,000 years for the following reasons: (1) It is considered likely that the USNRC will require demonstration of criticality control for longer than 10,000 years, in keeping with the 1 million years time horizon recently recommended by the National Academy of Science to the Environmental Protection Agency for performance assessment related to a nuclear repository (Ref. 5.59), and (2) The chemistry calculations showed that by 100,000 years the material of interest (which depended on the case being considered) had largely been removed from the waste package or reached a steady state.

Both boron (B) and gadolinium (Gd) were considered as WP internal criticality control materials for this analysis. The results of this analysis will be used to assure that the type and amount of criticality control material used in the waste package design will prevent criticality.

Since the differences between the MIT fuel and the ORR fuel are not expected to be significant (see Section 7.2.3 and Assumption 4.3.7), and since the MIT fuel has a much higher enrichment, and will generally be more reactive with respect to criticcality, the analyses of this document are focused primarily on the MIT fuel.

For reference purposes, the following should be noted:

- The MIT fuel having an enrichment of 93.5% (^{235}U) is classified as highly enriched uranium (HEU) and the ORR fuel having an enrichment of 20% is classified as medium enriched uranium (MEU).

- The reference conditions for the chemistry calculations will involve the codisposal of HLW (high level waste from reprocessing of spent fuel) glass in the same waste package with the DOE SNF.

2. Quality Assurance

The Quality Assurance (QA) program applies to this analysis. The work reported in this document is part of the waste package design analyses that will eventually support the License Application Design phase. This activity, when appropriately confirmed, can affect the proper functioning of the MGDS waste package. The *Classification of Permanent Items* QAP-2-3 evaluation entitled *Classification of the Preliminary MGDS Repository Design* (Ref. 5.1) has identified the waste package as an MGDS item important to safety, waste isolation, and physical protection of materials (TBV-228; Ref. 5.1). The Waste Package Operations responsible manager has evaluated this activity in accordance with QAP-2-0, *Conduct of Activities*. The *Engineering Development* (Ref. 5.3) activity evaluation has determined that work performed for this analysis is subject to *Quality Assurance Requirements and Description* (Ref. 5.2) requirements. As specified in NLP-3-18, *Documentation of QA Controls on Drawings, Specifications, Design Analyses, and Technical Documents*, this activity is subject to QA controls.

All design inputs which are identified in this analysis are for the preliminary stage of the design process; some or all of these design inputs will require subsequent confirmation (or superseding inputs) as the waste package design proceeds. Consequently, the use of any data from this analysis for input into documents supporting construction, fabrication, or procurement is required to be controlled and tracked as TBV or TBD in accordance with NLP-3-15, *To Be Verified (TBV) and To Be Determined (TBD) Monitoring System*, or other appropriate procedures.

3. Method

The method used for this analysis involves the following steps:

- Basic EQ6 (software package, Section 6.1) capability for tracing the progress of reactions with evolution of the chemistry, including the estimation of the concentrations remaining in solution and the composition of the precipitated solids. (EQ3 is used to set up EQ6 calculations; it does not simulate reaction progress.)

- Evaluation of available data on the range of dissolution rates for the materials involved, to be used as material/species input for each time step.

- "Pseudo flow-through" mode in which:

    1) Water is added continuously to the waste package and builds up in the waste package over a sequence of time steps (typically 15 to 18 steps per sequence, except for the initial sequence which is in the range 200 to 600 steps, with the times for the individual EQ6 timesteps determined automatically by the program and ranging from 0.01seconds to 1000 days). The time per sequence, including the initial sequence, is kept constant and is determined from the selected drip rate, e.g., 1 mm/yr, and the percentage of added water selected, usually 10%.

    2) Simulation of the flushing action of removing the water added during one EQ6 sequence and adjusting the amount of water and solutes accordingly to use as input to the next EQ6 sequence.

- Determination of fissile concentrations in solution as a function of time (from the output of EQ6 sequences over times up to 140,000 yrs) and calculation of the amount of fissile material released from the waste package as a function of time (which thereby reduces the chance of criticality within the waste package).

- Determination of concentrations of neutron absorbers, such as Gd, in solution as a function of time (from the output of EQ6 sequences over times up to 140,000 yrs) and calculation of the amount of neutron absorbers retained within the waste package as a function of time.

Further detail on the specific methods employed for each step is available in Section 7 of this analysis.

4. Design Inputs

All design inputs are for preliminary design; these design inputs will require subsequent qualification (or superseding inputs) before this analysis can be used to support procurement, fabrication, or construction activities, unless otherwise noted.

4.1 Design Parameters

This section presents the design parameters used in the analysis.

4.1.1 Waste Package and Waste Form Materials and Performance Parameters

This section provides a brief overview of the chemical characteristics of different waste packages. The emphasis is on the chemical composition and reactivity, rather than on the physical configurations within different waste packages, although the configurations were used for volume calculations to determine the overall chemistries and for calculations of surface areas for use in the rate equation in the EQ6 program.

4.1.1.1 DOE SNF Canister

The preliminary design (TBV) for the DOE SNF canister is taken from Refs. 5.38 and 5.55. The canister is composed of stainless steel XM-19 forming a right circular cylinder which contains a stainless steel 316L basket. DOE-owned SNF is to be loaded into the basket. The dimensions for the DOE SNF canister are 439.3 mm for the outer diameter with a 15 mm wall thickness. The length of the canister is defined for this analysis as the length of four stacked fuel assemblies plus tolerances plus between-layer (axial) separator plate thicknesses as required. The DOE SNF canister designs contain 16 MIT or 10 ORR DOE SNF fuel basket locations in four layers. Stainless steel/boron alloy is used to separate each layer from the adjacent layer within the canister (Ref. 5.48). In the MIT SNF canister, a stainless steel/boron alloy is also used in the basket between each assembly. Table 4.1.1.1-1 provides a summary of the total amount of material in the MIT DOE SNF canister. Further detail on the individual MIT assemblies is provided below in Section 4.1.1.2.

Table 4.1.1.1-1. MIT SNF Material Quantities	
Material	Mass per DOE SNF canister (g)
U-235	32912
U-234	352
U-238	1936
Al	414000

4.1.1.2 SNF Characteristics

The details of the MIT fuel assembly were obtained from the MIT fuel Appendix A data and the MIT plate/assembly drawings (R3F-3-2, R3F-1-4) provided by SRS (Ref. 5.4) (TBV). The MIT fuel assembly is constructed from a collection of 15 flat plates tilted at a sixty degree angle so that the resulting assembly has a parallelogram cross-section instead of the more common square or hexagon shape. The MIT fuel length values used in these analyses are shorter than the original as-built length of the MIT assembly because the top and bottom ends of the assembly, which do not contain uranium materials, have been removed by cutting. The fuel plates consist of an aluminum cladding over an aluminum/uranium alloy. The maximum fuel mass for the MIT assemblies is 514.25 grams of U-235 with an enrichment of 93.5 weight percent and one weight percent of U-234 (Assumption 4.3.3). The amount of aluminum present in the U-Al_x alloy is 30.5 weight percent. Multiplying these per/assembly numbers by the number of assemblies per canister, 64, gives the corresponding values in Table 4.1.1.1-1.

Fuel Plates

The flat plates are 2.552 +0.000, -0.002 inches wide, and 23 inches long. All 15 plates are the same size and have a finned cladding surface with a thickness of 0.080 ±0.003 inches and a fin height of 0.010 ± 0.002 inches. The fuel alloy is 0.030 +0.000, -0.002 inches thick, 2.177 +0.000, -0.1875 inches wide, and 22.375 ±0.375 inches long.

Fuel Element

The aluminum outer shroud which encloses the 15 fuel plates on 4 sides is an equal sided parallelogram structure with a 2.405 inch outside dimension perpendicular to the parallelogram sides (not along the parallogram edges) having two 0.044 inch thick walls parallel with the fuel plates and two 0.188 inch thick comb plates into which the fuel plates fit. The length (after cutting) is 23.368 inches. The fuel plates are evenly spaced within this rhomboid and angled 60

degrees off the comb plate. Drawing R3F-1-4 (Ref. 5.4)) shows a fuel plate center-to-center spacing of 0.158 inches, which is the spacing of the notches on the comb plates.

Fuel Degradation Rate

The rate of corrosion of aluminum under the conditions of interest is not to be well known, but it is assumed that it be fast compared to other rates of corrosion of materials in the waste package (Assumption 4.3.28). Evidence of the range of uncertainty is given by the following examples: (1) Corrosion tests reported in Ref. 5.5 on aluminum clad spent fuel showed penetration of the aluminum cladding in 45 days; (2) Ref. 5.6 shows a graph of the corrosion rate of Al versus % nitric acid. At 0% acid the rate is 1 mm/yr. For MIT fuel, the height of the "ribs" in the cladding is 0.01 in, or 0.254 mm. Thickness between bottom of rib and the fuel is 0.015 in., or 0.381 mm. At a corrosion rate of 1 mm/yr this thickness would be penetrated in 139 days, or about 3 times as long as the case reported by Howell (Ref. 5.5). Therefore, a corrosion rate of 1 mm/yr was initially used for this analysis. Because complete degradation of the fuel in only a few days appeared unrealistically rapid, the rate was adjusted for subsequent simulations to result in complete degradation of the fuel in about 10 years.

4.1.1.3 HLW Canister and Contents

As mentioned in Section 1, the chemistry calculations of this document reflect configurations in which the DOE SNF is co-disposed with HLW glass. The reference container for the HLW glass is the Savannah River pour canister. This is a cylindrical stainless steel Type 304L can with an approximate 610 mm outer diameter, a 9.525 mm wall thickness (Ref. 5.7, pp. 3.3-4) (TBV), and a nominal length of 3 m. The canister inside volume is 0.736 m^3 and the glass weight is 1682 kg (Ref. 5.7, pp. 3.3-6). High Level Waste (HLW) glass (Ref. 5.7, pp. 3.3-1) is poured into the canisters until 85% of the volume is filled. The nominal dimensions of the pour canister are used for these analyses.

Whereas the geochemical code EQ6 has been used for modeling the degradation of this glass (Ref. 5.8), attempts to combine this approach with the additional complexity required for an entire waste package have not succeeded. This appears to be caused by numerical difficulties in handling such a large computational problem. Instead, a conservative value (see Table 4.1.1.3-3) was chosen for the corrosion rate for the glasses, based on the initial rate of corrosion. Another reason for choosing initial rates is that some observations have shown, after a period of weeks to years during which the rate slows, a subsequent increase to rates resembling the initial value (Ref. 5.9 and 5.10). Whereas efforts have been made to design glasses that will not be subject to this eventual rate increase, it does not appear possible to guarantee that the rate will not increase

over the course of decades or centuries. Therefore, for this report, high conservative rates have generally been selected. A non-conservative slow glass dissolution rate was also used in a few cases. (See Table 4.1.1.3-3 and references cited therein.) Composition data for these glasses are presented in Tables 4.1.1.3-1 and 4.1.1.3-2. Reaction rates for the WP metal and glass materials are presented in Table 4.1.1.3-3.

Table 4.1.1.3-1. Composition of HLW (Ref. 5.11, Attachment I, pp. 3-4, 3-9)

Component	Weight %	Mol. Wt.	g-Atoms, 1st element	g-Atoms, 2nd element	2nd element	g-Atoms, oxygen
Ag	5.00e-02	1.08e+02				
Al2O3	3.96e+00	1.02e+02	7.77e-02			1.17e-01
B2O3	1.03e+01	6.96e+01	2.95e-01			4.43e-01
BaSO4	1.40e-01	2.33e+02	6.00e-04	6.00e-04	S	2.40e-03
Ca3(PO4)2	7.00e-02	3.10e+02	6.77e-04	4.51e-04	P	1.81e-03
CaO	8.50e-01	5.61e+01	1.52e-02			1.52e-02
CaSO4	8.00e-02	1.36e+02	5.88e-04	5.88e-04	S	2.35e-03
Cr2O3	1.20e-01	1.52e+02	1.58e-03			2.37e-03
Cs2O*						
CuO	1.90e-01	7.95e+01	2.39e-03			2.39e-03
Fe2O3	7.04e+00	1.60e+02	8.82e-02			1.32e-01
FeO	3.12e+00	7.19e+01	4.34e-02			4.34e-02
K2O	3.58e+00	9.42e+01	7.60e-02			3.80e-02
Li2O	3.16e+00	2.99e+01	2.12e-01			1.06e-01
MgO	1.36e+00	4.03e+01	3.37e-02			3.37e-02
MnO	2.00e+00	7.09e+01	2.82e-02			2.82e-02
Na2O	1.10e+01	6.20e+01	3.55e-01			1.77e-01
Na2SO4	3.60e-01	1.42e+02	5.07e-03	2.53e-03	S	1.01e-02
NaCl	1.90e-01	5.84e+01	3.25e-03	3.25e-03	Cl	
NaF	7.00e-02	4.20e+01	1.67e-03	1.67e-03	F	
NiO	9.30e-01	7.47e+01	1.24e-02			1.24e-02
PbS	7.00e-02	2.39e+02	2.93e-04	2.93e-04	S	
SiO2	4.56e+01	6.01e+01	7.59e-01			1.52e+00
ThO2*	2.10e-01	2.64e+02	7.95e-04			1.59e-03
TiO2*	9.90e-01	7.99e+01	1.24e-02			2.48e-02
U3O8	2.20e+00	8.42e+02	7.84e-03			2.09e-02
Zeolite*						
ZnO*	8.00e-02	8.14e+01	9.83e-04			9.83e-04
Np	7.51e-04	2.37e+02	3.17e-06			

Table 4.1.1.3-1. Composition of HLW (Ref. 5.11, Attachment I, pp. 3-4, 3-9)						
Component	Weight %	Mol. Wt.	g-Atoms, 1st element	g-Atoms, 2nd element	2nd element	g-Atoms, oxygen
Pu	1.23e-02	2.39e+02	5.16e-05			
Am*						
Tc	1.08e-02	9.99e+01	1.08e-04			
Zr	2.64e-02	9.12e+01	2.90e-04			
Pd*						
Sn*						
Ce	2.38e-02	1.42e+02	1.68e-04			
Ba	3.48e-02	1.37e+02	2.53e-04			
Nd	2.44e-02	1.44e+02	1.70e-04			
Sm	6.81e-03	1.50e+02	4.53e-05			
					Total g-Atoms =	2.71e+00
* Not considered at this time in the interest of simplifying the calculations, because the percentages present were too small to be given by the source and/or they were too small to affect pH or solubility of the fissile species. The number of chemical components must be limited to assure convergence of the EQ3/6 calculations.						

Table 4.1.1.3-2. Composition of HLW		
Element	g-Atoms	Atom Fraction
Al	7.77e-02	1.64e-02
B	2.95e-01	6.24e-02
Ba	6.00e-04	1.27e-04
Ca	1.64e-02	3.47e-03
Cr	1.58e-03	3.34e-04
Cu	2.39e-03	5.05e-04
Fe	1.32e-01	2.78e-02
K	7.60e-02	1.61e-02
Li	2.12e-01	4.47e-02
Mg	3.37e-02	7.12e-03
Mn	2.82e-02	5.95e-03

Table 4.1.1.3-2. Composition of HLW		
Element	g-Atoms	Atom Fraction
Na	3.65e-01	7.71e-02
Cl	3.25e-03	6.87e-04
F	1.67e-03	3.52e-04
Ni	1.24e-02	2.63e-03
P	4.51e-04	9.53e-05
Pb	2.93e-04	6.18e-05
S	4.01e-03	8.48e-04
Si	7.59e-01	1.60e-01
U	7.84e-03	1.66e-03
O	2.71e+00	5.71e-01
Np	3.17e-06	6.69e-07
Pu	5.16e-05	1.09e-05
Tc	1.01e-04	2.13e-05
Zr	2.84e-04	6.01e-05
Ce	1.68e-04	3.54e-05
Nd	1.70e-04	3.59e-05
Sm	4.53e-05	9.56e-06
Total	4.74e+00	1.00e+00

Table 4.1.1.3-3. Reaction Rates for Waste Package Materials								
Material	Rate μm/yr	Rate gm/m²/d	Area* cm²	Rate**/yr	Rate**/sec	Density gm/cm³	Rate gm/sec	Rate moles/sec
Alloy 625[1]	1.008e-02		1.000e+00	1.008e-06	3.196e-14	8.440e+00	2.698e-13	4.500e-15
316L[2]	1.000e-01		1.000e+00	1.000e-05	3.171e-13	7.593e+00	2.522e-12	4.207e-14
304L[3]	1.500e-01		1.000e+00	1.500e-05	4.756e-13	7.900e+00	3.758e-12	6.874e-14
Carbon Steel[4]	3.000e+01		1.000e+00	3.000e-03	9.513e-11	7.832e+00	7.451e-10	1.371e-11
A516[5]	2.223e+01		1.000e+00	2.223e-03	7.050e-11	7.832e+00	5.522e-10	1.000e-11
B Stainless Steel[6]	8.000e-01		1.000e+00	8.000e-06	2.537e-12	7.745e+00	1.965e-11	3.775e-13

Table 4.1.1.3-3. Reaction Rates for Waste Package Materials								
Material	Rate μm/yr	Rate gm/m²/d	Area* cm²	Rate**/yr	Rate**/sec	Density gm/cm³	Rate gm/sec	Rate moles/sec
HLW glass[3]		2.791e-02	1.000e-04	1.019e-03	3.230e-11		3.230e-11	1.529e-11
HLW glass[4]		2.000e-04	1.000e-04	7.300e-06	7.300e-13		2.315e-13	1.096e-14

* Area in cm² for metals, conversion factor from m² to cm² for HLW.
** Rate in cm³ for metals, grams for HLW.
[1] Rate assumed to be approximately 10% of corrosion rate of 316L stainless steel, specifically 4.5e-15 moles/cm²/sec. (Assumption 4.3.10).
[2] Ref. 5.16, p. 11.
[3] Ref. 5.16, p. 11.
[4] Ref. 5.36, p. 47, rate in water at 30°C at short times.
[5] Ref. 5.36, p. 47, value for carbon steel rounded to 1.0e-11 moles/cm²/sec.
[6] Ref. 5.16, p. 12, rate doubled for conservatism (Assumption 4.3.27).
[7] Ref. 5.9, p. 4 high degradation rate cases.
[8] Ref. 5.36, Fig. 6.2-5, pH ca. 5.5-8.5, approximate average value, low degradation rate cases.

4.1.2 Water Chemistry

It was assumed that the composition of water entering the waste package would be the same as for water from well J-13 (Assumption 4.3.1). Water from this well has been analyzed repeatedly over a span of at least two decades (Ref. 5.12). This composition is reproduced in Table 4.1.2-1.

Table 4.1.2-1. Analyzed Composition of J-13 Well Water		
J-13 water	Molality	Mole Fr.
Na	1.99e-03	1.20e-05
Si	1.02e-03	6.11e-06
Ca	3.24e-04	1.95e-06
K	1.29e-04	7.74e-07
C	1.45e-04	8.69e-07
F	1.15e-04	6.89e-07
Cl*	2.15e-04	1.29e-06
N	1.42e-04	8.53e-07
Mg	8.27e-05	4.97e-07
S	1.92e-04	1.15e-06
B	1.24e-05	7.44e-08
P	1.27e-06	7.63e-09
H	1.11e+02	6.67e-01
O	5.55e+01	3.33e-01
Total	1.67e+02	1.00e+00

* Adjusted from the nominal value to produce electrical neutrality.

4.1.3 Metal Chemistry

The following metals are considered directly in computer models for waste package degradation: Alloy 625 (currently selected for the inner corrosion resistant barrier), 304L stainless steel (used for containment of glass waste forms and support structures inside a waste package), 316L stainless steel (used in basket structures for spent nuclear fuel), borated 316L stainless steel (B stainless steel) (used in basket structures for criticality control), XM-19 stainless steel (used for DOE SNF canister and assumed to have twice the corrosion rate of 316L -- Assumption 4.3.27) and carbon steel (used for outer corrosion allowance barrier). Table 4.1.3-1 shows the composition data for the metals. Reaction rates for the metals are given in Table 4.1.1.3-3.

Table 4.1.3-1. Composition of Metals

Alloy 625, Ref. 5.16, p. 10*		316L Stainless Steel Ref. 5.14, p. 14		B Stainless Steel 20% B removed, SS316B6A, Ref. 5.14, p. I-12		304L Stainless Steel, Ref. 5.14, p. I-4		XM-19 Stainless Steel, Ref. 5.15		Carbon Steel, Ref. 5.14, p. I-1	
Element	Wt%	Element	Wt%	Element	Wt%	Element	Wt%	Element	Wt%	Element	Wt%
Cr	21.5	C	0.03	B	1.2841	C	0.03	C	0.06	Fe	98.535
Ni	58.0	Mn	2	C	0.0301	Mn	2	Mn	5	Mn	0.9
Mo	9.0	P	0.045	N	0.1003	P	0.045	P	0.04	S	0.035
Nb	1.8	S	0.03	Si	0.7524	S	0.03	S	0.03	P	0.035
Fe	5.0	Si	0.75	P	0.0451	Si	0.75	Si	1	Si	0.275
Mn	0.5	Cr	17	S	0.0301	Cr	19	Cr	22	C	0.22
Ta	1.8	Ni	12	Cr	19.061	Ni	10	Ni	12.5		
S	0.015	Mo	2.5	Mn	2.0064	N	0.1	Mo	2.25		
Si	0.5	N	0.1	Fe	60.639	Fe	68.045	N	0.3		
P	0.015	Fe	65.545	Ni	13.5433			Nb	0.2		
C	0.1			Mo	2.508			V	0.2		
Co	0.93							Fe	56.42		
Ti	0.4										
Al	0.4										
Total	99.96		100		99.9998	Total	100	Totat	100	Total	100

* The analysis used this composition for runs that include "r", as in Ualla10rmm. Runs without "r" used a simplified analysis in which values for Cr, Ni, Nb, and Mo were used with the balance assigned to Fe.

4.1.4 Thermodynamic Data

It was assumed that the data in the thermodynamic data bases provided in conjunction with the EQ3/6 computer code package (Refs. 5.18, 5.19, 5.20, and 5.21) are sufficiently accurate for the purposes of this report (Assumption 4.3.8).

It should be noted, however, that two instances of doubtful data were identified; in both cases use of the values is conservative. Consequently, the data were retained. These relate to: (1) the solid, $Na_4UO_2(CO_3)_3$, and (2) chromate/dichromate ion, as discussed below.

1. The modeling often predicts the formation of significant amounts of the solid, $Na_4UO_2(CO_3)_3$, e.g., about 3.5% of the total mass of deposited material or 99.5% of the total mass of U plus Pu solids. This compound is not known as a mineral. This could mean simply the right conditions for its formation never occur in nature, but could also mean that there is some small error in the thermodynamic data for this solid. The impact on the results would be small, inasmuch as other uranium solids, which do occur as minerals, are very

close to saturation under the conditions for which the models predict the formation of this carbonate. In the present instance, the formation of the solid did not occur in the simulation, owing to the rate of water infiltration, no questionable consequences result.

2. As noted in Ref. 5.17, the modeling of reactions with Cr-containing steels in the presence of air predicts the oxidation of the Cr to chromate or dichromate. This would result in the production of very significant quantities of acid. There appears to be no direct metallurgical evidence for the generation of this acid. It would appear that, if oxidation to chromate does occur, it must be very slow. However, it could still be fast enough to be of consequence in the repository. Observations do indicate the attainment of low pH, e.g., 4 or less, in corrosion pits in such steels, but do not indicate whether this arises from the production of dichromate or from the hydrolysis of Cr^{+++} ions. Such hydrolysis does produce low pHs in solutions of $CrCl_3$ and $Cr(NO_3)_3$. Possibly the thermodynamic data for chromate ions are modestly in error, but enough to produce an erroneous modeling result. It is evidently difficult to obtain accurate thermodynamic data for chromate (see Ref. 5.22, pp. 355-357, and Ref. 5.23, pp. 249-250) owing to the great insolubility of CrO_3 and of chromates in general. Beyond this initial effort, the accuracy of the thermodynamic data for Cr have not been investigated in conjunction with this report.

It is assumed (Assumption 4.3.8) that the thermodynamic data are sufficiently accurate. This is conservative because the production of acid will lower the pH more than would otherwise be true and this results in a somewhat higher preferential solubility of neutron absorber (compared to fissile material) in the waste package and transport out to the surrounding environment. This increases the probability of a criticality inside the waste package. The effect on criticality external to the waste package will be analyzed in a separate study.

4.1.5 Solid Densities

Table 4.1.5-1 presents those mineral and non-mineral solid densities that were used in evaluating potential gravitational separation of fissile solid precipitates from neutron absorbers.

Table 4.1.5-1. Solid Densities

Solid	Density, g/cm^3	Reference
Gd_2O_3	7.4	5.39, p. B-113
Gibbsite	2.42	5.45, p. 236
Goethite	4.26	5.45, p. 240
Gold	17.0	5.45, p. B-115
Kaolinite	2.61	5.45, p. 318
Monazite	5.25	5.45, p. 413
Quartz	2.65	5.45, p. 504
Rhabdophane	4.0	5.45, p. 516
Soddyite	4.7	5.45, p. 568
Xenotime	4.7	5.45, p. 679

4.2 Criteria

The *Engineered Barrier Design Requirements Document* (EBDRD; Ref. 5.24) requirement EBDRD 3.7.1.A indicates that:

> Packages for SNF and HLW shall be designed so that the in situ chemical, physical, and nuclear properties of the waste package and its interactions with the emplacement environment do not compromise the function of the waste packages or the performance of the underground facility or the geologic setting.

Similarly, EBDRD 3.7.1.2.G indicates that:

> The container shall be designed so that neither its in situ chemical, physical and nuclear properties, nor its interactions with the waste form and the emplacement environment, compromise the function of the waste package or the performance of the natural barriers or engineered barriers.

This analysis contributes to satisfying the above two requirements by evaluating the chemical processes that will occur as the DOE SNF canister, waste form, and the HLW glass canisters, degrade following breach of the waste package. The results of this analysis will be used as input to criticality analyses which will determine if any of the resulting degraded configurations cause failure of the criticality control function of the waste package. While the EBDRD also contains several criteria which relate to criticality control, they are not relevant to this analysis, which deals only with the composition of the degraded configurations and does not involve any criticality (i.e., k_{eff}) calculations. Those calculations and any assesment of whether the criticality control criteria are met will be performed in the subsequent criticality analyses.

4.3 Assumptions

All assumptions are for preliminary design; these assumptions will require verification before this analysis can be used to support procurement, fabrication, or construction activities.

4.3.1 It is assumed that J-13 well water fills all voids within waste packages. It is further assumed that the composition of this water will remain as given in Ref. 5.12 for up to 100,000 years. The basis for the first part of this assumption is that it provides the maximum degradation rate with the potential for the fastest flushing of the neutron absorber from the DOE SNF canister and from the waste package, and is, thereby conservative. The basis for the second part of the assumption is that there is no basis for predicting any change in this composition over a 100,000 year time period. This assumption is used in Section 4.1.1, Section 4.1.2, and in Sections 7.1 through 7.4.

4.3.2 It is assumed that the density of J-13 well water is 1.0 g/cm^3. The basis is that for dilute solutions, the density differs extremely little from that for pure water and that any differences are insignificant in respect to other uncertainties in the data and calculations. Moreover, this number is used only initially in EQ3/6 to convert concentrations of dissolved substances from parts per million to molalities. The assumption applies throughout Sections 7.1 through 7.4.

4.3.3 It is assumed that the MIT fuel contains one weight percent U-234. The basis for this assumption is comparison to published information on other research reactor fuel of similar enrichment (Ref. 5.47). This assumption is used in Section 4.1.1.2 and in Sections 7.1, 7.2, and 7.3.

4.3.4 In assuming that the water entering the waste package can be approximated by the J-13 water it is implicitly assumed that: (1) the infiltrating water will have only a minimal contact, if any at all, with undegraded metal in the corrosion allowance barrier, and (2) that any effects of contact with the drift liner will be minimal after a few thousand years. The basis for the first part of this assumption is that the water should move rapidly enough through openings in the waste package barriers that its residence time in the corroded barrier will be too small for significant reaction to occur. Furthermore, the water flowing through the barriers will be in contact with the corrosion products left from the barrier corrosion which created the holes in the first place, but these corrosion products will closely resemble iron oxides and hydroxides in the overlying rock. Consequently, the water should already be close to equilibrium with these compounds and would be unaffected by further contact with them, even if it flowed slowly enough to

permit significant reaction. The second part of this assumption is justified by the following: (1) The drift liner of the top of the drift is expected to collapse with the roof support, well before 1000 years, (2) The travel time of water through the liner, while probably faster than the time through holes in the waste package barriers, will still be much less than the travel time through the rock above the repository; (3) Even if the drift liner lasted beyond the 3000 to 10000 years to breach the waste package, the alkalinity would not be much different from that expected to be produced during the HLW glass degradation phase. This assumption applies throughout Sections 7.1 through 7.4.

4.3.5 In some simulations, it is assumed water may circulate freely enough in the partially degraded WP that all degraded solid products, i.e., clay in the degraded HLW canisters and soddyite in degraded SNF canisters, may react with each other through the aqueous solution medium. The basis is that this provides one bound for the extent of chemical interactions within the WP and conservatively simulates phosphate in the clayey mass immobilizing Gd in the codisposal canister. This assumption is used in Section 7.3.2.1.1.

4.3.6 In some simulations, no interaction was permitted between degraded products of HLW canisters and those of the SNF canisters. The basis is that the clayey material may effectively prevent any significant circulation of the aqueous solution between the two regions. This provides a bound for the extent of the chemical interaction opposite to that of Assumption 4.3.5. This assumption is used in Section 7.3.2.1.1.

4.3.7 With respect to the need for separate geochemistry calculations for ORR fuel, it is assumed that the uranium silicide will not produce any additional degradation products. The basis for this assumption is that the amount of silicon in the ORR fuel is very small compared to that already present in the system from the HLW glass and from the J-13 water. This assumption is used in Section 7.2.3.

4.3.8 It has been assumed that the data base supplied with the EQ3/6 computer package is sufficiently accurate for the purposes of this report. The basis is that the data have been carefully scrutinized by many experts over the course of several decades and carefully selected by Lawrence Livermore National Laboratory (LLNL) for incorporation into the data base (Ref. 5.18). Every run of either EQ3 or EQ6 documents automatically what data base is used. The data bases include references internally for the sources of the data. The reader is referred to this documentation, included in electronic files labeled data0 that accompany this report, for details. Nevertheless, this review and documentation does not absolutely guarantee that all the data are adequate. In this connection, see discussion of

the data for chromium and uranium in Section 4.1.4. The assumption applies throughout Sections 7.1 through 7.4.

4.3.9 In general it is assumed that chromium and molybdenum will oxidize fully to chromate (or dichromate) and molybdate, respectively. This is based on the available thermodynamic data which indicate that in the presence of air the chromium and molybdenum would both oxidize to the +6 valence state. Laboratory observation of the corrosion of Cr and Mo containing steels and alloys, however, indicates that this oxidation, if it in fact occurs at a significant rate in respect to the time frame of interest, is extremely slow. For the present analyses, the assumption is made that over the times of concern the oxidation will occur. This is conservative for times of several thousand years after waste package breach, when the high pH solution from the degrading HLW glass, or from any drift liner effects, has been flushed out of the waste package, because it will cause acidification of the solution and the subsequent increase of solubility and transport of neutron absorber out of the WP thereby separating it preferentially from fissile material. It also has the consequence that the time interval during which the pH will remain at a particular value, e.g., 10 or 7, is limited. Such cases are considered separately. This assumption applies throughout Sections 7.1 through 7.4 generally.

4.3.10 It is assumed, in the absence of data for relevant conditions, that the corrosion rate of Alloy 625 is no more than 10 percent of the corrosion rate of 316L stainless steel. The justification for this assumption is that Alloy 625 is generally assumed to have corrosion properties similar to Alloy 825 (Refs. 5.50 and 5.51), and the most recent measurements of Alloy 825 corrosion rate indicate that it is less than 10 percent of that for 316L (Ref. 5.51). The conservatively high corrosion rate assumed for Alloy 625 resulted in virtually no effect on the simulations, because very little of the Alloy 625 had reacted by the time all of the other materials had degraded. Therefore, further analysis of the sensitivity to the corrosion rate wasn't necessary. This assumption applies to Sections 4.1.3 and 7.1 through 7.4.

4.3.11 It is assumed that the inner corrosion resistant barrier will react so slowly with the infiltrating water as to have negligible effect on the chemistry. The bases consist of the facts that this metal corrodes very slowly compared (1) to other reactions in the waste package and (2) to the rate at which soluble corrosion products will likely be flushed from the package. This assumption applies to Sections 7.1 through 7.4.

4.3.12 It is assumed that gases in the solution in the waste package will remain in equilibrium with the ambient atmosphere outside the waste package. In other words, it is assumed

that there is sufficient contact with the gas phase in the repository to maintain equilibrium with the CO_2 and O_2 present, whether or not this be the normal atmosphere in open air or rock gas that seeps out of the adjacent tuff. Under these conditions the partial pressure of CO_2 exerts important controls on the pH and carbonate concentration in the solution and hence on the solubility of uranium, gadolinium, and other elements. As discussed in Reference 5.28, the measured composition of J-13 water is not in equilibrium with the partial pressure of CO_2 in the atmosphere. By adjusting the average measured composition of the water slightly, well within the standard deviation of the measurements, it is possible to determine a partial pressure of CO_2 nearly ten times atmospheric (Ref. 5.29, Table 8, and Ref. 5.39, F-210), with which this water was apparently in equilibrium at depth in the well. Computer runs j13avg1.3o, j13avg19.3o, j13avg20.6o, and j13avg21.6o (provided on tape, Ref. 5.30) show the details of these adjustments. This high partial pressure is close to the maximum found by measurement of the rock gas composition (Ref. 5.29, Table 8). Therefore this high partial pressure was conservatively chosen for the majority of the computer runs used in this analysis. The basis for this assumption is that it minimizes the pH and thereby conservatively maximizes the solubility of Gd and the likelihood that this neutron absorber can be separated from the U. The high CO_2 tends to increase the concentration of free carbonate ion and its complexation with the dissolved U (uranyl ion), thereby tending to increase the solubility of U, but this is moderated by the reduction of the pH. There is little overall net effect for otherwise comparable conditions. This assumption was used throughout Section 7.

4.3.13 For purposes of estimating the probability that water dripping into the waste package will contact the contents of the DOE SNF canister, it is assumed that the water is flowing in a predominantly vertical direction, downward with gravity. The corollary to this assumption is that the probability of contact will be equal to the fraction of the waste package horizontal area which covers the DOE SNF canister. The assumption (and its corollary) do not explicitly consider the following two processes:

1) the initially downward flow of the drop entering the clayey mass is deflected, or diffused, by inhomogeneities, voids, or surfaces of undegraded material, and

2) for standing water there will be some regions of complete circulation with downward flow matched by upward flow.

A comprehensive flow analysis incorporating these processes is beyond the scope of this study. Instead, the justification is that for each path which could encounter the canister by such a diversion, there will be a flow path which would have been estimated to encounter

the DOE SNF canister but will be diverted away from it. This assumption was used in Section 7.4.3.1.

4.3.14 For purposes of estimating the probability of acidic water making gadolinium oxide soluble in the DOE SNF canister, it is assumed that the DOE SNF canister will not contribute significantly to the acidification. The justification for this assumption is that the corrosion will be primarily from the outside of the DOE SNF canister and the corrosion products will be carried away from the DOE SNF canister, rather than into it. Since this assumption tends to underestimate the solubility of gadolinium oxide, and hence underestimate the removal rate from the waste package, it is not conservative with respect to the use of gadolinium oxide as a criticality control material. However, the assumption is only used for comparing gadolinium oxide to the preferred alternative, gadolinium phosphate, where its effect is to de-emphasize the benefit of gadolinium phosphate with respect to gadolinium oxide. Therefore, with respect to the overall recommendation of this study, for gadolinium oxide, the assumption is conservative. This assumption is used directly in Section 7.4.4.1 and implicitly in Section 7.4.5.

4.3.15 It is assumed that the HLW glass will degrade at a rate no more than about 50% higher than the initial rate measured experimentally. The basis for this assumption is, whereas the initially observed rates of degradation always decrease with time, it has sometimes occurred that the rate subsequently increases (Ref. 5.9). The subsequent increase evidently depends upon nucleation of secondary phases. However, there is no satisfactory theory to predict when nucleation may start, which means that no matter how long an experiment is run, nucleation may still begin sometime later. To guard conservatively against underestimating release rates, hence the potential to form substantial deposits outside the waste package, the initial rate was increased by 50% as a conservative margin. This assumption applies to Sections 7.1 through 7.4.

4.3.16 It is assumed that if the gadolinium is used as the criticality control material (instead of boron), then carbon steel will be used as the SNF basket material and as the carrier for the gadolinium. The justification for this assumption is the superior performance in terms of the following:

1) higher yield strength,

2) more uniform distribution of iron oxide resulting from corrosion, and

3) production rate of iron oxide which more nearly corresponds to the release rate of the uranium aluminide from the SNF.

These benefits are discussed more fully in Section 7.4.4. This assumption is used directly in Section 7.4.4.1 and implicitly in Section 7.4.5.

4.3.17 To estimate the conditional probability that acidic water will contact the DOE SNF canister, given that the acidic water has resulted from the corrosion of the stainless steel of the HLW glass canisters, it is assumed that:

1) the average height of the clay surface above the waste package bottom is uniformly distributed between the diameter of the DOE SNF canister and the diameter of the waste package, and

2) the top of the DOE SNF canister (or that of its remnant) is uniformly distributed between the diameter of the DOE SNF canister and the height of the clay surface.

It is further assumed that the probability of the clay above the DOE SNF canister having a significant amount of corroding steel, is approximated by the ratio of the average depth of the DOE SNF canister divided by the maximum depth (which is the waste package diameter minus the DOE SNF canister diameter). The justification for this assumption is that it approximates the probability of water contacting an object by the fraction, covered by the area of the object, of the total area into which the water can flow. This assumption is used for comparison purposes only, to calculate the probability of criticality for a non-recommended alternative. It is used in Section 7.4.4.1.

4.3.18 It is assumed that reaction rates are reasonable, but at the high end of applicable ranges. The basis for this assumption is that it is highly conservative. This assumption applies throughout Sections 7.1 through 7.4.

4.3.19 It is assumed in the open system flow through modeling that all solids that are deposited remain in place; no solids are entrained or otherwise re-mobilized. The basis for this assumption is that it conservatively maximizes the size of potential deposits of fissile material inside the WP. This assumption applies throughout Sections 7.1 through 7.4.

4.3.20 It is assumed that the corrosion rates will not be significantly enhanced by biological mediated corrosion. The bases for this assumption are that even at the time that the repository is closed there will be little organic material present to serve as nutrients for biological activity and that by the time the corrosion barriers are breached essentially all of such material will most likely have decayed to carbon dioxide and dissipated. Whereas a few organisms can use CO_2 directly as a nutrient and two other essential factors necessary for biological activity are present (water and an energy source, in this case

chemical disequilibrium between the metal and atmospheric oxygen), the impact on corrosion is likely to be low and the effect on the chemistry of fissile isotopes and neutron absorbers is expected to be negligible. This assumption applies to Sections 7.1 through 7.4.

4.3.21 It is assumed that sufficient decay heat is retained within the waste package over times of interest to cause convective circulation and mixing of the water inside the package. The basis for this assumption is discussed on p. 5-7 of Ref. 5.14. This assumption applies to Sections 7.1 through 7.4.

4.3.22 It was assumed that uranium aluminide would corrode at a rate resembling that for aluminum metal. The basis for this assumption is that the aluminide is thermodynamically unstable in the presence of water and atmospheric oxygen to approximately the same degree as is aluminum metal. Consequently, rather rapid corrosion is likely to occur. If the degradation occurs in a time frame much shorter than that for the HLW or other metals, errors in the degradation have no significant impact on the results of the analyses in this report. This assumption applies to Sections 7.1 through 7.4.

4.3.23 It is assumed, in some cases, that following breach of the outer barriers, the HLW canister will breach sufficiently long before the DOE SNF canister containing the DOE spent fuel breaches that all the HLW will have degraded and the highly alkaline resultant solution will have been flushed out and replaced by essentially unmodified J-13 water. The basis for this assumption is that the proposed DOE SNF canister wall is thicker than the HLW canister and will be constructed of a more corrosion resistant metal. The assumption is conservative because the pH will be close to neutral and the U will be retained within the degraded DOE SNF canister.

4.3.24 It is assumed that the crystal shapes of gibbsite or kaolinite, goethite, rhabdophane, and soddyite will sufficiently resemble each other that differences in shapes will not lead to a significant difference in settling rates within the DOE SNF canister or waste package. The basis for this assumption is that all three minerals tend to crystallize in tabular to elongated forms (Ref. 5.45, pp. 236, 240, 318, 516, and 568). Because all of them differ from spheres in similar ways, it is expected that their settling rates, if all other factors such as size and density were the same, would be nearly the same. This assumption is used in Section 7.4.1.

4.3.25 For purposes of estimating the fraction of a basket plate surface area which will eventually settle to the bottom intact (rather than corroding in its initial configuration) it is assumed that a carbon steel pit can be represented by a cross section dimension equal to the pit depth, while a stainless steel pit will be represented by a cross section dimension equal to the 1/10 of the pit depth (so that there are 100 times as many square cells for stainless steel). The justification for this assumption is that it falls within the range of observations for carbon steel (Ref. 5.36, Section 5.3.6). It is conservative for stainless steel because the observations indicate a cross section dimension less than 1/10 of the pit depth (for pits which have penetrated more than 1mm). This assumption is used in Section 7.4.4.2.

4.3.26 For purposes of estimating the fraction of a basket plate surface area which will eventually settle to the bottom intact (rather than corroding in its initial configuration) it is assumed that all pits grow at a uniform rate, and the only randomness is the total number of pits and their distribution. The justification for this assumption is that it is conservative because random pitting rates will result in some pits not penetrating through the plate so that they will be less effective in producing a cutout. This assumption is used in Section 7.4.4.2.

4.3.27 It is assumed that chemically XM-19 is equivalent to 316L stainless steel because of similar chemical compositions (see Table 4.1.3-1). The corrosion rate for XM-19 is conservatively assumed to be twice that for 316L stainless steel. This assumption is used in Section 4.1.3.

4.3.28 It is assumed that aluminum will corrode at a rate which is fast compared to the degradation rates of other material in the waste package in general, and material in the basket of the DOE SNF canister, in particular. This assumption is conservative with respect to the published data, as illustrated in Refs. 5.5 and 5.6, and as explained in Section 4.1.1.2. This assumption is used in Section 4.1.1.2.

4.3.29 For purposes of estimating the fraction of neutronically significant material which could fall to the bottom of the basket in the DOE SNF canister, it is assumed that the waste package is oriented such that the large basket plates (shown horizontal in Figure 7.4-3) actually are horizontal. It is further assumed that the disposition of material from the plates which are angled to the large plates (shown in Figure 7.4-3 and described in Refs. 5.38 and 5.55) will be the same as for the horizontal plates. This assumption is made for modeling purposes only. The basis for this assumption is that it is conservative. Any material resting on top of a non-horizontal basket plate would tend to slide down the plate to the corner formed by the intersection of the plate with the canister wall. There would

be one such corner for each basket plate, and the collection of such corners would be a less favorable geometery for criticality than the one collection at the bottom assumed here. The same considerations apply to corroded material from the angled plates. This assumption is used in Section 7.4.4.2

4.3.30 It is assumed that the drip rates of water into the repository will vary within the range 0.1 mm/yr to 10 mm/yr over the long term. This range of drip rates is the same as the range of filtration rates given in TSPA-95 (Ref. 5.36); the range is lower than that given in the CDA (Ref. 5.25). Infiltration rate is the net flow into the ground at a small distance beneath the surface (precipation minus evapotranspiration, minus runoff). Drip rate is the net flow into the repository. The difference is the lateral diversion, away from the repository, by relatively impervious layers between the surface and the repository. This difference is uncertain at the present time, but experiments are expected to provide definitive information within the next few years. The CDA specifies an upper limit for the range of infiltration rates which is much higher than 10 mm/yr. The justification for not using a much higher upper limit for the drip rate range is based on the following: (1) except in regions where the lateral diversion mechanisms (layers) are broken by a nearly vertical fault or similar geologic structure, the drip rate must be significantly lower than infiltration rate; (2) the assumption of a low drip rate is conservative with respect to reaction rates which can be enhanced by buildup of ionic strength or deviation of pH from neutrality; (3) the only criticality enhancing effect of a high drip rate is the faster removal, from the waste package, of neutron absorbers already in solution, which is already discounted by extending the run times until the absorber was removed, for those cases which showed significant absorber depletion by this mechanism.

4.4 Codes and Standards

No codes or standards are applicable to this analysis.

5. References

5.1 *QA Classification Analysis of Preliminary MGDS Repository Design*, Document Identification Number: B00000000-01717-0200-00134 REV 00, Department of Energy Office of Civilian Radioactive Waste Management (OCRWM).

5.2 *Quality Assurance Requirements and Description*, DOE/RW-0333P, REV 7, CRWMS M&O.

5.3 *Perform Probabilistic Waste Package Design Analyses*, QAP-2-0 Activity Evaluations, WP-25, Civilian Radioactive Waste Management System (CRWMS) Management and Operating Contractor (M&O).

5.4 *Data Package from Savannah River Criticality Analysis of MIT and ORR SNF*, (includes WSRC-TR-95-0302 Appendix A data sheets 59 and 217 for MIT and ORR fuel, as well as drawings R3F-3-2, R3F-1-4, M-11495-OR-001, 003, and 004) RPC Batch Number MOY-970605-02, CRWMS M&O.

5.5 Howell, J. P., *Corrosion of Aluminum-Clad Spent Fuel in Reactor Basin Water Storage*, Westinghouse Savannah River Company, WSRC-MS-94-0524, 1995, p. 1.

5.6 Cook, E., Horst, R., and Binger, W., *Corrosion*, Volume 17, 1961, p. 251.

5.7 *Characteristics of Potential Repository Wastes*, DOE/RW-0184-R1; Volume 1, U.S. DOE OCRWM.

5.8 Bourcier, Wm. L., *Waste Glass Corrosion Modeling: Comparison with Experimental Results*, Materials Research Society Symposium Proceedings, 1994, v. 333, pp. 69-82.

5.9 Bates, J., Strachan, D., Ellison, A., Buck, E., Bibler, N., McGrail, B. P., Bourcier, W., Grambow, B., Sylvester, K., Wenzel, K., and Simonson, S., *Glass Corrosion and Irradiation Damage Performance*, Plutonium Stabilization & Immobilization Workshop, December 11-14, 1995, Washington, D. C.

5.10 Bates, John, *Viewgraph*, last in the set entitled "Leaching Studies", Identifier ITT-96-051-LWG 5/2/96-P-5, Identification number MOY-970911-13, 1996.

5.11 *DHLW Glass Waste Package Criticality Analysis*, Document Identifier Number: BBAC00000-01717-0200-00001 REV 00, CRWMS M&O.

5.12 Harrar, J. E., Carley, J. F., Isherwood, W. F., and Raber, E., *Report of the Committee to Review the Use of J-13 Well Water in Nevada Nuclear Waste Storage Investigations*, UCID-21867, 1990, Lawrence Livermore National Laboratory , Livermore, CA.

5.13 *Standard Specification for Nickel-Chromium-Molybdenum-Columbium Alloy (UNSN06625) Plate, Sheet, and Strip*, ASTM B443-93, American Society for Testing and Materials, Philadelphia, PA.

5.14 *Material Compositions and Number Densities For Neutronics Calculations (SCPB: N/A)*, Document Identifier Number: BBA000000-01717-0200-00002 REV 00, CRWMS M&O.

5.15 *Standard Specification for Heat-Resisting Chromium and Chromium-Nickel Stainless Steel Plate, Sheet, and Strip for Pressure Vessels*, ASTM A240/A240M REV91A, American Society for Testing and Materials, Philadelphia, PA.

5.16 *Criticality Evaluation of Degraded Internal Configurations for the PWR AUCF WP Designs*, Document Identifier Number: BBA000000-01717-0200-00056 REV 00, CRWMS M&O.

5.17 *Degraded Mode Criticality Analysis of Immobilized Plutonium Waste Forms in a Geologic Repository*, Document Identifier Number: A00000000-01717-5705-00014 REV 01, CRWMS M&O.

5.18 Wolery, Thomas J., *EQ3/6, A Software Package for Geochemical Modeling of Aqueous Systems: Package Overview and Installation Guide (Version 7.0)*, UCRL-MA-110662 PT I, 1992, LLNL.

5.19 Daveler, Stephanie A., and Wolery, Thomas J., *EQPT, A Data File Preprocessor for the EQ3/6 Software Package: User's Guide, and Related Documentation (Version 7.0)*, UCRL-MA-110662 PT II, 1992, LLNL.

5.20 Wolery, Thomas J., *EQ3NR, A Computer Program for Geochemical Aqueous Speciation-Solubility Calculations: Theoretical Manual, User's Guide, and Related Documentation (Version 7.0)*, UCRL-MA-110662 PT III, 1992, LLNL.

5.21 Wolery, Thomas J., and Daveler, Stephanie A., *EQ6, A Computer Program for Reaction Path Modeling of Aqueous Geochemical Systems: Theoretical Manual, User's Guide, and Related Documentation (Version 7.0)*, UCRL-MA-110662 PT IV, 1992, LLNL.

5.22 Latimer, W. M., and Hildebrand, J. H., *Reference Book of Inorganic Chemistry, Revised Edition*, 1940, The MacMillan Co., New York.

5.23 Latimer, W. M., *The Oxidation States of the Elements and Their Potentials in Aqueous Solutions, 2nd ed.*, 1952, Prentice-Hall, Inc., New York.

5.24 *Engineered Barrier Design Requirements Document*, YMP/CM-0024, REV 0, ICN 1, Yucca Mountain Site Characterization Project.

5.25 *Controlled Design Assumptions Document*, Document Identifier Number: B00000000-01717-4600-0032 REV 04, ICN 03, CRWMS M&O.

5.26 *10CFR Part 60; Disposal of High-Level Radioactive Wastes in Geologic Repositories; Design Basis Events; Final Rule*, U.S. Nuclear Regulatory Commission, Federal Register, Volume 61, Number 234, January 1, 1997.

5.27 *Inconel Alloy 625*, 5th Edition, Inco Alloys International, Publication T-42, 1985.

5.28 *Evaluation of the Potential for Deposition of Uranium/Plutonium from Repository Waste Packages*, Document Identifier Number: BBA000000-01717-0200-00050 REV 00, CRWMS M&O.

5.29 Yang, I. C., Rattray, G. W., and Yu, P., *Interpretation of Chemical and Isotopic Data from Boreholes in the Unsaturated-Zone at Yucca Mountain, Nevada*, U. W. Geological Survey Water-Resources Investigations, Report WRIR 96-4058, 1996.

5.30 *Electronic Media for BBA000000-01717-0200-00059 REV 00*, Colorado Trakker Tape, RPC Batch Number MOY-971215-07, CRWMS M&O.

5.31 Seidell, A., *Solubilities of Inorganic and Metal Organic Compounds*, Vol. 1, 3rd ed., 1953, D. van Nostrand.

5.32 Wefers, K., and Misra, C., *Oxides and Hydroxides of Aluminum*, Alcoa Technical Paper, No. 19, Revised, 1987, Alcoa Laboratories.

5.33 Busenberg, E., *The Products of the Interaction of Feldspars with Aqueous Solutions at 25 °C*, Geochimica et Cosmochimica Acta, Vol. 42, 1978, pp. 1679-1686.

5.34 Vaniman, D. T., Bish, D. L., Chipera, S. J., Carlos, B. A., and Guthrie, G. D., Jr., *Summary and Synthesis Report on Mineralogy and Petrology Studies for the Yucca Mountain Site Characterization Project, Volume 1, Chemistry and Mineralogy of the Transport Environment at Yucca Mountain*, Yucca Mountain Milestone Report Number 3665, 1966, Los Alamos National Laboratory.

5.35 Fleer, V. N., and Johnston, R. M., *A Compilation of Solubility and Dissolution Kinetics Data on Minerals in Granitic and Gabbroic Systems*, AECL-TR-328-2, Atomic Energy of Canada Limited, Pinawa, Manitoba, Canada.

5.36 *Total System Performance Assessment - 1995: An Evaluation of the Potential Yucca Mountain Repository*, Document Identifier Number: B00000000-01717-2200-000136 REV 01, CRWMS M&O.

5.37 Langmuir, D., *Aqueous Environmental Geochemistry*, 1996, Prentice-Hall, Upper Saddle River, NJ.

5.38 *Evaluation of Codisposal Viability for Aluminum-Clad DOE-Owned Spent Fuel: Phase I Intact Codisposal Canister*, Document Identifier Number: BBA000000-01717-5705-00011 REV 01, CRWMS M&O.

5.39 Weast, R. C., ed., *CRC Handbook of Chemistry and Physics, 58th Ed.*, 1977, CRC Press, Inc., Cleveland, OH.

5.40 Spahiu, K., and Bruno, J., *A selected thermodynamic database for REE to be used in HLNW performance assessment exercises*, SKB Technical Report 95-35, 1995, Swedish Nuclear Fuel and Waste Management Co., Stockholm, Sweden.

5.41 Jonasson, R. G., Bancroft, G. M., and Nesbit, H. W., *Solubilities of Some Hydrous REE Phosphates with Implications for Diagenesis and Sea Water Concentrations*, Geochimica et Cosmochimica Acta, Vol. 49, 1985, pp. 2133-2139.

5.42 Palache, C., Berman, H., and Frondel, C., *The System of Mineralogy*, 7th ed., vol. II, 1951, John Wiley & Sons, Inc.

5.43 Gaudin, A. M., *Principles of Mineral Dressing*, 1939, McGraw-Hill Book, Co.

5.44 Wills, B. A., *Mineral Processing Technology*, 4th ed., 1988, Pergamon Press.

5.45 Roberts, W. L., Jr., Rapp, G. R., Jr., and Weber, J., *Encyclopedia of Minerals*, 1974, van Nostrand Reinhold Co.

5.46 Jensen, Mead L., and Bateman, Alan M., *Economic Mineral Deposits, 3rd ed., Revised Printing*, 1981, John Wiley & Sons, New York.

5.47 *International Handbook of Evaluated Criticality Safety Benchmark Experiments*, NEA/NSC/DOC(95)03/I, Volume II.b, Nuclear Energy Agency, Organization for Economic Co-operation and Development, November 4, 1996 update.

5.48 *Criticality Safety and Shielding Evaluation of the Codisposal Canister in the Five-Pack DHLW Waste Package*, Document Identifier Number: BBA000000-01717-0200-00052 REV 01, CRWMS M&O.

5.49 Technical Data, Nitronic 50 Alloy, ALTECH, AL Tech Specialty Steel Corporation, Dunkirk, NY 14048, ASTM TP XM-19, American Society for Testing and Materials, Philadelphia, PA.

5.50 *Immersion Studies on Candidate Container Alloys for the Tuff Repository*, 1991, Nuclear Regulatory Commission, NUREG/CR-5598.

5.51 Roy, A. J., Fleming, D. L., and Lum, B. Y., *Stress Corrosion Cracking of Fe-Ni-Cr-Mo, Ni-Cr-Mo and Ti Alloys in 90 °C Acidic Brine*, UCRL-JC-128477, 1997, LLNL.

5.52 *Initial Waste Package Probabilistic Criricality Analysis*, Document Identifier Number: B00000000-01717-2200-00079 REV 01, CRWMS M&O.

5.53 *1994 ASME Boiler and Pressure Vessel Code*, Section II, American Society of Mechanical Engineeers, 1995.

5.54 *Standard Specification for Pressure Vessel Plates, Carbon Steel, for Moderate-and-Lower-Teperature Service*, ASTM A516/A516M-90, American Society for Testing and Materials, Philadelphia, PA.

5.55 *Disposal Criticality Analysis for Aluminum-based Fuel in a Codisposal Waste Package - ORR and MIT SNF - Phase II*, Document Identifier Number: BBA000000-01717-0200-00060 REV 00, CRWMS M&O.

5.56 *Report on External Criticality of Plutonium Waste Forms in a Geologic Repository*, Document Identifier Number: BBA000000-01717-5705-00018 REV 00, CRWMS M&O.

5.57 *Structural Evaluation of MIT-SNF Codisposal Canister*, Document Identifier Number: BBA000000-01717-0200-00051 REV 00, CRWMS M&O.

5.58 *Probabilistic External Criticality Evaluation*, Document Identifier Number: BB0000000-01717-2200-00037 REV 00, CRWMS M&O.

5.59 *Technical Bases for Yucca Mountain Standards*, National Research Council of the National Academy of Science, National Academy Press, 1995, Washington, DC.

6. Use of Computer Software

This section describes the computer software used to carry out the analysis.

6.1 EQ3/6 Software Package

The EQ3/6 software package originated in the mid-1970's at Northwestern University. Since 1978 Lawrence Livermore National Laboratory has been responsible for its maintenance. It has most recently been maintained under the sponsorship of the Civilian Radioactive Waste Management Program of the U.S. Department of Energy. The major components of the EQ3/6 package include: EQ3NR, a speciation-solubility code; EQ6, a reaction path code which models water/rock interaction or fluid mixing in either a pure reaction progress mode or a time mode; EQPT, a data file preprocessor; EQLIB, a supporting software library; and several (>5) supporting thermodynamic data files. The software deals with the concepts of the thermodynamic equilibrium, thermodynamic disequilibrium, and reaction kinetics. The supporting data files contain both standard state and activity coefficient-related data. Most of the data files support the use of the Davies or B-dot equations for the activity coefficients; two others support the use of Pitzer's equations. The temperature range of the thermodynamic data on the data files varies from 25°C only for some species to a full range of 0-300°C for others. EQPT takes a formatted data file (a data file) and writes an unformatted near-equivalent called a data1 file, which is actually the form read by EQ3NR and EQ6. EQ3NR is useful for analyzing groundwater chemistry data, calculating solubility limits and determining whether certain reactions are in states of partial equilibrium or disequilibrium. EQ3NR is also required to initialize an EQ6 calculation.

EQ6 models the consequences of reacting an aqueous solution with a set of reactants which react irreversibly. It can also model fluid mixing and the consequences of changes in temperature. This code operates both in a pure reaction progress frame and in a time frame. In a time frame calculation, the user specifies rate laws for the progress of the irreversible reactions. Otherwise, only relative rates are specified. EQ3NR and EQ6 use a hybrid Newton-Raphson technique to make thermodynamic calculations. This is supported by a set of algorithms which create and optimize starting values. EQ6 uses an ODE integration algorithm to solve rate equations in time mode. The codes in the EQ3/6 package are written in FORTRAN 77 and have been developed to run under the UNIX operating system on computers ranging from workstations to supercomputers. Further information on the codes of the EQ3/6 package is provided in Ref. 5.18 through 5.21.

In this study EQ3/6 was used to provide:

1) a general overview of the nature of chemical reactions to be expected,

2) the degradation products likely to result from corrosion of the waste forms and canisters, and

3) an indication of the minerals, and their amounts, likely to precipitate within the WP.

The programs have not been used outside the range of parameters for which they have been verified. The EQ3/6 calculations reported in this document used version 7.2b of the code and were executed on the Hewlett-Packard 9000 Series 735 workstation.

The EQ3/6 package has been verified by its present custodian, Lawrence Livermore National Laboratory, but it has not been qualified under the Management and Operating Contractor Quality Administrative Procedure (M&O QAP). Therefore all the results are considered TBV with respect to any design or procurement decisions or specifications.

6.2 Software Routines for Chaining Successive EQ6 Cases

The following software routines were developed specifically for this study for the purpose of facilitating the setup and execution of successive cases of EQ6, by transforming the output of one case to the input of the following case. An individual EQ6 run diluted the solution constituents to reflect the inflow of fresh water and the routines periodically remove water and solutes corresponding to the inflow. The routines also read the output of one run and reformat it as input for the next run. The data reformatting aspect of these routines was verified by visual inspection in accordance with QAP-SI-0, 5.3.2C by an individual independent of the person doing the original development. The mathematical algorithm for these routines is given in attachment I. It has also been verified by hand calculations by an individual independent of the person doing the original development in accordance with QAP-SI-0, 5.3.2C. Both the progam and the hand calculation are documented in Attachment II, in accordance with QAP-SI-0, 5.3.2D.

6.2.1 File bldinpt.bat

This is a UNIX shell script which does the following:

1) runs the program (EQ6) to build the initial input (bldinput.c),

2) executes the initial iteration of EQ6,

3) runs the program (nxtinput.c) to transfer the output from one iteration to the input of the next iteration,

4) runs the next iteration of EQ6, and

5) repeats steps 3 and 4 until a specified number of iterations have been reached, or until an abnormal condition occurs (which causes nxtinput.c to write an error message to a file which is read and interpreted by this script file).

6.2.2 File bldinput.c

This C program builds the EQ3/6 input from a template and an input file containing casename, date, and maximum simulation time.

6.2.3 File nxtinput.bat

This shell script runs the same iteration loop as bldinput.bat, but starts from the output of a previous iteration.

6.2.4 File nxtinput.c

This C program reads the output and pickup (program file names) files of an EQ3/6 iteration and generates the input file for the next iteration. In this process it makes two basic data changes:

1) the amounts of all the species in solution are reduced to simulate the flushing out of an amount of solution corresponding to an infusion of fresh water into the waste package as calculated by EQ6, and

2) some alternative species are switched into, or out of, the basis set for the chemical reactions, according to which member of the alternative set has achieved the largest concentration.

6.2.5 File pitgen.c

This C program does the following:

1) generates a rectangular array of square locations (nodes) on a rectangular plate,

2) randomly selects, from this array, the locations for the occurrence of pits, and

3) after each of a specified number of pits is generated, scans the array to detect the areas which are completely encircled by pits, defines these areas as cutouts (which serve as paths for certain solid corrosion products, or their precipitates, to settle to lower parts of the DOE SNF canister), and counts the area (number of square locations) enclosed in the cutouts.

6.3 Spreadsheets

Spreadsheet analyses were performed with Microsoft Excel version 97, loaded on a PC. The specific spreadsheets used for results reported in this document are included for reference in the attachments.

7. Design Analysis

The purpose of this section is to model the degradation processes in the codisposal waste package which may result in segregation of fissile material from neutron absorber material. For postclosure, the low probability and consequences of a criticality must provide reasonable assurance that the performance objective of 10CFR60.112 is met. This analysis contributes to satisfying the above requirements for postclosure by determining the distribution over time of fissile and absorber materials which affect criticality. The probability of such events is addressed in a separate analysis.

Four HLW canisters (of the 5-pack design) and one DOE SNF canister of the M&O design containing uranium aluminide spent fuel from the MIT research reactor were modeled in this analysis of the codisposal waste package system. (The use of four canisters is, from the chemical point of view, more conservative than using five, as in the current design, because this would tend to result in less removal of uranium from the waste package and hence a greater probability of a criticality.) In particular, the analysis uses EQ6 to determine the concentrations of neutronically active species in solution and in solid precipitates within the waste package for time periods up to 100,000 years following emplacement. These parameters are to be determined for the range of drip rates expected, 0.1 mm/yr to 10 mm/yr, which will permit an estimate of the amount of each neutronically significant species remaining in the waste package as a function of time. This range of drip rates is consistent with the infiltration rates given in TSPA-95 (Ref. 5.36); the range is lower than that given in Ref. 5.25. The justification for this choice is given in assumption 4.3.30, together with an explanation of the difference between drip rate and infiltration rate.

Section 7.1 describes the degradation scenarios evaluated. Section 7.2 describes the degradation products of the waste forms and the basket in the DOE SNF canister. Section 7.3 describes the evolution of the solids and solution in the waste package. Section 7.4 summarizes the results for use in the design and design analysis documentation for this waste package prepared for disposal of SRS canisters (Ref. 5.4).

7.1 Degradation Scenarios

This analysis is based on the premise that some number of waste packages will be penetrated by water during the post-closure time period of interest (up to at least 100,000 years). This premise is consistent with the present specification of waste package barrier materials and our present understanding of their corrosion rates. The analyses presented in this document are concerned with products of the degradation of the contents of waste package. The analyses are concerned

with both the initial degradation products and the subsequent evolution of the system of the products mixing, and interacting, to varying degrees. The ranges of rates for these degradation processes are given in Section 4.1. The specific products which result directly from these degradation processes are partly determined by the specific aqueous chemical environment as the processes are taking place.

The degradation environment, in turn, is partly determined by other processes which are taking place simultaneously. In particular, the HLW glass degradation products will cause the pH to increase. If the SNF degrades in a high pH environment, most of the released uranium could go directly into solution. In contrast, when the SNF degrades in a near-neutral pH environment (characteristic of inflowing J-13 water) most of the released uranium will go directly into precipitated solids. To provide some guidance in determining the appropriate environment, the estimated periods of degradation for the various basket materials, which were used for most of the computer simulations, are given in Table 7.1-1. A few simulations were performed with a slower degradation rate for the glass. Outputs for individual computer runs (Ref. 5.30) echo the data specified in the input file and used for each individual run.

Table 7.1-1. Typical Corrosion Periods/Lifetimes of Materials which can Affect Criticality

Item/Material	Volume (cm^3)	Mass (g)	Surface Area (cm^2)	Degradation Rate ($g/cm^2/sec$)	Duration of degradation (years since exposure)	Absolute Lifetime[A] (yrs since emplacement of WP)	Absolute Lifetime[B] (yrs since emplacement of WP)
316 SS	6.68e+04	5.31e+05	1.62e+05	2.52e-12	4.12e+04	4.62e+04	5.10e+04
XM-19[1]	6.05e+04	4.77e+05	7.00e+04	3.76e-12	5.74e+04	6.24e+04	N.A.
Al[2]	4.04e+04	1.09e+05	3.65e+04	5.81e-09	1.63e+01	5.02e+03	9.78e+03
Fuel meat[3]	2.34e+04	5.12e+04	6.23e+05	2.60e-10	1.00e+01	5.01e+03	9.77e+03
304L	3.66e+05	2.89e+06	4.54e+05	3.76e-12	5.36e+04	5.86e+04	N.A.
Alloy 625	4.05e+05	3.42e+06	1.88e+05	2.66e-13	2.16e+06	2.17e+06	N.A.
B stainless steel[4]	1.37e+04	1.06e+05	6.74e+04	1.97e-11	2.53e+03	7.53e+03	N.A.
A516 steel[5]	1.37e+04	1.06e+05	6.74e+04	5.52e-10	9.03e+01	N.A.	9.85e+03
HLW glass[6]	2.42e+06	6.89e+06	5.65e+06	3.23e-11	1.20e+03	6.20e+03	N.A.
HLW glass[7]	2.42e+06	6.89e+06	5.65e+06	2.31e-13	1.67e+05	N.A.	1.77e+05

[A] Breach of the DOE SNF canister is assumed to occur 1000 years after exposure, which in turn is assumed to occur following breach of Alloy 625 at 4000 years after emplacement of the waste package. Thus, the entry in the 7th column, where applicable, is 5000 years greater than the time entered in the 6th column.

[B] Analyses of alternative corrosion periods. Breach of the DOE SNF canister is assumed to occur following degradation of the HLW and flushing out of the soluble products at 5756 years after breach of Alloy 625 at 4000 years after emplacement of the waste package. Thus, the entry in the 8th column, where applicable, is 9756 years greater than the time entered in the 6th column.

[1] Density from Ref. 5.49. [2] Density from Ref. 5.39, p. B-85.

[3] Density from Ref. 5.48, p. II-2.

[4] Density from Ref. 5.14, p. I-12. Material used for boron absorber only.

[5] Density from Ref. 5.14, p. I-12. Material used for gadolinium absorber only.

[6] HLW glass, nominal reaction rate.

[7] HLW glass, low reaction rate from Ref. 5.36.

For all cases in these analyses the perspective has been taken that, following breach of the outer barriers, all void spaces in the waste package fill completely with water resembling that in well J-13 (Assumption 4.3.1). All the solid forms become covered by water, and, for a waste package in which all canisters have been breached, there is a standing water volume of about 2.9 m^3 per package. As discussed in Ref. 5.17, this situation is most conservative with respect to producing a criticality within the waste package. Moreover, it is assumed that sufficient decay heat is retained within the waste package over times of interest to cause convective circulation and mixing of the water inside the package (Assumption 4.3.21).

As a consequence of the above considerations, the duration and products of the degradation processes are primarily determined by the corrosion rates and thicknesses of the metal and glass waste forms, canisters, and DOE SNF canister basket. Additional factors which could affect dissolution rates are omitted by implication, based on the following:

- All solid surfaces within a canister are wetted, once the canister is breached. This assumption (Assumption 4.3.1) is used because it is conservative. Other assumptions which in a variety of complex ways could result in only part of the surface being wetted would produce less corrosion of metal and consequent lower acid production from the oxidation of Cr to chromate. This in turn would reduce the potential removal of neutron absorbers.

- Localized corrosion will, at specific locations, penetrate into corrosion resistant materials more rapidly than will general corrosion. The corrosion products will be the same in both cases, except perhaps transiently within pits and crevices, and, consequently, modeling will predict the same products.

- Biological processes, which are not included in the EQ6 chemistry model, will account for only an insignificant fraction of total metal corrosion. (Assumption 4.3.20)

7.2 Degradation Products

This section describes the products of the degradation processes for the waste forms and criticality control material. The evolution of the solution and solids in the waste package is described in Section 7.3.

7.2.1 Degradation of HLW

The water chemistry and degradation products generated during the HLW degradation phase were estimated with EQ6, and the resulting outputs are archived in the electronic attachments (Ref. 5.30). The most immediately important parameter of this degradation is pH. The behavior of this parameter during the HLW degradation period is given in Tables 7.2-1 and 7.2-2. Table 7.2-1 shows the simulated evolution for different drip rates for cases run with atmospheric partial pressure of CO_2 for waste packages under conditions such that both HLW and SNF (MIT spent fuel) are initially exposed to water at about the same time. Because the initial pH is higher for these cases and the neutralizing effect of CO_2 is less, these runs simulate maximum probable pH values. Because the SNF has little effect on the pH, cases for HLW alone with atmospheric partial pressure of CO_2 would be almost identical to the above cases and were not run. Table 7.2-2 shows simulations for an elevated partial pressure of CO_2, corresponding to conditions to reconcile the measured data for J-13 water with thermodynamic data. These simulations were for waste packages in which only HLW is initially exposed to water. These simulations start at lower pH and tend to remain lower owing to the higher CO_2 pressure. Consequently, they simulate those minimum pH conditions that are most likely to dissolve and remove Gd from the waste package and thereby possibly result in a criticality. Again, because the SNF has little effect on the pH, cases for HLW plus SNF with the higher partial pressure of CO_2 would be almost identical and were not run.

Table 7.2-1. Drip rate Summary of pH for the Case in which the SNF is Exposed to the High pH of the Degrading HLW Glass, Atmospheric CO_2 Partial Pressure.

Drip rate, mm/yr	Average pH‡	Peak pH	Final pH	Time at run end, yrs	EQ6 run*
0.1††	10.0	10.2	10.2	1300	UAIIa0:1rmm
1.0†	9.6	10.1	10.1	1020	UAIIa1rmm
5.0	9.6	9.9	8.7	2830	UAIIa5rmm
10.0	9.7	9.8	9.0	1420	UAIIa10rmm

* See Ref. 5.30 for full details. Key to file names: UAI[I, II, ...][a, b, c, . i,.][I][1, 2:1, ...][r]mm; UAI refers to uranium aluminide fuel; the Roman numeral indicates the flushing sequence -- because of file size limitations the full flushing simulation must be run piecemeal; "a" refers to sequences starting with both fuel and HLW present at atmospheric partial pressure of CO_2 and best estimates for degradation rates at near neutral conditions; "b" refers to sequences starting with degradation of HLW and flushing of its degradation products before fuel is exposed to the water and at an elevated partial pressure of CO_2 (to obtain concordance of water analyses and thermodynamic data); "c" refers to a run for degradation of the fuel canister in the absence of HLW or its degradation products; "d" refers to runs beginning after flushing out of high concentration of alkali from the HLW and use of Gd_2O_3 plus carbon steel in the canister instead of borated steel; "e" refers to runs to which $GdPO_4 \cdot H_2O$ and carbon steel replaced borated steel; the arabic number refers to the drip rate in mm/yr (0:1 was used to designate 0.1 in the file name); the "r" sometimes present in the file name means that minor errors in the input data were corrected (revised); the "i" refers to cases in which all solid phosphates produced during the degradation of HLW are isolated from the model system after the HLW has fully degraded and the soluble products flushed out before the cases are continued and reaction with the SNF begins; and the "mm" refers to millimeters.

† This run attained too high an ionic strength to permit further continuation of the flushing scheme. Peak pH occurred at the end of the run, but was still increasing.

†† This run attained too high an ionic strength to permit further continuation of the flushing scheme. Peak pH occurred just before the end of the run, decreasing from 10.169 to 10.159 in about 165 years. The final pH is unreliable owing to the high ionic strength (about 3.1 m).

‡ Estimated from visual examination of abbreviated output files. Typical behavior is for pH to increase rapidly initially and then reach a quasi-steady state value. For the 5 and 10 mm/yr cases, only the first part of the run is considered. Later, pH decreases at a moderate rate and reaches other quasi-steady state values.

Table 7.2-2. Drip rate Summary of pH for the Case in which the SNF is Exposed to the High pH of the Degrading HLW Glass, Elevated CO_2 Partial Pressure.

Drip rate mm/yr	Average pH‡	Peak pH	Final pH	Time at run end, yrs	EQ6 run*
0.1†	9.6	9.7	9.7	618	UAIIb0:1rmm
1.0††	9.4	9.6	9.6	444	UAIIb1rmm
5.0	9.4	9.4	8.7	2830	UAIIb5rmm
10.0	9.2	9.2	8.8	1415	UAIIb10rmm

* See Ref. 5.30 for full details.

† This run attained too high an ionic strength to permit further continuation of the flushing scheme. Peak pH occurred at the end of the run, but was still increasing.

†† This sequence failed to converge for the second run. No adjustments were made to extend the sequence because it would provide no further insights to the nature of the reaction.

‡ Estimated from visual examination of condensed output files. Typical behavior is for pH to increase rapidly initially and then reach a quasi-steady state value. For the 5 and 10 mm/yr cases, only the first part of the run is considered. Later, pH decreases at a moderate rate and reaches other quasi-steady state values.

Analysis of the indicated EQ6 outputs indicates the production mostly of smectite clays, whereas the experiments show clay and other silicate minerals forming after a considerable (a few years) initial delay. This comparison shows that the modeled and experimental results (Ref. 5.8) differ only in respect to the model predicting immediate precipitation of secondary phases and the experiments finding a few years delay in the formation of very similar products. The differences in the products are small; in other words, the same elements are predicted to precipitate as found and in nearly the same proportions. In the time frames of interest to the present analysis, a delay of a few years in the beginning of precipitation, as compared to model results, is of no consequence. This result is found to be relatively independent of whether degradation of the SNF is taking place simultaneously or following the degradation of the HLW and its corrosion products. This accords with expectations, since the SNF degradation products are only a small fraction of the HLW.

The geochemical simulation predicts the precipitation of much of the B released from the glass as borax, which is well known to be moderately soluble in water. To evaluate the reliability of the simulation with respect to B, a separate case was run for just solid borax plus pure water for comparison with the measured solubilities for this mineral. This yielded a simulation of 21.6 g $Na_2B_4O_7$ per kg of water at an ionic strength of 9.7 and 25°C (Ref. 5.30). The measured solubility at this temperature is 31.5 g $Na_2B_4O_7$ per kg of water (Ref. 5.31, p. 1149). In view of the fact that the option used for calculation of activity coefficients is known to be only

approximate at ionic strengths approaching 1, and very unreliable at ionic strengths in excess of 2, this agreement is reasonable. In other words, it is reasonable to conclude that borax will indeed precipitate, but that it will redissolve and be flushed from the system about 50% sooner [(31.5-21.6)*100/21.6] than shown by the simulations.

In the presence of a large supply of CO_2, either from the atmosphere or from the rock gas, the highly alkaline solution generated by the degrading HLW is neutralized to a pH between 9 and about 10. The exact value depends on the rate of flushing by infiltration, being lower for faster infiltration owing to the lower pH of the J-13 water infiltrating into the waste package. Tables 7.2-1 and 7.2-2 indicate that the maximum at a drip rate of 5 mm/yr is in the range 9.4 to 9.9 (Runs UAIIa5rmm and UAIIb5rmm, Ref. 5.30), as compared to about 10 at a drip rate of 0.1 mm/yr (Runs UAIIa0:1rmm and UAIIb0:1rmm, Ref. 5.30). These conditions produce total dissolved carbonate concentrations of about 0.13 to 0.52 molal and 1.1 to 1.4 molal, respectively. These large concentrations of carbonate would be sufficient to dissolve all the uranium in MIT spent fuel as it degrades, if that SNF degradation took place while the HLW degradation process was generating a high pH. This possibility is described further in Section 7.2.2.1.

7.2.2 Degradation Products of Aluminum and Uranium Aluminide

The composition and disposition of the immediate degradation products of these materials depends on the degradation environment, particularly the pH, which is likely to be high, if the HLW glass is degrading simultaneously, and if the solution resulting from the dissolution of soluble HLW degradation products is in contact with the degrading surfaces of the SNF. The pH of the solution in contact with the degrading SNF surfaces is likely to be near neutral otherwise.

The initial corrosion product of aluminum metal in water is typically an alumina gel (Ref. 5.32, p. 4). In the course of sufficient time this amorphous highly hydrous material crystallizes to the minerals bayerite or gibbsite. These observations agree with those of Busenberg (Ref. 5.33), who observed experimentally in tests lasting up to 400 hours that alkali feldspars first degrade to a gelatinous alumina layer, followed by crystallization to gibbsite and later to kaolinite in presence of the silica released from the feldspar. These results lead to the conclusion that aluminum in the presence of J-13 water, which is high in silica, will produce crystalline hydroxides or oxides of aluminum or some clay mineral, as is appropriate to the chemistry of the system. Accordingly, the computer simulations used in the analyses in this report allow the aluminum metal to produce the equilibrium products in keeping with the thermodynamic data. The computer simulations show that initially most of the aluminum degrades to a smectite clay, i.e., it combines with silica and other components of the water with a small proportion of diaspore (AlOOH).

A necessary input to the modeling process is the degradation (corrosion) rate of aluminum. Whereas the rate of corrosion of aluminum under the conditions of interest seems not to be well known, it will be fast compared to rates of corrosion of other materials in the waste package. Howell (Ref. 5.5) reports tests that show penetration of aluminum clad spent fuel in 45 days. Cook, et al. (cited in Ref. 5.6) report corrosion of aluminum as a function of the concentration of nitric acid; at 0% acid the rate is shown as 1 mm/yr (see Section 4.1.1.2 for the measured data). Initially for the present analyses, the latter rate was chosen, but the simulations showed complete degradation in only a few weeks. Because this seemed unreasonably fast, the rate was adjusted to provide complete corrosion in 10 years. This is still very short compared to the time frames of interest.

No corrosion rates for the uranium aluminide were found. In the absence of such information and in keeping with thermodynamic stabilities it was assumed that the aluminide would corrode at a rate resembling that for aluminum metal (Assumption 4.3.22). As for the metal, the rate was adjusted to result in complete degradation in about 10 years.

7.2.2.1 SNF Degradation in a High pH Environment

The modeling results indicate that the uranium for this case initially mostly precipitates as the mineral soddyite, $(UO_2)_2SiO_4 \cdot 2\ H_2O$. At high pH the uranium subsequently dissolves as a uranyl carbonate complex and is flushed from the waste package by water flowing through the package (if the package bottom is breached) or flowing across the top surface of ponding water (which flowpath is mixed with the rest of the pond in the waste package, or in the DOE SNF canister containing the SNF). This flushing is at a volumetric rate equal to the inputed inflow rate (the product of the drip rate multiplied by the horizontal cross section area). For an drip rate of 5 mm/yr, cases UAlIa5rmm, UAlIIa5rmm , and UAlIIIa5rmm (Ref. 5.30) give the simulated concentrations of species in solution and the various solids which precipitate. A summary of the estimated time history of ^{235}U (from the SNF), ^{238}U (from the HLW), and boron (present in the HLW and borated steel), the most neutronically active species present in the waste forms is given in Table 7.2-3.

Table 7.2-3. Time History for Simultaneous Degradation of SNF and HLW (Initially High pH Environment)
(Computer Runs UAIIa5rmm, UAIIIa5rmm, and UAIIIIa5rmm, Ref. 5.30)*

Time (yrs)	pH	Total U in solution, kg	^{235}U in solution, kg	Total U in WP, kg	^{235}U in WP, kg	Boron in solution, kg	Boron total in WP, kg
0		Trace	0	162	35.5	Trace	221
12.5	9.2	2.3	2.3	162	35.3	2.1	221
310	9.2	27.6	14.3	122	14.3	3.6	210
1001	9.9	13.5	3.38	34.2	3.4	7.3	177
1207	9.9	12.3	2.69	12.3	2.7	6.7	166
1999	8.8	0.03	5.6E-03	2.6E-02	5.6E-03	6.8	125
2996	8.8	1.1E-05	2.4E-06	1.1E-05	2.4E-06	7.2	67
4008	8.8	4.3E-09	9.4E-10	4.3E-09	9.4E-10	6.3	7.4
5006	7.8	1.9E-12	4.2E-13	1.9E-12	4.2E-13	3.4E-03	3.4E-03
6003	7.6	8.6E-16	1.9E-16	8.6E-16	1.9E-16	3.9E-04	3.9E-04

* For consistency, the data are taken from the output files at times close to even thousands of years and at a few times of particular interest. At 10 years, the uranium aluminide fuel has entirely degraded, followed by the first flushing operation at 12.5 years (3.9E+08 sec). Most of the uranium released from the waste initially precipitates as soddyite, which has redissolved by 310 years. The HLW glass is fully degraded by 1207 years. Borax simulated to precipitate very early in the runs is completely redissolved at 3992 years. The simulation stopped at 6869 years and was not readjusted to continue. To run EQ3/6, the quantities of materials must be normalized to 1 kg of water initially; because the waste package contains about 2917 kg of water, the values in the output files are multiplied by this factor to obtain the numbers entered into the table. During the simulation, the volume of water in the package was gradually increased by 10% and a corresponding amount of solution removed all at once every 12.5 years (3.9E+08 seconds) for a total of 555 flushing operations.

The reduction in concentrations of U and B with time is due to the flushing action of the infiltrating water. Continuing release of B from borated steel maintains its concentration well above that in J-13 water to the end of this simulation, eventually reaching a quasi-steady state.

The following observations on these data are of interest. There is an initial rise of pH from a starting value of 8.50 to 9.19 in 10 years. This simulation was started with water initially adjusted to achieve agreement between the chemical analyses of J-13 water and the thermodynamic data, as described in Ref. 5.28, p. 74ff, with a further subsequent adjustment to the normal atmospheric partial pressure of CO_2. This last adjustment results in a loss of CO_2 from the solution and a rise in pH. The time of 10 years is the simulated time for all of the Al metal and uranium aluminide to have corroded. The U concentration at this time was simulated to be about 735 ppm. This amounts to about 6% of the total amount of the ^{235}U by weight, the rest being present as the mineral soddyite. About 1% of the original inventory of ^{235}U was simulated to have been flushed out of the package at this time. The flushing action results in the removal of sufficient uranium to dissolve all the soddyite at about 310 years. The simulation shows that at about 1200 years all of the HLW glass has degraded, the pH has risen to about 9.9, and about 47% of the original U inventory has been flushed out. All of the uranium solids are simulated to have dissolved, which means that the remaining 53% (13 kg for 2.9 m^3 of water having a U concentration of 4460 ppm) of the original inventory would all be in solution. At a slower infiltration, rate less uranium will be flushed out and perhaps the U concentration could rise to about twice this value, or about 10,000 ppm. At this time, the simulated concentration of B in solution, which arises primarily from degradation of the HLW, is about 2100 ppm. This concentration of U in the presence of the B is not expected to pose any criticality problem. Therefore, while this configuration is possible, it does not impose any requirements on the design, as contrasted with some of the configurations in which the SNF degrades in a neutral pH environment, as described in the following sections.

7.2.2.2 SNF Degradation in a Neutral pH Environment

Uranium aluminide was assumed to degrade at the same rate and in essentially the same manner as described in Section 7.2.2. In the present case, the U in the fuel again alters to soddyite, $(UO_2)_2SiO_4 \cdot 2\ H_2O$, but nearly all of the U remains insoluble in this or other minerals throughout the remaining course of the modeling. This case is based on the assumption (Assumption 4.3.23) that, following breach of the outer barriers, the HLW canister will breach sufficiently long before the DOE SNF canister containing the DOE spent fuel breaches, that all the HLW will have degraded and the highly alkaline resultant solution will have been flushed out and replaced by essentially unmodified J-13 water. The assumption is conservative because the pH will be close to neutral and the U will be retained within the degraded DOE SNF canister. See also Sections 7.3.2.1.1, 7.3.2.1.2, and 7.3.2.1.3.

A corollary to this assumption is that the time history of the HLW degradation (such as that shown in Table 7.2-2) will have no effect on the degradation of the SNF. Of particular

importance in this regard are the clayey solids with which the fissile uranium degradation products from the SNF can be mixed. In such a case, the water bound to the clay could provide sufficient moderator for a criticality.

In accordance with Assumption 4.3.5, the solid products of the glass degradation were kept in the model, and the water composition present at the time that the highly alkaline solution would be flushed out and the pH brought back to about 7.6 was used for further reaction. Because the code (EQ6) models everything in the reactive system simultaneously, retention of the degradation products in the model means that a change in one part of the degrading DOE SNF canister, such as a change in pH next to corroding steel, will quickly propagate to all parts of the canister and possibly dissolve some constituent, such as phosphate, from the clayey mass. This could in turn affect other aspects of the model, such as immobilizing Gd. Thereby, to some degree, the retained solids and water composition will influence the course of the future chemical evolution of the system. In fact models, notably case UAlIIIc0:1mm (Ref. 5.30), run for this scenario showed a substantial effect in respect to immobilization of the Gd attributable primarily to release of phosphate from the fluorapatite, Ca_5FPO_4, simulated to form as a part of the clayey mass during the degradation of the HLW. Specifically, in this case virtually all of the Gd is retained as a solid phosphate, the phosphate having been derived evidently from dissolution of a small proportion of the apatite in the solids produced earlier (see Table 7.2-4 and Figure 7.2-1). The various peaks in the concentrations in the time span from about 30,000 to 70,000 years arise from changes in acid production from Cr oxidation and other pH changes related to the exhaustion (complete degradation) of some of the metals.

Table 7.2-4. Calculated History for Case in Which All Solids from Glass Degradation Allowed to Continue to React with All Waste Package Contents, Including SNF Together with Gd_2O_3 Absorber, After Flushing out of Highly Alkaline Solution

Data extracted from file UAIIIIc0:1rmm				
Time, yrs	pH	Gd, ppm * 1E04	Pu, ppm * 1E05	U, ppm * 1E03
5.755E+03	7.4576	0		6.26E+00
5.758E+03	7.4324	1.08E-04		5.99E+02
5.760E+03	7.2715	1.05E-04		2.51E+02
7.863E+03	7.1814	8.55E-01	3.08E-02	9.44E+01
8.498E+03	7.1723	8.92E-01	3.04E-02	8.36E+01
8.956E+03	7.1404	1.13E+00	3.01E-02	6.02E+01
1.151E+04	7.0168	2.40E+00	3.21E-02	2.14E+01
1.233E+04	6.9767	3.12E+00	3.35E-02	1.59E+01
1.297E+04	6.954	2.34E+00	3.44E-02	1.45E+01
1.589E+04	6.8823	5.24E+00	3.78E-02	8.95E+00
1.953E+04	6.8306	1.06E+01	4.08E-02	6.79E+00
2.172E+04	6.8175	1.32E+01	4.16E-02	6.46E+00
2.375E+04	6.8176	2.17E+00	4.16E-02	6.61E+00
2.438E+04	6.8203	1.39E-02	9.84E-02	7.07E+00
2.501E+04	6.8244	1.52E-02	7.83E-02	7.25E+00
3.669E+04	6.7949	1.04E-02	4.08E-01	8.50E+00
4.101E+04	6.8453	3.45E-03	6.30E+01	1.37E+01
4.838E+04	6.8029	6.47E-03	2.07E+00	1.23E+01
5.046E+04	8.8184	2.87E-02	4.40E-02	1.11E+01
5.112E+04	6.8225	9.86E+00	4.07E-02	1.09E+01
5.569E+04	6.841	1.85E+01	3.92E-02	1.06E+01
6.078E+04	6.862	2.02E+01	3.75E-02	1.05E+01
7.474E+04	7.1263	4.01E+00	2.46E-02	1.69E+01
9.161E+04	7.2077	3.07E+00	2.24E-02	2.06E+01
1.422E+05	7.1978	3.93E+00	2.25E-02	1.93E+01

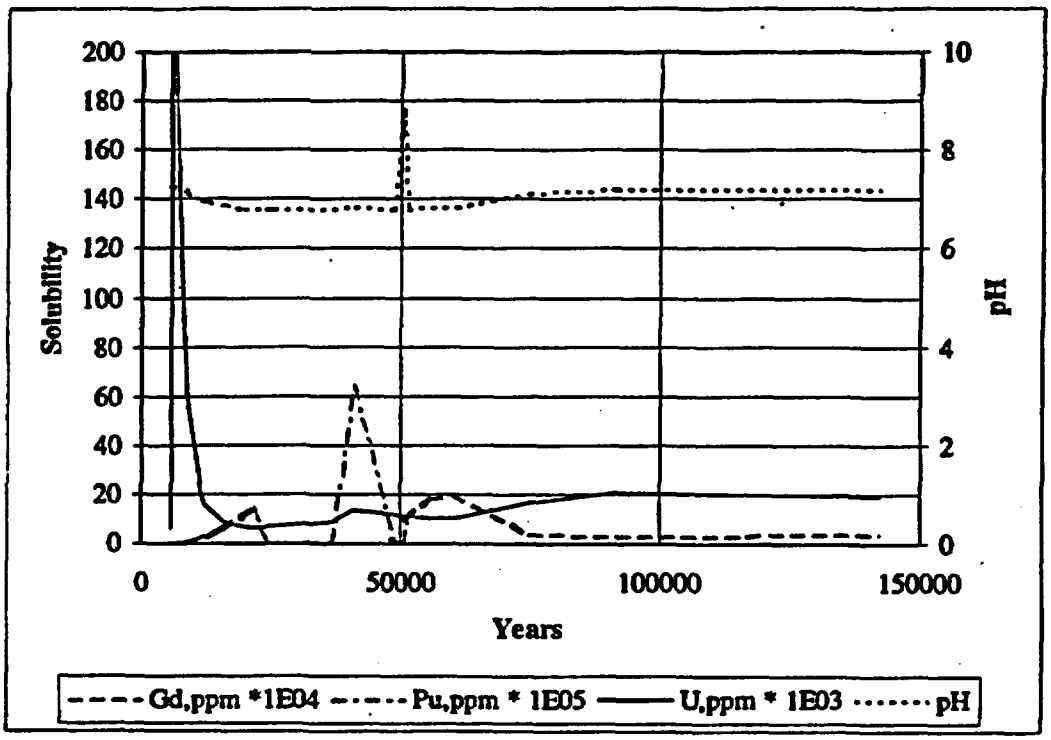

Figure 7.2-1. Plot of Case in Which All Solids from Glass Degradation Allowed to Continue to React with All Waste Package Contents, Including SNF Together with Gd_2O_3 Absorber, After Flushing out of Highly Alkaline Solution

Under a different scenario (Assumption 4.3.6), the clayey solids may have become sufficiently isolated from the DOE SNF canister that there is no or minimal chemical interaction and that the water is nearly identical to unaffected J-13 water. Because of the effect of residual phosphate on Gd immobilization, as noted above (case UAIIIc0:1mm, Ref. 5.30), in this second scenario (case UAIIIci0:1mm, Ref. 5.30), all phosphate solids were removed from the clayey mass, and the phosphate concentration reset to the value in J-13 water. In this case, the great majority of the Gd was simulated to be removed from the waste package (see Tables 7.2-5, 7.3-2, and Figure 7.2-2). In the figure, the peak in the Gd aqueous concentration results from the increasing solubility of the Gd solid first formed, $GdOHCO_3$, as the pH decreases, until the time at which all of this solid has dissolved. Thereafter the Gd is flushed out and its concentration decreases. The

U peak at about 40,000 years arises from complex interrelationships among aqueous complexes of uranyl ion with carbonate and hydroxide ions, whose concentrations are changing.

Table 7.2-5. Calculated History for Case in Which All Solids from Glass Degradation Isolated from All Other Waste Package Contents, Including SNF Together with Gd_2O_3 Absorber, After Flushing out of Highly Alkaline Solution

Data extracted from file UAIIIIci0:1mm				
Time, yrs	pH	Gd, ppm * 1E04	Pu, ppm * 1E08	U, ppm * 1E04
5.755E+03	7.7523	2.25E-14	3.10E+01	2.07E-08
5.755E+03	7.7522	3.10E-03	3.10E+01	1.04E+03
5.755E+03	7.6068	1.61E-01	2.23E+01	3.54E+02
6.401E+03	6.912	1.11E+00	3.21E+01	3.55E+01
7.784E+03	6.7365	3.84E+00	4.46E+01	2.77E+01
1.224E+04	6.6393	1.06E+01	5.58E+01	2.94E+01
1.516E+04	6.6125	1.40E+01	5.93E+01	2.92E+01
2.245E+04	6.6005	1.68E+01	6.12E+01	3.03E+01
2.757E+04	6.6112	1.62E+01	6.01E+01	3.19E+01
3.121E+04	6.6146	1.60E+01	5.98E+01	3.28E+01
3.414E+04	6.6061	1.69E+01	6.07E+01	3.33E+00
3.633E+04	6.5303	2.73E+01	7.03E+01	2.93E+01
3.923E+04	6.3373	9.42E+01	1.04E+02	2.47E+01
4.068E+04	6.281	1.35E+02	1.18E+02	2.47E+02
4.361E+04	6.2134	2.10E+02	1.37E+02	2.55E+01
4.723E+04	6.1715	2.70E+02	1.50E+02	3.48E+01
5.240E+04	5.9749	7.71E+02	2.28E+02	3.50E+01
5.604E+04	5.8989	1.13E+03	2.67E+02	3.56E+01
5.673E+04	5.889	1.19E+03	2.73E+02	3.57E+01
5.823E+04	5.8645	9.40E+02	2.89E+02	3.69E+01
6.034E+04	5.8402	6.80E+02	3.07E+02	3.84E+01
6.338E+04	5.8267	4.26E+02	3.08E+02	3.78E+01
6.412E+04	5.8231	3.80E+02	3.09E+02	3.76E+01

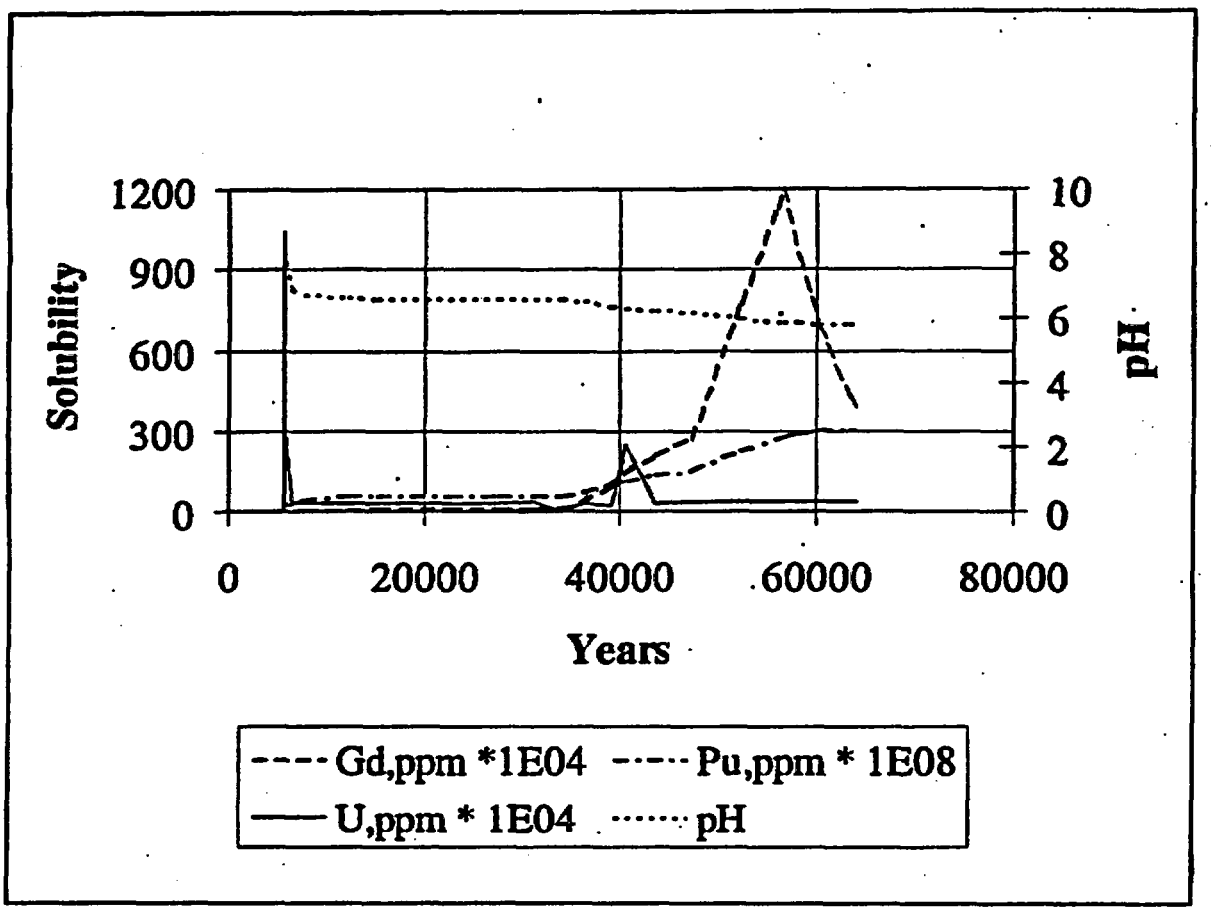

Figure 7.2-2. Plot of Case in Which All Solids from Glass Degradation Isolated from All Other Waste Package Contents, Including SNF Together with Gd_2O_3 Absorber, After Flushing out of Highly Alkaline Solution

Runs UAIIc5mm (Ref. 5.30) modeled the degradation of the fuel starting with J-13 water and in the absence of the HLW. Comparison of the solids simulated to be produced during the degradation of the HLW and the subsequent flushing of the alkaline solution (runs UAIIIb5mm and UAIIc5mm) run with the modification of these solids simulated during continuations of the modeling (runs UAIIIb5mm, UAIIVb5mm, UAIIIe0:1mm, UAIIIc0:1mm, UAIIIci0:1mm, and UAIIId0:1mm; Ref. 5.30) shows the changes to be minimal, except for the cases in which all phosphate solids have been removed from the clayey material. In the last cases, the significant effect is for Gd solids only.

7.2.3 Degradation Products of Uranium Silicide

The Oak Ridge Research reactor uses uranium silicide as the nuclear fuel. No corrosion rates for the uranium silicide are available in the literature. In the absence of such information, and in keeping with thermodynamic stabilities, it was assumed that the silicide would corrode at a rate approximating that for aluminum metal (Assumption 4.3.7). The uranium would react in a similar manner to uranium released from the uranium aluminide, specifically to form soddyite or some other uranyl silicate and, therefore, effectively was modeled by the simulations for that compound. The silicon would oxidize to the tetravalent state and largely precipitate as insoluble silica minerals, such as quartz or chalcedony, and silicates. The amount of silicon in the fuel is small compared to the silica already in the system, arising from the HLW glass and from the rather high concentration in the J-13 water. Thus, in this case also the relevant scenario was effectively bounded by the simulations for the uranium aluminide, except for the mass of uranium compared to other components. Consequently, no further modeling was required for this fuel and none was performed.

7.3 Evolution/Removal of Reaction Products and Chemical Configurations Relevant to Criticality

The important issue then devolves to whether or not the neutron absorber, B or Gd, will remain associated with the fissile material. This issue was studied through the model simulations described in the following subsections. The neutron absorbers evaluated with respect to this potential separation are boron and gadolinium.

7.3.1 Worst Case Removal of Boron

Initial modeling cases dealt with the use of B stainless steel as a component of the DOE fuel canisters. Modeling of this case (reaction of an uranium aluminide package with the solution remaining after flushing of the initially alkaline solution) indicated that the boron was flushed from the package after it was released from the borated steel (e.g., run UAlIIIb5mm, Ref. 5.30; runs UAlIb5mm and runs UAlIIb5mm model the degradation and flushing of the HLW, Ref. 5.30). Table 7.3-1 gives the time history of the results for flushing of B released from the borated steel, as well as U released from the fuel. To highlight the evolution of the borated stainless steel degradation process, the start time for this case, 5755 years is taken to be the time of water penetration of the DOE SNF canister, which is also the starting time for corrosion of the borated stainless steel in the canister basket.

Table 7.3-1. Time History of Boron Concentration in a Codisposal Waste Package Relying on B Stainless Steel for Criticality Control*

Time, yrs	pH	Uranium in solution, ppm	Uranium total in WP, kg	Boron in solution, ppm	Boron total in WP, kg
5755	7.75	2.1E-12	35.5	1.4E-01	1.37
5813	7.12	5.6E-03	35.5	8.38	1.37
6531	6.9	3.2E-03	35.5	22.5	1.02

* The initial time corresponds to that at which the pH was simulated to have returned to approximately the original value, run UAIIIb5mm (Ref. 5.30). At that time the concentrations of U and B are very low owing to the flushing action. The two following entries are for times immediately following additional flushing operations, run UAIIIb5mm (Ref. 5.30).

It should be noted that the amount of boron remaining in the last column, last line, 1.02 kg is approximately equal to that given by a straight line decline from the initial value at 5755 years to zero approximately 2500 years later (0.93 kg). This table also shows that after the source of an element in the waste package has been degraded, or its solid degradation products have been dissolved, the concentration of elements being released from the respective solids declines rapidly. Examples include the decrease in U after the initially formed soddyite has dissolved and the decrease in B after the borax has gone back into solution. Therefore, it is clear that the concentration of B in the waste package will decrease rapidly following the complete degradation of the borated steel at about 2500 years after breach of the DOE SNF canister or about 7000 years after breach of the waste package. This rapid decline of the boron concentration with time shows that the B stainless steel plates are not a completely effective criticality control technique, and that it will be necessary to evaluate less soluble neutron absorbers.

7.3.2 Worst Case Removal of Gadolinium

The removal rate of gadolinium depends on its solubility, which in turn depends strongly on the pH and on certain ionic species which affect the solubility, particularly phosphate, fluoride, and carbonate. Over the pH range of interest the pH strongly influences the concentrations of the free phosphate, $PO_4^{=}$, and carbonate, $CO_3^{=}$, i.e., phosphate or carbonate not bound to hydrogen or other ions as in HPO_4^{-} and HCO_3^{-}. It should be borne in mind that the phosphate concentration in J-13 water, or, more to the point, in water infiltrating through Yucca Mountain and entering the waste package, is small and uncertain. The same uncertainty applies to the analyses for fluoride in this water; fluoride has possible relevance because of interactive effects among Gd fluoride and phosphate chemical species, both solid and aqueous. To study this implication,

several computer models were constructed to investigate the behavior of systems in which borated steel was replaced by carbon steel and either gadolinium oxide or phosphate. In the Gd phosphate case the J-13 water composition was modified by removing all phosphorous both from the composition of water and of the metals that had not yet corroded, some of which contain small amounts of this element. In another test with Gd oxide the phosphate in the water was kept, but the fluoride was removed. Because the phosphates become more soluble with decreasing pH, the parameters for these cases were chosen (from within the range of physical possibility) to simulate the worst case (highest solubility of Gd) by minimizing the pH. Specifically, this meant, in view of the potential production of acid from oxidation of Cr in the B stainless steels to chromate, a low drip rate. A low rate will minimize the flushing out of any acid produced. Similarly, a high partial pressure of CO_2 will reduce the pH.

7.3.2.1 Gadolinium Added as Gd_2O_3

The simplest form for adding Gd is Gd_2O_3. However, this form must still be evaluated with respect to long term Gd solubility. The EQ6 analyses described in this section show that, if the phosphate present in the clayey material and associated water at the time that the highly alkaline solution is flushed away, the P released as phosphate from the corroding steel will limit the amount of Gd that dissolves and assures that about 20% (225 g) of the Gd will remain in the waste package after 60,000 years. This conclusion is relatively independent of the drip rate. See Tables 7.2-4, 7.3-2, and Figure 7.2-1.

Table 7.3-2. Time History Gd Concentration in a Codisposal Waste Package Relying on Gd_2O_3 for Criticality Control (Run UAIIIIc0:1mm, Ref. 5.30)

Time, yrs	pH	Gd in solution, pkg, g	Gd_2O_3 mol/kg H_2O	Gd in $GdOHCO_3$ mol/kg H_2O	Gd in $GdPO_4.H_2O$ mol/kg H_2O	Gd in solids, g/pkg	Total Gd in pkg, g
5755	7.7523	6.49E-15	1.11E-03	0	0	1022	1022
5758	7.6068	4.69E-02	1.10E-03	1.68E-05	4.80E-06	1022	1022
5766	7.2042	8.72E-02	9.98E-04	1.80E-04	5.14E-05	1022	1022
5851	7.1149	1.20E-01	0.00E+00	1.74E-03	4.93E-04	1022	1022
6401	6.9120	3.11E-01	0	1.73E-03	4.93E-04	1022	1022
7080	6.8013	6.56E-01	0	1.73E-03	4.93E-04	1022	1022
11507	6.6502	2.77E+00	0	1.73E-03	4.93E-04	1018	1021
15149	6.6125	4.07E+00	0	1.72E-03	4.93E-04	1014	1018
19535	6.5998	5.37E+00	0	1.71E-03	4.93E-04	1010	1016
25372	6.6055	4.85E+00	0	1.70E-03	4.93E-04	1006	1010
30390	6.6197	4.51E+00	0	1.69E-03	4.93E-04	1002	1007
34825	6.6067	4.92E+00	0	1.69E-03	4.93E-04	999	1004
39973	6.3066	3.35E+01	0	1.59E-03	4.93E-04	955	988
45010	6.2012	6.61E+01	0	1.42E-03	4.93E-04	877	943
50185	6.0452	1.55E+02	0	1.04E-03	4.93E-04	701	857
55305	5.9108	3.11E+02	0	2.47E-04	4.93E-04	339	651
56728	5.8890	3.46E+02	0	0	4.93E-04	226	572
59713	5.8461	2.19E+02	0	0	4.93E-04	226	445
61903	5.8336	1.56E+02	0	0	4.93E-04	226	382
64120	5.8231	1.11E+02	0	0	4.93E-04	226	337

7.3.2.1.1 Gadolinium Loss when Infiltrating Water has the Same Concentration of Phosphate as J-13 Water

Two cases were examined in which the infiltrating water had the same concentration of phosphate as in J-13 water. In both cases the model was set up such that the DOE SNF canister would breach at the time that the initially highly alkaline solution from the HLW had been flushed out. Gd_2O_3 and A516 carbon steel were added in place of borated steel, and the drip rate set at 0.1mm/yr. For the first of these cases (Run UAIIIIc0:1rnm, Ref. 5.30), when the DOE SNF canister was breached, the water composition simulated to be present was kept unchanged. Also, all the solids present were kept and allowed to react with all other components of the waste package (Assumption 4.3.5). These solids included the precipitated solids present in the clayey mass resulting from degradation of the HLW glass and from the partial degradation of the metals.

In the second case (Run UAlIIIci0:1mm, Ref. 5.30) all the precipitated solids were removed from the clayey mass, on the premise that these solids were sufficiently isolated physically from the DOE SNF canister that chemical interaction would be so limited as to be negligible (Assumption 4.3.6). Also, the concentration of phosphate in the residual water was reduced to that present in J-13 water. In all of these cases the phosphorous content of the A516 steel was kept.

For the first case (Run UAlIIIc0:1rmm), Table 7.2-4 and Figure 7.2-1 show the course of the changing solubilities of U, Gd, and Pu, together with pH, for times modeled in this run up to nearly 150,000 years. This plot starts just after the flushing out of the soluble products of the HLW, at about 6000 years after breaching of the HLW canisters. Initially, the model shows a sharp increase over about 8 years in the U concentration from a very low value (0.006 ppm) up to about 0.25 ppm as the uranium aluminide is degrading. By about 11 years, following the complete degradation of the fuel, the concentration has decreased to less than 0.1 ppm and remains at comparably low values for the rest of the simulation. The pH has simultaneously decreased by a few tenths of a pH unit. The irregularities in the plot primarily reflect times when one or another of the materials in the waste package, e.g., carbon steel, become completely corroded (See Section 7.2.2.2). The simulation indicates that Gd_2O_3 should react with phosphate in the J-13 water and the carbon steeel to form an insoluble Gd phosphate. The rare earth oxides are modestly soluble in water (Ref. 5.39, pp. B-85 to B-178; Ref. 5.40, pp. 14-15) which means that enough should readily enter the solution to react with the dissolved phosphate and precipitate as the phosphate monohydrate. These phosphates form rather readily (Ref. 5.40 and 5.41). In fact the anhydrous phosphate, monazite, may also form in the presence of the phosphate and gadolinium present at the concentrations likely to exist in the repository. Monazite persists in nature for the very long periods of time required to weather enclosing igneous and metamorphic rocks, erosion of the weathered rock, stream transport to the ocean, and concentration into beach placers, from which it sometimes is mined for its content of rare earths (Ref. 5.42). Under the conditions simulated by the modeling (note that the previously formed solid phosphates were allowed to react freely with all other materials present and the residual phosphate concentration in the water at the time that the DOE SNF canister breached was much higher than in J-13 water) the pH did not fall below 6.8, and the resulting Gd loss from the waste package was only 0.034 g in 142,000 years.

In the second case (Run UAlIIIci0:1mm, Ref. 5.30), phosphate solids and phosphate in excess of that in J-13 water removed, the Gd_2O_3 first would alter to $GdOHCO_3$, which then slowly would partially alter to $GdPO{\cdot}H_2O$ (See Table 7.2-5 and Figure 7.2-2). The phosphate for this conversion comes from the corroding carbon steel, not from the water or other solid phosphates, and the limited amount of P in the steel limits the total amount of Gd that is retained. In other words the phosphate being added to the system by the infiltrating J-13 water and that released

from corrosion of the steel is insufficient to fix all the Gd as phosphate before a large share of the much more soluble hydroxycarbonate has dissolved and been flushed out. The remainder of the Gd, about 80%, is flushed from the package at the low drip rate of 0.1 mm/yr at 50,970 years following breach of the DOE SNF canister. The run modeled another 7380 years during which, per waste package, 2.0E-05 moles of $GdPO_4H_2O$ (0.3 mg of Gd) was simulated to dissolve, thereby being (at least mostly) washed away. At a higher drip rate more phosphate will enter the waste package in the J-13 water, but, because the phosphate concentration in this water is uncertain, the concentration might be no more than 1/10 as high as that used in the modeling. In other words, at an drip rate of 1 mm/yr, but 1/10 the phosphate concentration, the same result would be obtained. Even at 10 mm/yr, a very significant loss of Gd over similar time frames might occur, especially in view of the expectation that with more water, more $GdOHCO_3$ would dissolve and be flushed out per unit time. These results demonstrate that reliance on Gd placed in the canister as Gd_2O_3 is questionable.

7.3.2.1.2 Gadolinium Loss when Infiltrating Water Contains no Phosphate

Run UAIIIId0:1mm (detailed time history in maxgdlos.wk3, Ref. 5.30) included no phosphorous in any form in the waste package and none in the infiltrating J-13 water. Gd was included as Gd_2O_3. The run indicated that sometime after 10,000 years, pH would drop to nearly 6.2 and the corresponding increase in Gd solubility (due to the combined effects of all the ionic species considered in EQ6, but mostly represented by pH) would result in a Gd loss of 61 grams in 43,000 years. If such a low pH could be maintained during a higher drip rate, the Gd loss could be correspondingly higher. For example, if this same pH (6.2) could be maintained, by the oxidation of B stainless steel chromium to chromate, in an drip rate 100 times larger (10 mm/yr), the resulting Gd loss could be as large as 6 kg. In view of the uncertainty concerning phosphate concentration in the infiltrating water, this large potential loss of Gd demonstrates the need to assure that a sufficient supply of phosphate will be available. Such an alternative is discussed in Section 7.3.2.2.

7.3.2.2 Gadolinium Added as $GdPO_4$

Run UAIIIIe0:1mm (Ref. 5.30) examined the case for adding Gd phosphate instead of the oxide and a flow through of water at a rate of 0.1 mm/yr, with no phosphate in the infiltrating water. This was intended to test whether the phosphate was sufficiently soluble to be completely dissolved and flushed out of the system. At the end of a simulation for 71,000 years, almost no Gd had been removed. The ending concentrations were, in ppm: Gd: 0.2×10^{-4}; U: 0.54×10^{-2}; and pH 5.79. It should be noted that the Gd solubility is much lower than would be predicted from the carbonate solubility limit used previously, particularly for such a low pH (see Table 7.3-3).

Table 7.3-3. Time History Gd Concentration in a Codisposal Waste Package Relying on $GdPO_4$ for Criticality Control (Run UAlIIIe0:1mm, Ref. 5.30)

Time, yrs	pH	Gd in solution, pkg, g	Reactant $GdPO_4.H2O$ mol/kg H_2O	Solid solution $GdPO_4.H2O$ mol/kg H_2O	Gd in solids, g/pkg	Total Gd in pkg, g
5755	7.7523	8.21E-16	2.23E-03	9.99E-15	1022.260	1022.260
5758	7.6068	1.292E-06	2.22E-03	1.08E-05	1022.281	1022.281
5766	7.2045	1.439E-06	2.11E-03	1.16E-04	1022.269	1022.269
5851	7.1152	8.317E-08	1.11E-03	1.11E-03	1022.260	1022.260
6401	6.9123	1.637E-07	0	2.23E-03	1022.260	1022.260
9900	6.6386	0.0017365	0	2.23E-03	1022.260	1022.262
19535	6.5996	0.0186087	0	2.23E-03	1022.214	1022.233
30418	6.6189	0.0428827	0	2.23E-03	1022.168	1022.211
40219	6.2991	0.0167068	0	2.23E-03	1022.122	1022.139
50185	6.0334	0.0065472	0	2.23E-03	1022.122	1022.129
61903	5.8236	0.0010487	0	2.23E-03	1022.122	1022.123
69979	5.7894	8.479E-05	0	2.23E-03	1022.122	1022.122

7.3.3 Persistence of Rare Earth Phosphates in Nature

Natural occurrences of the rare earth phosphates, monazite and xenotime, which are widely distributed in small amounts in many rocks, indicates that $GdPO_4$, once formed, will not quickly be dissolved and transported in natural waters. This greatly bolsters confidence that this form of Gd, if added to a waste package, will persist for many thousands of years. The light rare earths are more concentrated in monazite and the heavy ones more so in xenotime. Both minerals survive for very long times during weathering and erosion as evidenced by their presence in river and beach sands, some reaching concentrations sufficient to serve as ores for the rare earth elements (Ref. 5.42, pp. 690-691 and 694-695). This is in keeping with their very low solubilities and their persistence as predicted by the modeling.

7.4 Configurations Having Separation Between Uranium and the Neutron Absorber

This section will summarize the scenarios and configurations likely to result in the separation of uranium from the neutron absorber material. The separations are with respect to the nominal waste package configuration having the following material locations:

- The neutron absorber iron is in the structural basket plates.

- The added neutron absorber, boron or gadolinium, is in plates (which may be B stainless steel or carbon steel, and which may be, or may not be, part of the structural basket).

- The uranium is uniformly distributed in the water in the DOE SNF canister. This is a worst-case representation of the most likely configuration in which the uranium aluminide particles adhere to the surfaces of the remaining basket material. At the maximum degree of hydration possible for the uranium aluminides, adherence could be equivalent to uniform distribution throughout the water, and it is shown in Ref. 5.38 that the homogenization throughout the water in the DOE SNF canister is more reactive, with respect to criticality, than is the configuration with the uranium in a narrow layer about the basket plates.

7.4.1 Separation Mechanisms

The separations between the uranium from the fuel and the neutron absorber placed in the basket of the DOE SNF canister for criticality control can arise from several mechanisms illustrated by the following:

- The uranium may become soluble and be removed from the waste package. This can only happen if the DOE SNF canister is breached while the HLW glass is degrading and causing a high pH, so that the uranium is sufficiently soluble that most of it is flushed out of the waste package by the action of the water which is causing the degradation of the HLW glass. The parameters of this case are summarized in Table 7.2-1. This case cannot lead to criticality within the waste package, and will, therefore, not be considered further in this study. It is however important for the consideration of the possibility of external criticality, and will be evaluated as part of that future study.

- The absorber may become soluble and be removed from the DOE SNF canister (and subsequently the waste package), leaving the uranium behind. This is particularly likely for boron once it is released by corrosion of its B stainless steel carrier matrix, but it is also possible for gadolinium if the pH becomes low and there is insufficient phosphate to precipitate the bulk of the gadolinium.

- The uranium (which is released by the rapid corrosion of the SNF matrix) can settle to the bottom of the waste package and collect on the lowest available surface, which may be the bottom of the canister for some of the particles, while most of the neutron absorber remains in the undegraded portion of the basket. The maximum amount of separation by this mechanism is discussed in Section 7.4.4.2. However, it is shown in Ref. 5.55 that the concentration of U available by this mechanism is insufficient for criticality.

- The uranium may remain distributed throughout the canister while some of the steel breaks from the basket plates (as cutouts caused by pitting corrosion perforating the periphery). This breaking steel could fall into the bottom of the canister together with its complement of gadolinium, thereby taking some of the gadolinium out of the region in which it is most effective in controlling criticality by absorbing neutrons.

The following subsections discuss the possible configurations in sufficient detail to provide input for the criticality evaluation of these configurations; these criticality evaluations are described in Ref. 5.55. The configurations resulting from the alternative neutron absorbers, boron and gadolinium, are treated in separate subsections, since they are not likely to be used together. Both alternatives rely on the additional criticality control support from the insoluble iron oxide resulting from the corrosion of basket material. This iron oxide criticality control is particularly effective when carbon steel is used as basket material, because carbon steel corrodes much faster than B stainless steel.

7.4.2 Evaluation of Differential Settling of Solid Particles of Different Densities

7.4.2.1 Calculations Based upon Mineral Engineering Practice

For a neutron absorber to be effective in preventing a criticality, it must remain intermixed with fissile material. The preceding sections have addressed the possibilities of separation of absorber from fissile material through chemical means. This section considers the potentiality of a physical separation.

The possibility of physical segregation of solids containing fissile nuclides from other sources was investigated by use of the principles employed by the minerals industry to achieve separations of valuable (ore) minerals from those of no commercial value (gangue). Of the numerous techniques that have been utilized, the only one that applies to the quiescent conditions that will be present within the repository is differential gravitational settling. Unfortunately, not all of the desired data for a full calculation of the potentiality for separation are known. Specifically, it would be desirable to calculate the settling rates of particles of different density, but this requires a knowledge of the viscosity of the medium. As the uranium aluminide degrades, it will initially produce an aluminous gel, as noted above in Section 7.2.2, which will have a very high, but unknown, viscosity. Later the viscosity of the more crystalline sediment would be required, which is likewise unknown, but surely even higher. Nevertheless, it is possible to utilize equations for hindered settling, which require only the average densities of the medium and its constituents to determine the size ratio of particles for equal settling rates (Ref. 5.43, pp. 186-198 and Ref. 5.44, pp. 336-342). (For these calculations the viscosity cancels out.) Specifically, the equation:

$$\frac{d_1}{d_2} = \frac{(\rho_2 - \rho_s)^{1/2}}{(\rho_1 - \rho_s)^{1/2}}$$

(where d_1 and d_2 refer to the diameter of particles of types 1 and 2, respectively; ρ_1 and ρ_2 refer to the densities of the particles, and ρ_s refers to the effective density of the slurry or suspension) gives the ratio of diameters for equal rates of settling of the particles (Ref. 5.43, p. 192, equation VIII.31; Ref. 5.44, p. 338, equation 9.9). Equation VIII.31 in Ref. 5.43 includes a parameter, m, which may vary between 0.5, for Stokes Law settling, to 1.0, for Newton's Law settling. Stokes Law applies well for settling of small particles, less than about 50 μm in diameter, and the Newton's Law to particles larger than about 0.5 cm, whose settling is controlled by turbulence produced by the settling itself. Whereas both the size and shape of the particles that will be produced are unknown, it seems certain that the sizes will be small, approaching the colloidal range, in view of the initial production of gelatinous alumina and generally fine grain size of individual particles in rust, and it is assumed that the shapes will be sufficiently similar that the shape effect will be small (Assumption 4.3.24). Consequently, the exponent was chosen as 0.5, as shown above. The equation assumes spherical particles.

Solids of interest in respect to differential settling within the DOE SNF canister, where it is most important to keep an absorber with the fissile material, are the degradation products gibbsite, $Al(OH)_3$, goethite, FeOOH, soddyite, $(UO_2)_2SiO_4 \cdot 2H_2O$, and rhabophane, $LnPO_4 \cdot H_2O$, or monazite, $LnPO_4$, where Ln refers to a mixture of the lanthanide (rare earth) elements. These have densities of 2.42, 4.26, 4.7, about 4.0, and about 5.25 g/cm^3, respectively (Ref. 5.45, pp. 236, 240, 568, 516, and 413 respectively). These were combined in the proportions that the products would be produced, as calculated from the initial inventories of uranium aluminide, aluminum metal, and steel in the canister (see Attachment IV), and with water, at a density of 1.0 g/cm^3, for volume fractions of water of 0.6 and 0.9 (Ref. 5.55) to obtain the average density of a suspension.

These data were used for calculating the diameter ratio for equal rates of settling of gibbsite compared to that of soddyite and for goethite compared to that of soddyite for the two different volume fractions of water. For each volume fraction two configurations were considered: one in which goethite was not mixed with the gibbsite and soddyite, and one in which it was. Details of the calculations are given in Attachment IV. At a water volume fraction of 0.6 with no admixed goethite, the diameter ratio for gibbsite versus soddyite is about 2, and at a volume fraction of 0.9 it is about 1.7. With admixed goethite and a volume fraction of 0.6, the diameter ratio for gibbsite versus soddyite is about 2.5 and for goethite versus soddyite is about 1.1; at a volume fraction of 0.9 these ratios are about 1.1 and about 1.07, respectively. The implications of these

results are that the soddyite would tend to settle faster than gibbsite, thereby producing a modest separation. However, this would occur early in the degradation and presumably the entire mass would collect on top of steel components of the basket structure. In such a case, the separation is of no importance to criticality because the fissile material would be adjacent to or mixed with the neutron absorber material. If B stainless steel is used to absorb neutrons, the mass containing the soddyite would settle directly on top of it. If Gd_2O_3 is added instead as the absorber, it would settle out somewhat faster, in view of its higher density, 7.4 g/cm^3 (Ref. 5.39, p. B-113) and thus lie on top of the steel basket structure mixed with or immediately below the soddyite. $GdPO_4$, density about 4.8 g/cm^3 (Ref. 5.45, pp. 413 and 679), if added, would also settle somewhat faster than the soddyite directly on the steel, and the rhabdophane, $GdPO_4 \cdot H_2O$ that would likely form from reaction with Gd_2O_3, density about 4 g/cm3 (Ref. 5.45, p. 516) would settle at about the same rate as the soddyite. Consequently, any separation that might occur between the degradation products of the aluminum and the fuel would be of no importance to criticality. As degradation of the DOE SNF canister continues with the corrosion of the steel, large quantities of iron oxides and hydroxides would be produced, but, as shown above, the potential for separation from fissile material is small. Moreover, any gadolinium present should remain admixed.

7.4.2.2 Analogy with Natural Placer Deposits

It is well known in nature than heavy minerals may to some degree become separated from lighter ones to form placer deposits. However, the degree of separation is not extreme in spite of the agitation and suspension in rivers and beaches responsible for the segregation. One might expect the greatest separation from very heavy minerals, such as gold, and much lighter common ones, such as quartz. The respective densities are 17 (Ref. 5.39, p. B-115) and 2.65 (Ref. 5.45, p. 504). Nevertheless, the percentage of gold in typical placers is very low. For example, in the famous placer deposits associated with the Mother Lode in California, values were only 30¢/cubic meter when gold was $20/troy oz. (Ref. 5.46, p. 276) which is only about 0.5 g/m^3. These deposits varied from 6 to 20 meters in depth, which says that the heavy mineral will not by itself settle to the bottom of the sediment. Using a density of gravel of about 2 g/cm^3, this amounts to only about 1/4 part per million. Even at $3/per ton (gold valued at $35/troy oz.), as cited for Klamath Mountain placers (Ref. 5.46, p. 277), the concentration is very low. Without stream or wave action to promote the differential settling of the gold the degree of concentration would be even less. Moreover, this degree of separation occurs in sands and gravels, not in fine grained materials, such as clays. Apparently, there are no known placer deposits for clay beds or their rock equivalent, shales. Thus, these analogies also argue that the probability of significant separation of the fine grained degradation products in the waste package as a consequence of gravitational settling is extremely low.

Examples of placer deposits rich in monazite include stream placers and flood plains in North and South Carolina (resource of 600,000 tons of rare-earth oxides), beach and river placers mostly along the Atlantic coast of Brazil (resource of 180,000 tons of rare-earth oxides), and beach placers in Australia (resource of 480,000 tons of rare-earth oxides) (Ref. 5.46, pp. 456-457). The deposits form slowly over great lengths of time as source rocks weather and erode and sand grains are washed and suspended repeatedly. Nevertheless, separation of the heavy minerals from lighter ones, such as quartz, is far from complete and further concentration is required before a product suitable for smelting is obtained. No placers in very fine grained sediments, such as clay, have apparently ever been discovered. .This implies that the differential settling required to produce a useful deposit does not occur when the grain size in the sedimenting solids is too fine. These observations indicate that, because there will be no agitation analogous to that required to produce placers and because the grain size of the particles will almost certainly be very fine, probably approaching colloidal sizes, the probability of gravitational separation of fissile and absorber materials within a waste package is extremely small.

7.4.3 Separation of B Absorber from U

This section relates to the use of boron as a criticality control material, for which purpose 1 - 2 kg of boron is added to the DOE SNF canister basket in the form of B stainless steel plates. It was shown in Ref. 5.38 that this quantity of boron was sufficient to prevent criticality as long as the basket remained intact. The corrosion resistant stainless steel is used as the boron carrier in order to keep the boron in place as long as possible; once the stainless steel corrodes, the highly soluble boron dissolves and is subsequently flushed from the DOE SNF canister and waste package. As explained in Section 7.2.2.1, the waste package initially has nearly 250 kg of boron in the HLW glass. Tables 7.2-3 and 7.3-1 show that a fairly likely scenario is for the boron from the degraded HLW glass to be dissolved, precipitated, re-dissolved, and removed from the waste package before 10,000 years. The boron added specifically for criticality control will be more effective than that occurring as part of the HLW glass, for two reasons:

1) the added boron is placed in the DOE SNF canister to be in close proximity to the enriched uranium where its neutron absorbing properties will be most effective, and

2) the B stainless steel will degrade much more slowly than does the HLW glass.

There is some possibility that some scenarios/configurations for aqueous degradation will avoid extensive corrosion of the borated steel; the calculation of a probability which might be associated with such a process is described in Section 7.4.3.1. In the meantime, the corrosion of

B stainless steel still poses the principal risk of criticality for the boron based criticality control methodology. The range of earliest times at which such a critical separation can occur is summarized in Section 7.4.3.1.

7.4.3.1 Degradation of the B Stainless Steel Basket

Calculations based on the assumed corrosion rate for B stainless steel, and summarized in Table 7.1-1, show that this criticality control material will be completely corroded away by 11,000 years, under aqueous attack. It is expected that most of the boron released from the corrosion of B stainless steel will be dissolved, because of the high solubility of boron, and this is verified by the EQ6 calculations summarized in Section 7.3.1. Because of this possible loss of criticality control material, the criticality control effectiveness of B stainless steel is questionable.

On the other hand, it is possible for the waste package to degrade in such a way that the B stainless steel in the DOE SNF canister is not contacted to a significant degree by circulating or flowing water, so that the corrosion rate of the B stainless steel is severely limited. Such a configuration is illustrated in Figure 7.4-1, which shows a degraded waste package in which the glass has degraded and formed a clayey mass filling most of the waste package, with the DOE SNF canister within the clayey mass at some unspecified distance (which may be zero) below the upper surface. As was shown in Table 7.1-1, the degradation of the HLW glass will occur in less than 2000 years following breach of the waste package, breach of the HLW canister, and initial exposure to water. However, all the canisters (HLW and codisposal) may not be contacted by water at once, and complete degradation to the configuration shown in Figure 7.4-1 may take considerably longer.

With respect to the removal of boron, the fraction of the time for which the DOE SNF canister will be contacted by water is of primary importance. To approximate the process by which water dripping on the waste package is converted to flow and circulation through the waste package, it is assumed that the primary direction of the water movement within the waste package is downward, so that probability of a dripping flow contacting a mass within the package will be equal to the fraction of the horizontal cross section area occupied by that mass (Assumption 4.3.13). For the DOE SNF canister this fraction is 0.29.

For any given waste package, the occurrence of a drip, and the location of that drip, might be independent of time, or might vary with time. In the latter case, the effect would be to convert the small probability of corrosion of B stainless steel (0.29) to a certainty, but over a longer period of time, which would be approximated by taking the nominal corrosion time of 11,000

years (following breach of the DOE SNF canister) given in Table 7.1-1, and dividing by 0.29 to get 38,000 years. Both viewpoints will be used for comparison of alternatives in Section 7.4.5.

An additional conservative aspect of this analysis is that it neglects other configurations which have even stronger prevention of water contacting the B stainless steel in the basket of the DOE SNF canister, for example, the configuration in which the clay covering the DOE SNF canister has insufficient permeability to permit any significant water flow over the B stainless steel.

7.4.3.2 Uranium Settled to the Bottom of the DOE SNF canister

As mentioned in Section 7.4.1, it is possible that the uranium aluminide particles will settle to the bottom of the waste package while much or most of the basket is still intact, thereby separating that uranium from the boron remaining in the basket. The quantitative analysis of this possibility is similar to that used for gadolinium as neutron absorber; further discussion of this configuration is deferred to Section 7.4.4.2.

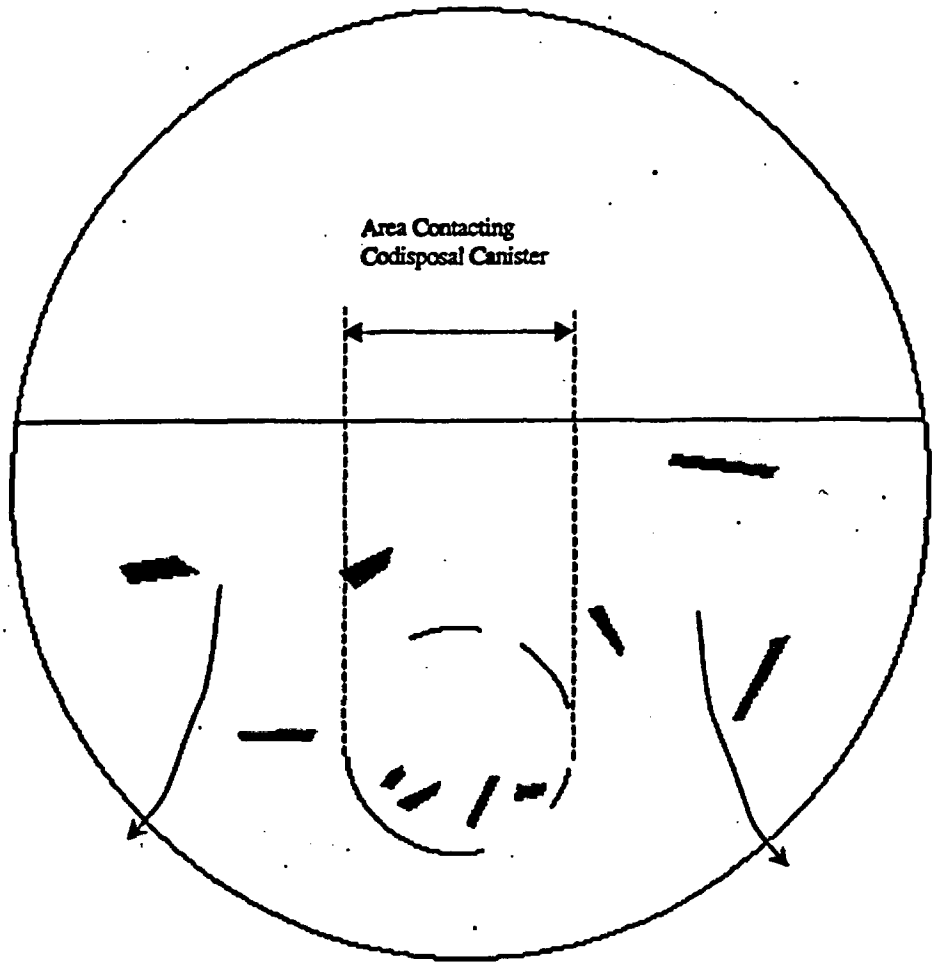

Figure 7.4-1. Boron Criticality Control: Likely Degraded Configuration Showing that Water Dripping into the Package may Bypass the DOE SNF Canister (or its Remnant), Thereby Retarding the Dissolution of the B Stainless Steel and the Removal of the Boron.

7.4.4 Separation of Gd Absorber from U

Unlike boron, gadolinium is basically insoluble, except for pH<6. Therefore, the corrosion resistant properties of stainless steel are not required and the benefits of carbon steel would make it the preferred alternative, not only for carrying the criticality control material (gadolinium), but also for the structural basket. The principal benefits of carbon steel in this regard are the following:

1) carbon steel has a significantly higher yield strength than stainless steel (260 MPa vs 172 Mpa, Refs. 5.53 and 5.54),

2) carbon steel will yield a more uniform spatial distribution of iron oxide, because its faster general corrosion rate will result in more iron oxide being released in the initial basket position, rather than after falling to the bottom in plates, as would stainless steel, and

3) the production rate of iron oxide from the oxidation of carbon steel more nearly corresponds to the release rate of the uranium aluminide from the SNF.

As with boron, the principal probability of criticality arises from the removal of gadolinium from the waste package due to solubility. The analysis of Section 7.3.2 shows that gadolinium is only soluble at low pH, and then only if there is a limited amount of phosphate present in the system. It is, therefore, useful to summarize the results in terms of the chemical form of the gadolinium used for criticality control.

7.4.4.1 Gadolinium as Gd_2O_3

The EQ6 simulations described in Section 7.3.2.1 show there is a possibility of low pH (as a result of complete oxidation of the chromium in stainless steel to chromate), and this low pH will be associated with a high solubility for gadolinium. In particular, Table 7.3-2 showed that the amount of gadolinium which is certain to be retained in the system is limited by the amount of phosphate present in the system when the gadolinium is released by the steel. Unless additional phosphate is added, the worst case gadolinium retention could be as low as 337 g. For this reason, the criticality control effectiveness of gadolinium can be said to be questionable.

However, configurations are possible in which the solution having pH lowered by the corroding stainless steel is not in direct contact with the Gd_2O_3 inside the DOE SNF canister. In such configurations the Gd will remain insoluble and not be lost from the waste package. Such a configuration is illustrated in Figure 7.4-2, which shows the stainless steel from the HLW

canisters degraded into small plates away from the likely locations of the uranium (which is most likely still in the DOE SNF canister or its remnant). In developing this simplified model it is assumed that the stainless steel of the DOE SNF canister will not contribute significantly to the acidification, since its corrosion will be primarily from the outside with the corrosion products carried away from the DOE SNF canister, rather than into it. (Assumption 4.3.14) It is further assumed that there will be no stainless steel in the basket because carbon steel is the preferable basket material when gadolinium (rather than boron) is the criticality control material, as was recommended in Section 7.4.4. (Assumption 4.3.16)

With the model described in the previous paragraph, this paragraph describes the method of estimating the conditional probability of criticality given that water is dripping into the waste package and that the water is accumulating in the clay formed from the HLW glass degradation products. The geometric model for this calculation is given in Figure 7.4-2. The probability of the solution from the degrading stainless steel contacting the Gd in the DOE SNF canister (given that water has dripped into, and collected in, the waste package) is the product of the probability that the water will directly contact the DOE SNF canister within the waste package (estimated as 0.29 in Section 7.4.1, above), multiplied by the probability that the clay above the DOE SNF canister (or its remnant) will contain a significant amount of corroding stainless steel. To estimate this latter probability it is assumed that:

1) the average height of the clay surface above the waste package bottom is uniformly distributed between the diameter of the DOE SNF canister and the diameter of the waste package, and

2) the top of the DOE SNF canister (or that of its remnant) is uniformly distributed between the diameter of the DOE SNF canister and the height of the clay surface.

It is further assumed that the probability of the clay above the DOE SNF canister having a significant amount of corroding steel, is approximated by the ratio of the average depth of the DOE SNF canister divided by the maximum depth (which is the waste package diameter minus the DOE SNF canister diameter). (Assumption 4.3.17) This gives the double integral

$$\frac{1}{D-d}\int_d^D dH \int_0^{H-d} \frac{h\,dh}{H-d}$$

where D is the diameter of the waste package and d is the diameter of the DOE SNF canister. This integral is normalized to (divided by) D-d, to give a value of 1/4(D-d)/D=0.19. Further

details of this integral are given in Attachment V. When this factor is multiplied by the 0.29 calculated earlier, the resulting conditional probability (of this process which is necessary for criticality to occur) given the increased dripping on the individual waste package is 0.055.

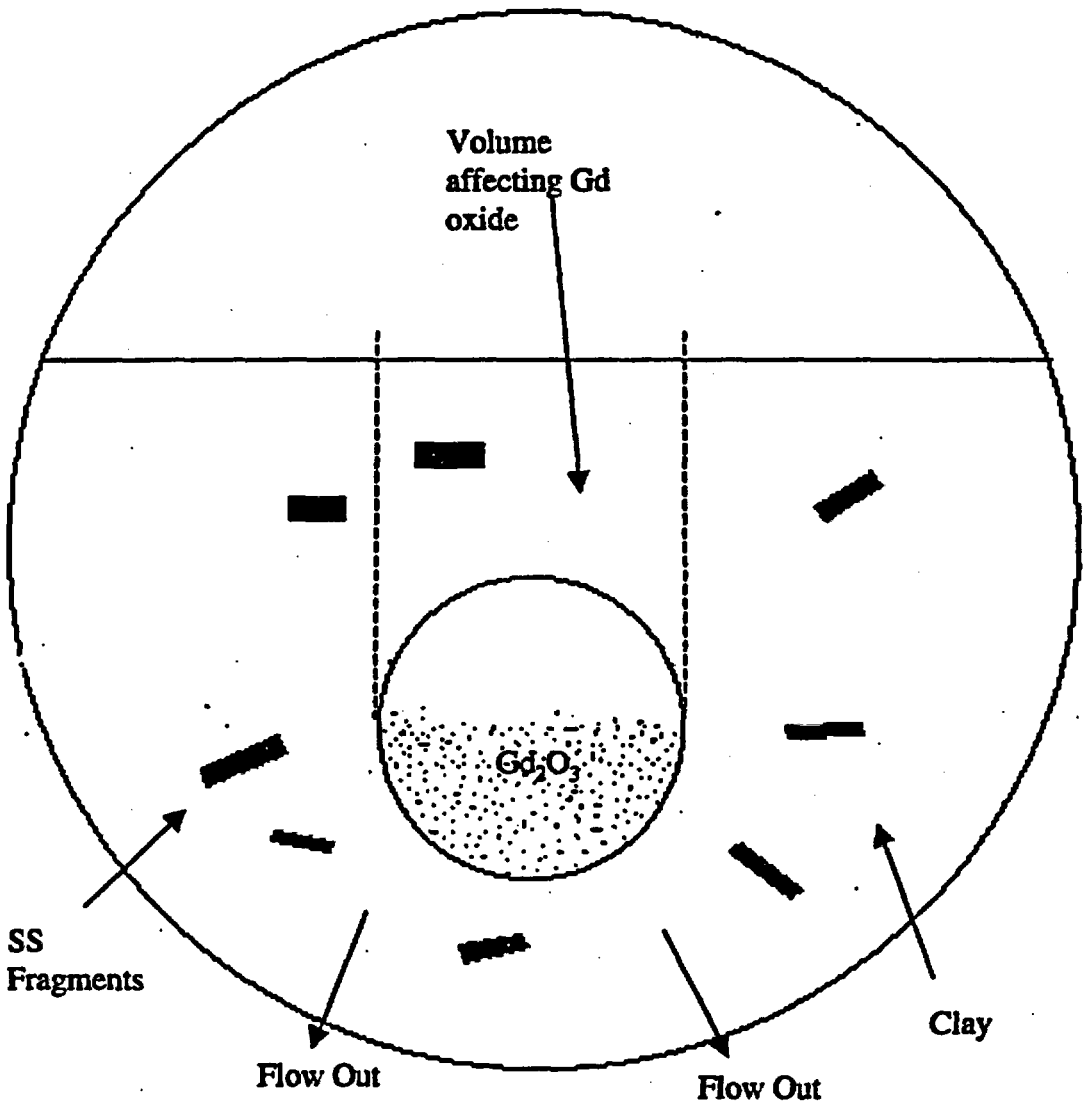

Figure 7.4-2. Gd_2O_3 Likely Configuration Which Will Keep Low pH Water Away from the Fissile Material in the DOE SNF Canister (or its Remnants)

As with the analysis of boron removal in Section 7.4.3.1, above, the occurrence of a drip, and the location of that drip, might be independent of time, or might vary with time. In the latter case, the effect would be to convert the small probability of contacting the DOE SNF canister (0.29) to a certainty, but over a longer period of time, which would be approximated by taking the nominal time to lose most of the gadolinium, 60,000 years following breach of the DOE SNF canister given in Table 7.3-2, and dividing by 210,000 years.

7.4.4.2 Gadolinium as $GdPO_4$

It has been shown in Section 7.3.2.2 that gadolinium incorporated as $GdPO_4$ will be sufficiently insoluble that it will remain in the waste package for more than several hundred thousand years. Therefore, the following two scenarios, which have already been suggested as the last two separation mechanisms described in Section 7.4.1, are presented to represent the opposite extremes for generating a separation of neutron absorber from fissile material while both remain inside the DOE SNF canister:

1) a major fraction of the uranium particles settles to the bottom through holes in the remaining basket plates, and

2) a significant fraction of the gadolinium is trapped in the steel cutout from the plates as a result of random pitting corrosion of a periphery for each cutout; these cutouts will settle to the bottom through holes (pits and cutouts) in the remaining basket plates.

For calculation convenience it is assumed that the waste package is oriented such that the large basket plates, shown horizontal in Figure 7.4-3, actually are horizontal and that the disposition of material from the plates which are angled to the large plates (shown in Figure 7.4-3 and described in Refs. 5.38 and 5.55) will be the same as for the horizontal plates (Assumption 4.3.29). The following analysis applies to both scenarios.

The geometry for this analysis begins with the waste package and DOE SNF canister for the highly enriched MIT SNF. Most of the fuel is contained in the volume within the four longest plates of the DOE SNF canister, and these plates are featured, in simplified form, in the drawing of Figure 7.4-3, which is a simplification of the complete basket description given in Refs. 5.38 and 5.55. For purposes of defining the maximum cutout, a random distribution of pits was simulated over the maximum unsupported basket plate span (15 cm x 60 cm x 0.8 cm thick). The pit penetrations at the surface were taken to be 0.8 cm square cells. This cell size approximates the volume (Assumption 4.3.25) corroded by a pit, by using a cube having

dimension equal to the thickness of the basket plate. In this manner, the maximum unsupported plate is divided into a 19 x 75 rectangular array, as shown in Figure 7.4-4. It is assumed that this pit size is appropriate to carbon steel. For stainless steel it is assumed that the pit cross section area is 1% of the carbon steel value (Assumption 4.3.25), so that there are 100x as many square cells on the reference basket plate.

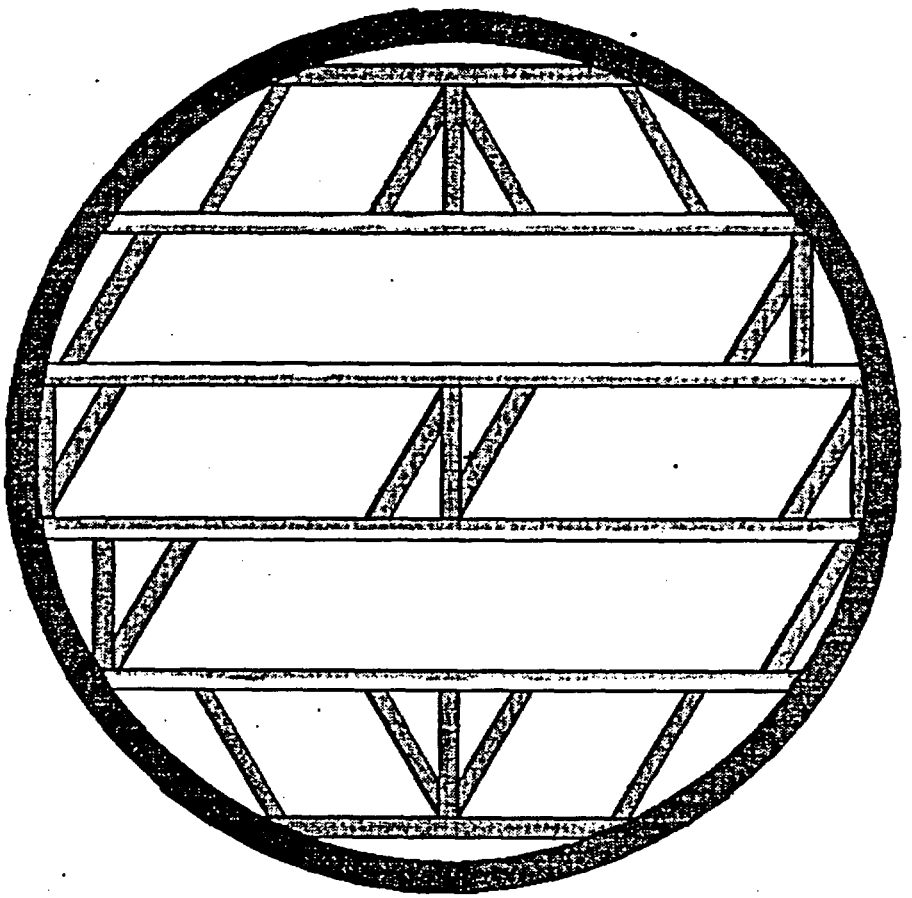

Figure 7.4-3. DOE SNF Canister Geometry for the MIT SNF

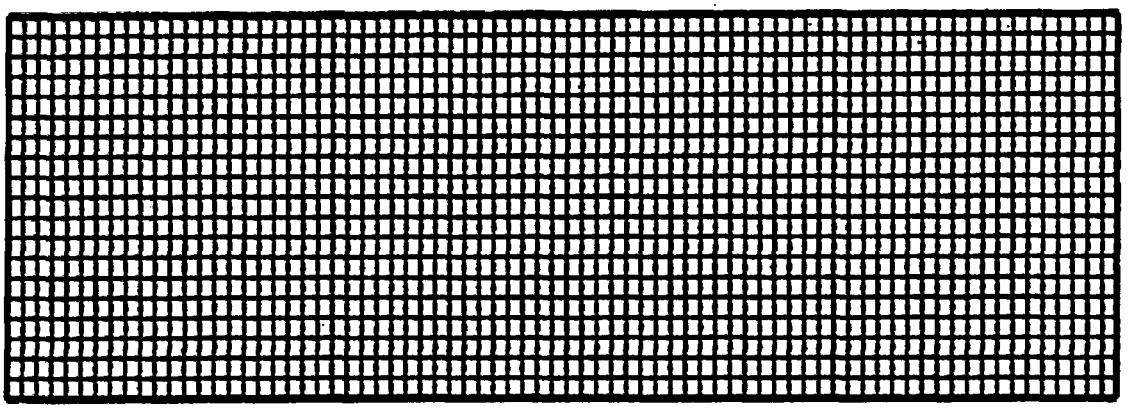

Figure 7.4-4. Grid of Square Pit Locations Typical of Carbon Steel

A cutout is defined as a region containing contiguous un-pitted cells, and completely surrounded by pits. Contiguous means adjacent in the horizontal or vertical direction; cells linked only by a diagonal are not considered contiguous. However, by the definition of contiguous for the interior of a cutout, diagonal neighbors are close enough to serve as a segment of the boundary of a cutout.

A computer program, pitgen.c, was used to randomly select, from the grid, the locations for the occurrence of pits. After each of a specified number of pits is generated, the program scans the array to detect the cutouts and count the area (number of square cells) enclosed in the cutouts. It is assumed that all pits grow at a uniform rate, and the only randomness is the total number of pits and their distribution (Assumption 4.3.26). For the reference 19 x 75 grid size (carbon steel) three realizations are illustrated by the three pairs of figures: Figures 7.4-5a and 7.4-5b; 7.4-6a and 7.4-6b; and 7.4-7a and 7.4-7b for pitting percentages of 42%, 49%, and 56%, respectively. The (a) figure of each pair uses a unique ASCII symbol to represent the locations of each cutout. The (b) figure represents all the cutout locations with the symbol '.'. All the figures represent the pit locations with the '+' symbol. In these figures there is an additional type of non-pitted cell which cannot be part of a cutout because it is linked, by a chain of contiguous unpitted cells, to a boundary, so that the region cannot be completely surrounded by pits. This exclusion from cutout status represents the fact that a partly corroded plate can maintain its position if it is welded at one end like a cantilevered beam. Obviously there is some limit to the length of such a cantilever. In keeping with the approximation of this study there was no attempt to estimate what

this limit should be. Instead, this limitation of cantilever capability is approximated by implementing it on the top and left boundaries of the grid (plate) and permitting the designation of cutout when the collection of unpitted cells intersects the lower or right border. A cantilever which connects opposite borders (thereby becoming a bridge) will not be counted as a cutout, in keeping with the additional support supplied by the connection to the opposite side. In the (a) figure of each pair, the space ' ' is used to identify the cantilever locations; in the (b) figure of each pair the 'o' symbol is used.

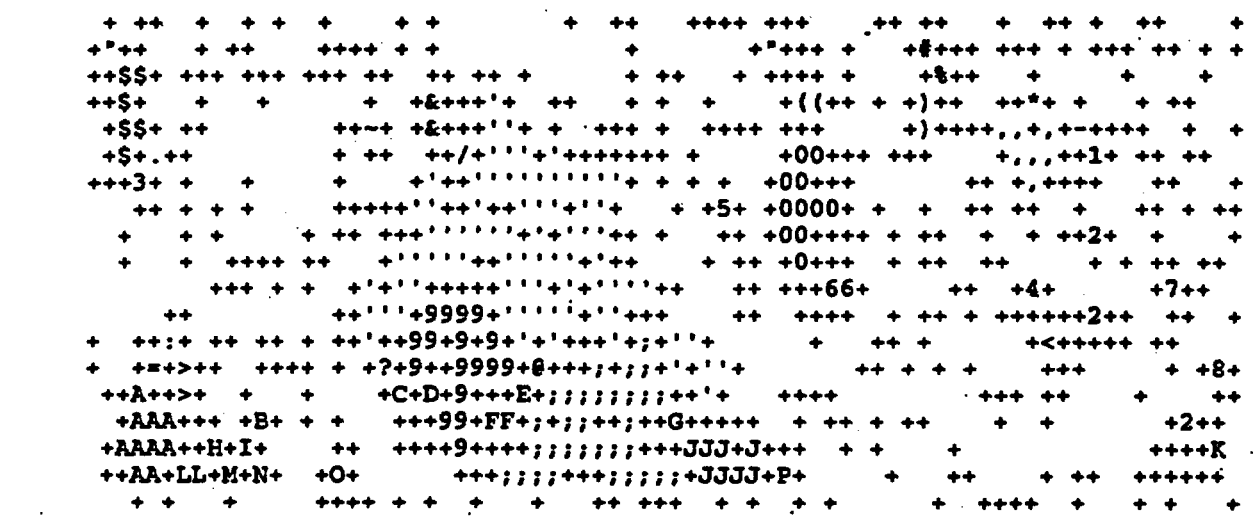

Figure 7.4-5a. Example Cutout Map for 19 x 75 Grid (Modeling Carbon Steel).
Pit fraction=0.421, cutout fraction=0.153, number of cutouts=47 avg cutout=4.638.
Symbols: '+' indicates a pit location; other printing ASCII characters indicate uniquely identified cutouts; blank space indicates a non-pitted location which is not part of a cutout because of connection to the upper or left boundary.

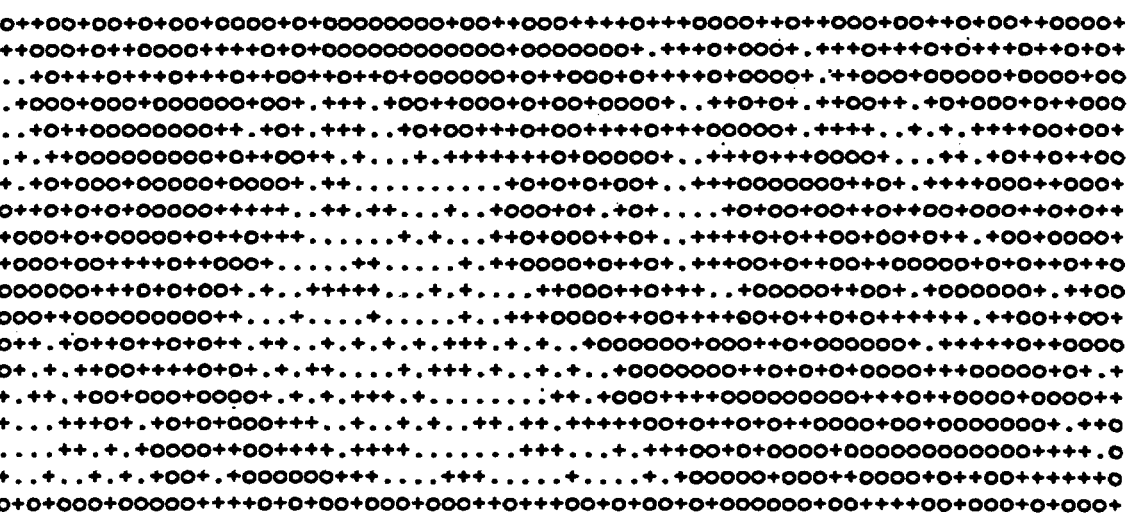

Figure 7.4-5b. Example Cutout Map for 19 x 75 Grid (Modeling Carbon Steel).
Pit fraction=0.421, cutout fraction=0.153, number of cutouts=47 avg cutout=4.638.
Symbols: '+' indicates a pit location; '.' indicates a cutout interior location; 'o' indicates a non-pitted location which is not part of a cutout because of connection to the upper or left boundary.

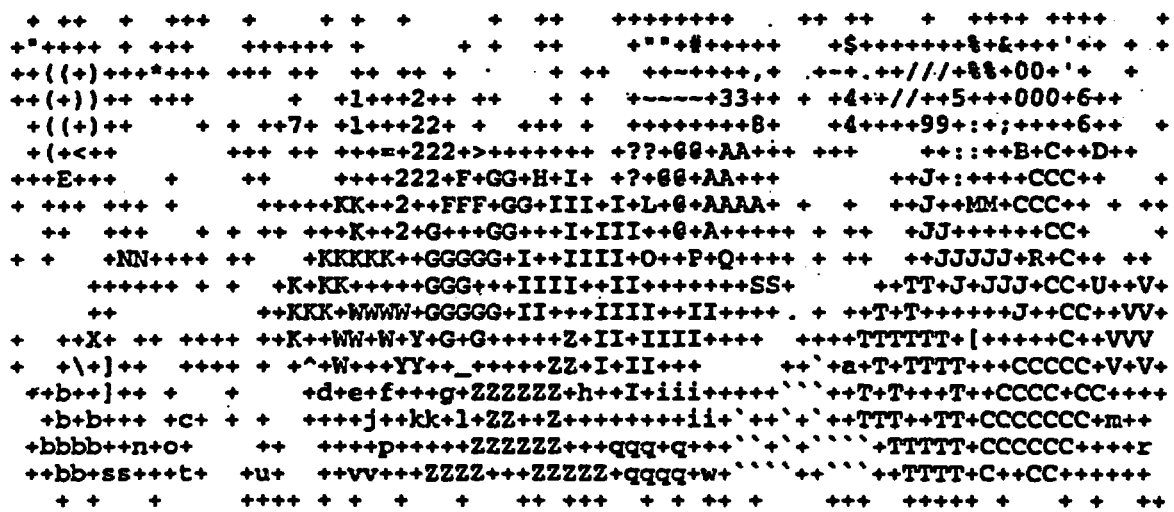

Figure 7.4-6a. Example Cutout Map for 19 x 75 Grid (Modeling Carbon Steel).
Pit fraction=0.491, cutout fraction=0.275, number of cutouts=86 avg cutout=4.558.
Symbols: '+' indicates a pit location; other printing ASCII characters indicate uniquely identified cutouts; blank space indicates a non-pitted location which is not part of a cutout because of connection to the upper or left boundary.

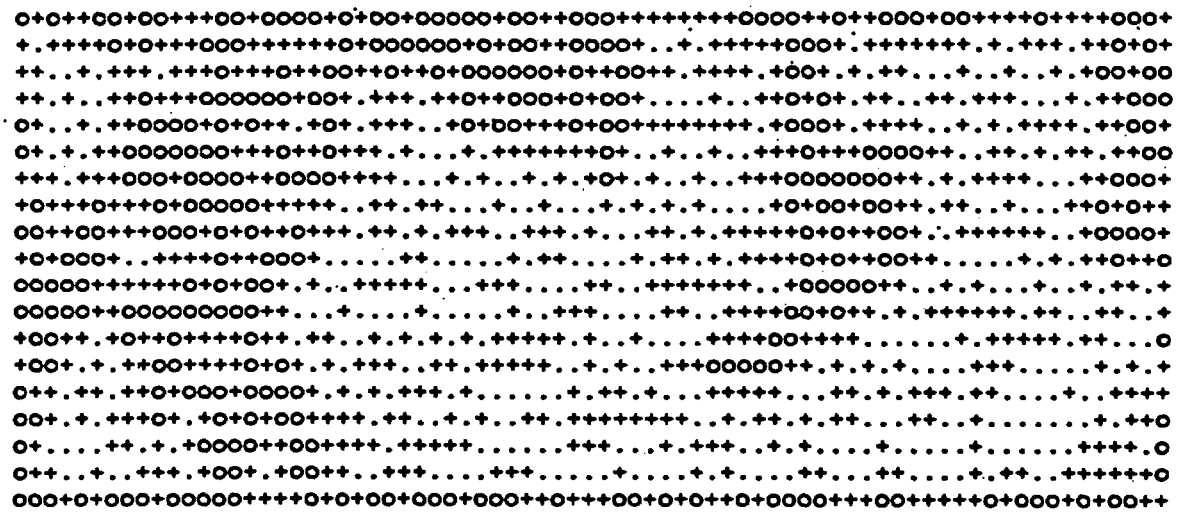

Figure 7.4-6b. Example Cutout Map for 19 x 75 Grid (Modeling Carbon Steel).
Pit fraction=0.491, cutout fraction=0.275, number of cutouts=86 avg cutout=4.558.
Symbols: '+' indicates a pit location; '.' indicates cutout interior location; 'o' indicates a non-pitted location which is not part of a cutout because of connection to the upper or left boundary.

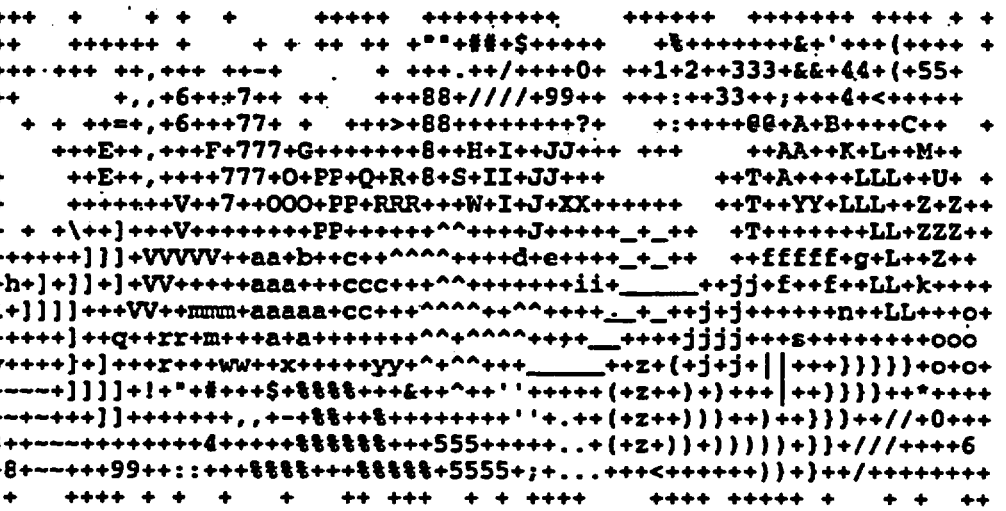

Figure 7.4-7a. Example Cutout Map for 19 x 75 Grid (Modeling Carbon Steel).
Pit fraction=0.561, cutout fraction=0.300, number of cutouts=121 avg cutout=3.537.
Symbols: '+' indicates a pit location; other printing ASCII characters indicate uniquely identified cutouts; blank space indicates a non-pitted location which is not part of a cutout because of connection to the upper or left boundary.

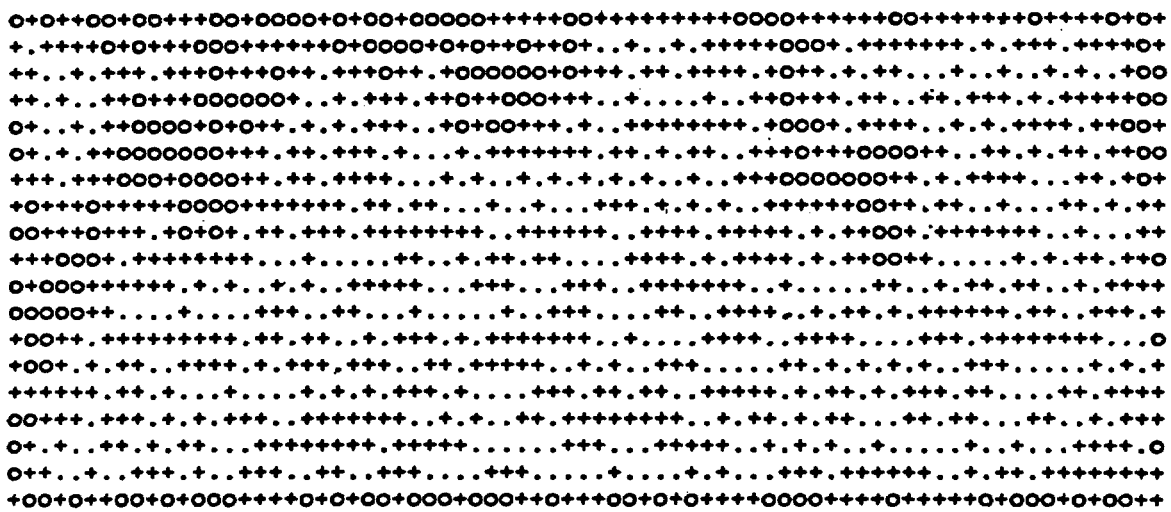

Figure 7.4-7b. Example Cutout Map for 19 x 75 Grid (Modeling Carbon Steel).
Pit fraction=0.561, cutout fraction=0.300, number of cutouts=121 avg cutout=3.537.
Symbols: '+' indicates a pit location; 'o' indicates a non-pitted location which is not part of a cutout because of connection to the upper or left boundary.

The symbol selection of the (a) series figures is most useful for visual verification of the horizontal or vertical adjacency of locations within an individual cutout. The symbol selection of the (b) series figures is most useful for visual verification of the complete surrounding of each cutout by pits ('+'symbols), and for the identification of cantilevered areas. Comparison of Figures 7.4-5b, 7.4-6b, and 7.4-7b illustrates the manner in which increasing the number of pits will decrease the cantilevered fraction (calculated as 1-(pitted fraction)-(cutout fraction)). Starting with nearly 50% cantilevered for 42% pitted (Figure 7.5-5b, which illustrates one complete cantilevered bridge from top to bottom at the left side of the figure) the sequence reduces to only 14% cantilevered for 56% pitted (Figure 7.5-7b).

Using the cutout analysis program, statistics for 100 realizations were generated for grid sizes representing both carbon steel (19 x 75) and stainless steel (190 x 750). The results are given in Table 7.4-1a and 7.4-1b.

Table 7.4-1a. Cutout Statistics for a 19 x 75 Grid (to Model Carbon Steel).

Pitfrac	Cutfrac	SDcutfrac	NumCutout	SDCutout	Avarea
0.070	0.000	0.000	0	0.196	1.500
0.140	0.001	0.001	1	0.790	1.212
0.211	0.003	0.003	3	1.545	1.503
0.281	0.013	0.010	9	3.218	2.163
0.351	0.059	0.033	22	4.762	3.735
0.421	0.189	0.057	47	6.829	5.726
0.491	0.299	0.041	80	8.001	5.298
0.561	0.318	0.022	114	8.260	3.962
0.632	0.292	0.011	141	10.225	2.957
0.702	0.246	0.007	153	9.150	2.287
0.772	0.192	0.005	144	13.394	1.899

Table 7.4-1b. Cutout Statistics for a 190 x 750 Grid (to Model Stainless Steel)

Pitfrac	Cutfrac	SDcutfrac	NumCutout	SDCutout	Avarea
0.070	0.000	0.000	4	1.775	1.011
0.140	0.000	0.000	51	6.577	1.082
0.211	0.002	0.000	256	15.959	1.219
0.281	0.009	0.000	830	28.571	1.575
0.351	0.051	0.005	2224	41.343	3.246
0.421	0.486	0.017	4997	63.750	13.859
0.491	0.484	0.002	8915	85.213	7.730
0.561	0.425	0.001	13003	88.518	4.663
0.632	0.360	0.000	16279	101.084	3.154
0.702	0.293	0.000	18040	95.424	2.313
0.772	0.224	0.000	17805	81.708	1.796

It should, of course, be noted that the times to corrode the stainless steel may be up to 2 orders of magnitude greater than for the carbon steel. Nevertheless, the following comparisons are important:

- The maximum cutout fraction for stainless steel is significantly greater than for carbon steel, as would be expected from the smaller pit size (finer resolution grid).
- The maximum cutout fraction for stainless steel occurs at a lower pitting fraction than for carbon steel, increasing the importance of cutouts as a mechanism for removing material.

The remainder of this section is devoted to an estimate of the worst case separation of the Gd from the U.

For carbon steel, the percent of Gd trapped in cutouts is estimated to be one half the cutout fraction to account for the fact that by the time the pit penetrates the 0.8 cm plate thickness, 50% of the plate thickness will also have been removed by bulk corrosion. The reason for this factor is as follows: the pitting corrosion factor for carbon steel (the carrier metal of choice for the $GdPO_4$ neutron absorber material) is 4 (Ref. 5.36, Section 5.4.4), which means that the pit penetration rate is 4 times the bulk corrosion rate; the bulk corrosion rate is then increased by a factor of 2 to account for corrosion from both surfaces, while the pit can only go from one surface at a time. This analysis provides a lower bound for the amount of Gd which will be removed to the bottom; since the Gd precipitate remaining from corrosion of the steel is not significantly hydrolized, it is all likely to remain on top of the remaining thickness of uncorroded plate and all be available to fall through the cutout when it develops. Furthermore, the Gd will not actually be emplaced in the basket structural steel, but rather in a thinner plate (0.25 cm) fastened to the structural basket plates (mostly the horizontal plates indicated in Figure 7.4-3), which is likely to be completely corroded before the cutout appears in the plate to which it is attached. It will all be available to fall through any cutout which appears beneath it.

As shown in Figure 7.4-3, the basket was approximated by the 4 largest plates, so that all the fuel is approximated as falling between these plates. Therefore, there are no cutouts or particulates falling through the top plate. Furthermore, the lowest plate approximates the bottom of the canister. Therefore, the probability of settling through the plates was estimated as the average of the probabilities of passing through 2 plates, 1 plate, and zero plates. For this calculation the probabilities of passing through the several numbers of plates is as follows: (1) zero plates, which requires no special conditions so the probability = 1; (2) one plate, probability = the sum of the fraction of area covered by pits plus the fraction cutout, and (3) two plates, probability is the square of the one plate pass-through.

This methodology is illustrated in Table 7.4-2, for the largest cutout fractions in Tables 7.4-1a and 7.4-1b. Typical calculations are given in the footnotes to the table, and further details are given in Attachment V.

Table 7.4-2. Worst Case (Maximum Cutout) Maximum U which can Settle to the Bottom and Minimum Gd which will Settle to the Bottom.

Material	% basket covered by pits	% cutout	Max % of U at bottom*	Min % of Gd at bottom †
Carbon steel	56	32	78	14‡
Stainless steel	42	49	83	45§

* For max U at bottom the min Gd at bottom is sufficient to prevent criticality.

† For min Gd at bottom the remaining Gd distributed will be sufficient to prevent criticality with all the U distributed.

‡ $(1+f+f^2)\ (0.32/2)/3$, where f=0.56+0.32

§ $(1+f+f^2)\ (0.49)/3$, where f=0.42+0.49

This approximation may overestimate the amount of material passing through the plates for the following reasons:

1) the pit holes may not be in sufficiently large contiguous groups to permit the passing of a large cutout falling from a plate above, and

2) much of the wider plates' cutouts/pits will fall on the canister wall, rather than on the plate below, which will be smaller area for the lowest plate.

To be precise, the settling uranium must still pass through the lowest plate in order to reach the bottom. By neglecting this last requirement (lumping the lowest together with the bottom), the amounts collecting at the bottom of the DOE SNF canister are overestimated, which is conservative.

7.4.5 Comparison of Probability of Criticality

This analysis is concerned with the occurrence of configurations which may be critical, and not with the actual occurrence of criticality per se. Nevertheless, the results of the calculations of configurations in Sections 7.4.3 and 7.4.4 can be used, together with probabilities of water infiltration and water retention (for moderation), to compare probability of criticality with the three alternative criticality control materials. This comparison is given in Table 7.4-3. The first line of this table gives the conditional probabilities for the occurrence of a geometry and geochemistry which removes the neutron absorber which was calculated in Sections 7.4.3.1 and 7.4.2.1 for the first two columns. For purposes of illustration, the time period covered by these

probabilities is taken to be 40,000 to 60,000 years. As explained in Section 7.4.3, for 40,000 years, the conditional probability of boron loss, given the infiltration (dripping) and collection of water in the DOE SNF canister, becomes 1. For Gd_2O_3, however, the 60,000 years coincides with the shortest time to achieve low pH and high Gd solubility, as given by the analysis in Section 7.4.4.1, so the probability that the low pH solution will contact the gadolinium remains as calculated in that section. The conditional probability of zero in the third column ($GdPO_4$) reflects the analysis summarized in Section 7.4.4.2, and would hold for upwards of several hundred thousand years. The second line of Table 7.4-3 is an adaptation of probability calculations made in Ref. 5.52. The items in the third line are the products of the first two lines. The details of the calculation of the second line are given in Attachment V.

Table 7.4-3. Comparison of Probabilities for Potentially Critical Configurations for Alternative Criticality Control Materials (time horizon: 60,000 years)

Description of system element	Criticality control material		
	boron	Gd_2O_3	$GdPO_4$
Conditional probability of a geometry and geochemistry which removes the indicated neutron absorber	1.0	0.075	0
Probability of required infiltration and water for moderator (same for all control alternatives)	0.007	0.007	0.007
Combined probability of criticality	7×10^{-3}	5.3×10^{-4}	0

8. Conclusions

This analysis investigated through simulation methods the likely geochemical conditions for the degraded waste package after the corrosion/dissolution of its initial form (so that it can be effective in preventing criticality). The conclusions drawn from this analysis are as follows:

- If the DOE SNF canister is breached while the HLW glass is still degrading, it is likely that the highly alkaline solution from the degrading HLW may dissolve a significant fraction of the uranium released by the degraded SNF. This dissolved uranium may be flushed from the waste package, thereby precluding the possibility of internal criticality. The maximum pH, and the consequent maximum uranium solubility, is decreased somewhat by an increased concentration of carbon dioxide, which may be possible in the repository environment, but not by enough to significantly affect this conclusion.

- The small difference in density between the uranium-containing particulates and the gadolinium-containing particulates expected in the degraded waste package will not result in significant horizontal stratification. This conclusion is based on a theoretical analysis using the range of possible settling velocities and on a review of the literature on the stratification in natural placer deposits.

- With the progressive degradation of the basket of the DOE SNF canister, some of the gadolinium can settle to the bottom in intact fragments of steel, but only while a significant fraction of the basket remains intact. The geometric hinderance of the remaining basket will limit the amount of gadolinium which can settle by this mechanism to less than 15% of the total.

- The criticality control effectiveness of B stainless steel is questionable because it may degrade in less than 20,000 years following exposure to water, releasing the highly soluble boron to be flushed from the DOE SNF canister and the waste package. Such a scenario may be delayed and/or reduced in probability by the following:

  1) only the fraction of the waste package flow, or circulation, intersecting the DOE SNF canister will be effective in causing the removal of boron, and

  2) the flow and circulation in the waste package is reduced with time by the increasing amount and density of clay.

- The criticality control effectiveness of gadolinium oxide is questionable because it may become soluble if the solution in the waste package becomes acidic, which can result from

the corrosion products of stainless steel. Such a scenario may be delayed and/or reduced in probability by factors reducing the overall flow effectiveness mentioned in connection with the B stainless steel conclusion, above, and by the limited mass of stainless steel fragments immediately upstream of the DOE SNF canister (which is the only place from which they can influence the pH in the DOE SNF canister).

- Gadolinium phosphate appears to be insoluble over the entire range of pH possible in the waste package generally and in the DOE SNF canister in particular. This conclusion is based on:

  1) EQ6 simulations which include consideration of all the types and amounts of materials which may be found in the waste package at any time, and

  2) the occurrence of very old rare earth phosphates in nature to such an extent that they form the principal ore for rare earth mining.

- Gadolinium initially loaded as gadolinium oxide into the codisposal basket may be rendered insoluble by combination with the phosphate present from other sources within the waste package. However, with the limited amount of such incidental phosphate available, most of the gadolinium required for criticality control will remain uncombined with phosphate, and, hence, be at risk of removal from the waste package.

- In the absence of experimental data on corrosion rates on uranium silicide (the fuel material for the ORR), a review of the thermodynamic constants indicates a probable corrosion rate no faster than that of the uranium aluminides used in the MIT fuel. Furthermore, the amount of silicon released by the corrosion of the uranium silicide will be much less than that already released by the degrading HLW glass. Therefore, it will be a conservative approximation if the degradation analysis of this document, for the MIT fuel, is applied to the ORR fuel as well. (Section 7.2.3)

- Since boron is highly soluble, the only way to delay/prevent its removal from the waste package is to encapsulate it in a corrosion resistant material, such as stainless steel, or, still better, zircaloy. If, on the other hand, gadolinium is used as the criticality control material, we rely on its fundamental insolubility. Gadolinium can, therefore, be encapsulated in a material chosen for properties other than corrosion resistance. Carbon steel seems to be the encapsulation material of choice for gadolinium because its corrosion releases iron oxide with a simultaneous increase in volume which provides a significant degree of criticality control in the form of moderator exclusion.

9. Attachments

This section contains general supporting information for the design analysis presented in the sections above. Supporting spreadsheets and other information provided as hardcopy are listed in Table 9-1.

9.1 Hardcopy Attachments

Supporting documentation, source listings of ancillary computer codes, and calculational spreadsheets provided as attachments in hardcopy form are listed in Table 9-1.

Table 9-1. List of Attachments

Attachment No.	Title	Date	No. of Pages
I	Algorithm for Successive Runs Simulating Flow and Transport	12/04/97	4
II	Scripts and Programs to Perform Simulations	12/04/97	9
III	Spreadsheets for EQ3/6 Calculations	12/15/97	100
IV	Hindered Settling Particle Diameter Ratios	12/05/97	8
V	Listing of pitgen.c, program to generate pit locations and analyse them for occurrence of cutouts	12/05/97	7
VI	Check of Flushing Routine	12/12/97	1
VII	MIT Codisposal Canister Sketch	12/12/97	1

9.2 Electronic Attachments

The following supporting documents are in electronic form on a Colorado Trakker® tape (Ref. 5.30) and are listed below.

```
UALIA1~1 ALL     46,760,725  12-10-97  3:30p UAlIa10rmm.allout
J13AVG1  3O         121,492  12-10-97  3:52p j13avg1.3o
UALIB5~1 ALL     39,406,705  12-12-97  9:58a UAlIb5mm.allout
UALIB5~2 ALL     39,650,595  12-10-97  3:35p UAlIb5rmm.allout
UALIIA~1 ALL      1,243,386  12-10-97  3:35p UAlIIa1rmm.allout
UALIB1~1 ALL      2,677,106  12-10-97  3:36p UAlIb1rmm.allout
UALIIB~1 ALL     37,553,075  12-12-97  9:59a UAlIIb5mm.allout
UALIA5~1 ALL     12,019,358  12-10-97  6:57p UAlIa5mmr.allout
```

UALIII~2	ALL	12,164,309	12-12-97	10:00a	UAlIIIb5mm.allout
UALIA0~1	ALL	3,891,709	12-11-97	3:21p	UAlIa0.1rmm.allout
UALIB0~1	ALL	1,524,819	12-10-97	3:49p	UAlIb0.1rmm.allout
UALIII~3	ALL	19,149,699	12-10-97	3:50p	UAlIIIci0.1mm.allout
UALIII~4	ALL	21,242,288	12-10-97	3:50p	UAlIIIe0.1mm.allout
J13AVG19	3O	123,821	12-10-97	3:52p	j13avg19.3o
J13AVG20	6O	108,477	12-10-97	3:52p	j13avg20.6o
J13AVG21	6O	100,093	12-10-97	3:52p	j13avg21.6o
BORAX	6O	67,755	12-10-97	3:53p	borax.6o
DATA0N~1	R3	2,325,742	12-10-97	3:53p	data0.nuc.R3
DATA0N~1	R5	2,310,952	12-10-97	3:53p	data0.nuc.R5
DATA0N~1	R7	2,328,835	12-10-97	3:53p	data0.nuc.R7
UALIIA~2	ALL	59,342,190	12-10-97	7:00p	UAlIIa5mmr.allout
UALIII~1	ALL	37,114,615	12-10-97	7:02p	UAlIIIa5mmr.allout
UALIIB~2	ALL	37,792,875	12-12-97	9:56a	UAlIIb5rmm.allout
UALIII~5	ALL	27,850,582	12-10-97	7:10p	UAlIIIc0.1rmm.allout
UALIB1~2	ALL	39,373,030	12-11-97	3:24p	UAlIb10rmm.allout
UALIBN~1	ALL	38,239,044	12-11-97	3:27p	UAlIbNF5mm.allout
UALIIB~3	ALL	29,843,831	12-11-97	3:28p	UAlIIbNF5mm.allout
UALIII~6	ALL	15,321,265	12-11-97	3:29p	UAlIIIc0.1mm.allout
UALIC5~1	ALL	22,234,209	12-11-97	3:31p	UAlIc5mm.allout
SS	OUT	68,949	12-06-97	4:46p	ss.out
UALIII~8	ALL	11,966,981	12-11-97	3:31p	UAlIIId0.1mm.allout
CS	OUT	70,921	12-06-97	4:44p	cs.out

Attachment I. Algorithm for Successive Runs Simulating Flow and Transport

Background

EQ6 is basically a batch code, with an individual run operating on a fixed set of reagents, which may be augmented by a set of reagents introduced at a fixed rate throughout the run. Using the fixed rate mechanism it is possible to simulate the input of water during the course of a single run. The removal of water is modeled between successive runs by restarting with the same amount of water as was standing in the waste package at the beginning of the previous run and with the amounts of solutes for the start of the new run being adjusted for the amount of water removed. For this purpose we have used the EQ3/6 capability to restart with the conditions at the end of the previous run, by incorporating the "pickup" file from the previous run into the "input" file for the next run. This process has been automated with a computer code to read the "pickup" and "output" files from one run, and adjust the amounts of solutes to reflect the removal of an amount of water required to bring the total standing water back to the standing water at the beginning of the previous run. Repetition of this sequence of computer codes will simulate the flushing action provide by a dripping into standing water which is circulating and overflowing to maintain a constant amount of standing water. This is especially useful when the drip rate becomes much higher than 1 mm/yr since it can simulate the dilution effect of the new water coming in.

This attachment describes how this automated system works and lists the source code for all of its component parts. The source code files are also included in the electronic files attachment (Attachment III). Because this scheme rapidly produces a great deal of output, the algorithm was set up to retain only the most essential information. This is done by creating two files, initially named "allin", which contains the input data for each of the successive runs, and "allout", which contains the important results but does not twice repeat the input file portion of the normal output file, nor other information which occupies considerable space. It is also important keep track of the concentrations at the end of each run, which are subsequently adjusted by the automated system; the file "allpick" is used for this purpose. Thus, the output from a "run" will be found in several files, each of which is a history of a chain of individual EQ6 runs.

Algorithm

In the following discussion "current run" refers to the one just completed, or the last one for which the EQ6 code has generated data. The "current run" is the one whose values are used for the source of data to set up the next run in the sequence.

In the algorithm, x = moles of solvent water at the end of the current run, y = moles of water at end of current run, and z = moles of water added by mixing in new J-13 water during the current run. z is delta moles of J-13 solution, as reported in the output file of EQ6, divided by an appropriate factor, e.g., 3. See the implementation section below for an explanation of this factor.

The algorithm calculates r = xy/(x+z).

From the pickup file, p = moles aqueous is read from the last column of the first table listing chemical composition data.

From the pickup file, q = total moles is read from the middle column of the first table listing chemical composition data.

The algorithm then replaces p by rp/y, and replaces q by q-p+rp/y. [r/y = x/(x+z)]

The algorithm then adjusts what is called the "logarithmic" basis species by using a ratio developed in the following steps:

a. It reads the value of the "logarithmic" species from pickup file (except for H+ and species O_2 and thereafter). This is the log of the molality of the uncomplexed basis species. Here this value is called g.

b. It takes the antilog, here called h, multiplies it by the reduction factor x/(x+z) to get h', takes the log of h' to get g' and replaces g by g' in the pickup file.

This procedure involves the assumption that the ratio of free to total aqueous species of an element at the end of the process of first admixing a solution in relatively large amounts, then removing a corresponding amount of the resulting solution, as the ratio would be if this process were performed during each step of reaction progress in EQ6. The resultant new set of logarithmic basis species need only be good enough to permit the Newton Raphson algorithm in EQ6 to converge.

Implementation of the algorithm

The objective is to change the pickup file to correspond to losses to the system that would result from outflow of solution produced by influx of a water solution, e.g., J-13 well water, from outside the system as changed by reaction within the system in such a way as to maintain the volume of influx equal, at least approximately, to the volume of efflux. To accomplish this:

1. From the output file, note the number of moles of J-13 added, e.g., delta J-13 divided by the mole fraction of oxygen in the solution that corresponds to free water (this excludes the oxygen tied up in sulfate, carbonate, etc.), and call this z. The methodology is described in the following paragraphs.

   Let z' be the number of moles of J-13 solution added. This needs to be modified by an appropriate factor, which for dilute solutions is 1/3. This factor is the atom fraction of oxygen in pure water; for pure water the solution would be normalized to two gram atoms of H plus one gram atom of O to yield a normalization factor of 1/3. In order to add the right number of moles

of water into the system, relative to the drip rate which is entered as the moles of solution added per second (the product of rk1, the rate of the pseudo-reaction which adds the water, and sk, the surface area over which this mythical reaction takes place), by means of the mixing option in EQ6 the "moles" of solution must be multiplied by 3, which is done by means of specifying a value of 3 for fx in the input file. [Most of this added water is added to the moles of solvent water, the rest entering clays and other hydrous solids.] This means that the number in the output file for delta moles of solution is three times the moles of water added to the system. Hence, to make the appropriate changes to the pickup file, delta moles must be divided by 3. [There exist other ways of setting up the problem, e.g., using mole fractions of oxides rather than of elements; so long as internal consistency is maintained between the way the run is set up in the input file and the algorithm, correct results can be obtained.]

For more concentrated solutions, the normalization factor must again be the ratio of moles of free water to moles of solution. The moles of free water may be determined by subtracting the gram atoms of sulfate, carbonate, water incorporated into aqueous complexes, etc. from the total number of gram atoms of oxygen in the solution. Thus, in this case, i.e., an inflowing concentrated solution, fx should be the ratio, moles of solution/moles of free water. Likewise, in making changes to the pickup file, delta moles must be divided by this factor. The default value in the algorithm is 3, but may be changed at run time.

The calculational scheme involves adding "new" solution, e.g., J-13 well water, as a special reactant, in keeping with the fluid mixing option in EQ6.

2. From the output file, note the number of moles of solvent water at the start of the current run, x, and the amount at the end of the current run, y.

3. To simulate flow and transport, it is necessary to periodically remove the water added, i.e., simulate it moving along the flow path. The need, then, is to subtract the amount of water added, minus the share of this added water that entered clays and other hydrous solids. In this way the water added is removed from the aqueous system, partly by entering solids and the rest by flowing out of the system. Conversely, water could be released from destruction of clays.

4. The total water entering or leaving clays (and other solids) = amount of solvent water initially present + the amount of solvent water in J-13 added - amount of solvent water present at the end. This yields the total water entering clays as $x + z - y$.

5. Of the amount of water that enters solids, the share that comes from newly added J-13 is $z/(x + z)$, the ratio of new solvent water to the total solvent water before solids are formed. Therefore, the amount of newly added water that enters solids is $z(x + z - y)/(x + z)$. To keep the total water in the system constant the remainder of the newly added water, s, needs to be removed.

6. Then, $s = z - z(x + z - y)/(x + z) = zy/(x + z)$. This amount in turn needs to be subtracted from the current amount of solvent water, y. Call this remainder r. After doing the algebra, one gets $r = y - zy/(x + z) = xy/(x + z)$

7. From this analysis one may conclude that, if the amount of water that may be released from clays is not too large, the proper amount of water for the next step (run) is r, so the fraction of solvent water remaining is r/y. This leads to the conclusion that the correct amount of moles in the aqueous solution is generally obtained by multiplying moles aqueous by $r/y = x/(x + z)$. However, if a large amount of water is released from clays and hydrates, the amount of solvent water could exceed 1 kg. This would result in overfilling of the void space. In such a case, the amount of water needs to be reduced further to limit the amount of solvent water to 1 kg. This is accomplished by adjusting the value of r so that the solvent water for the next run will be calculated to be 1 kg.

   The final objective is to adjust the pickup file, which will be read into the new "input" file. In particular, the algorithm will adjust values for the parameters listed as "moles", "moles aqueous", and "logarithmic basis species".

8. From the pickup file, call "moles aqueous" p. Then, following the conclusion in step 7, one gets a new quantity, called $m = rp/y$. This is the new amount to enter in the "moles aqueous" column to replace p.

9. Next one needs to correct the "moles" column. Call the entry here q, which is the sum of "moles aqueous" and moles solid. The number of moles of solid remains the same, and the aqueous portion is to be adjusted to equal m. Moles of solid is q - p. Thus, the new quantity should be $q - p + m = n$.

10. Repeat steps 9 & 10 for all elements, except for gases, e.g., $O_2(g)$.

11. Correct logarithmic basis species. These entries are the logarithms of the molalities of uncomplexed basis species. The logic is to decrease these molalities in the same proportion as used for decreasing the total moles of aqueous species. This is easily accomplished by reading a value of the logarithmic basis species, taking the antilog, multiplying by the reduction factor, taking the log, and entering the result as the new value of the logarithmic basis species.

Attachment II. Scripts and Programs to Perform Simulations

bldinput.bat

```
echo "did not run bldinput" >sfile
count=1
bldinput
read status <sfile
if [ "$status" != "go" ]
then
  echo $status
  echo "job terminated"
  exit
fi
echo $count
while [ $count -lt 20 ]
do
  mv bldinput.out input
  eq6dR136.opt
    cat input >> allin
    cat pickup >> allpick
    cat output >> allout
    cat tab >> alltab
  nxtinput
  read status <sfile
  if [ "$status" != "go" ]
  then
    echo $status
    echo "job terminated"
    exit
  fi
  count=`expr $count + 1`
  echo $count
done
exit
```

bldinput.in

```
root        date         creator        delmaxtime
autofloII    08/16/97     Automated          2.1e+08

#include <stdio.h>
#include <string.h>
#include <stdlib.h>
#include <math.h>
```

```
float  getfloat(char*,int,int);
void setup(),bldpick(),infromstd(),infromlast(),
   strinsert(char*,char*,int,int);
int locate0(char*,FILE*),locateall(char*,FILE*),tobar(char*,int);

float duration,delmaxtime;
char dummy[100],buffer[90],lookahead[90];
char froot[20],cname[20],fname[20];
FILE *fin,*fout,*fp,*ftemp,*fstd,*foutout,*finin,*fsfile;

void main()
{int i,j,k,flag;
fsfile=fopen("sfile","w");
fprintf(fsfile,"go\n");
flag=1;
fout=fopen("bldinput.out","w");/*file to be moved to input*/
if(flag==1) infromstd();
/*else infromlast();*/}

void infromstd()
{int i,j,k;
char tempstr[20],datestr[10];
fstd=fopen("input","r");/*template for initial input file*/
fin=fopen("bldinput.in","r");/*filename,creator,duration)*/
fgets(dummy,100,fin);/*readthrough labels of setup data*/
fscanf(fin,"%s %s %s %f",froot,datestr,cname,&delmaxtime);
strcpy(fname,froot);
strcat(fname,"1.6i        ");
locate0("|EQ",fstd);
strinsert(dummy,fname,22,strlen(fname));
fputs(dummy,fout);
locate0("|Created",fstd);
strcat(cname,"          ");
strinsert(dummy,datestr,9,8);
strinsert(dummy,cname,30,strlen(cname));
fputs(dummy,fout);
locate0("| starting time",fstd);
i=tobar(dummy,1);
if(i<0)
  {printf("couldn't find |");
  exit(0);}
i=tobar(dummy,i+1);
if(i<0)
  {printf("couldn't find |");
  exit(0);}
i=tobar(dummy,i+1);
```

```
if(i<0)
  {printf("couldn't find |");
  exit(0);}
sprintf(tempstr,"%12.5e",delmaxtime);
k=strlen(tempstr);
j=tobar(dummy,i+1);
if(j<0)
  {printf("couldn't find |");
  exit(0);}
strncat(tempstr,"       ",j-i-1-k);
strinsert(dummy,tempstr,i+1,j-i-1);
fputs(dummy,fout);
while(fgets(dummy,90,fstd)!=NULL)fputs(dummy,fout);}

void strinsert(char inline[90],char insert[90],int start,int len)
{int i;
for(i=0;i<len;i++) inline[start+i]=insert[i];}

int locate0(char sstring[50],FILE *fp)
{int i=0;
while(fgets(dummy,90,fp)!=NULL)
  {if(strncmp(dummy,sstring,strlen(sstring))==0)return i;
  i++;
  fputs(dummy,fout);}
return 0;}

int tobar(char line[100],int start)
{int i;
i=start;
while((i<strlen(line))&&(line[i]!='|'))i++;
if(line[i]=='|')return i;
else return -1;}
```

nxtinput.bat

```
count=1
while [ $count -lt 40 ]
do
  mv bldinput.out input
  eq6dR136.opt
    cat input >> allin
    cat pickup >> allpick
    cat output >> allout
  nxtinput
  read status <sfile
  if [ $status = "stop" ]
  then
    exit
  fi
  count=`expr $count + 1`
  echo $count
done
exit
```

nxtinput.c

```
#include <stdio.h>
#include <string.h>

#include <stdlib.h>
#include <math.h>
double getfloat(char*,int,int),gettobar(char*,int);
void setup(),bldpick(),infromstd(),infromlast(),
   convert(double,double,FILE*,FILE*),
   strinsert(char*,char*,int,int);
int locaterw(char*,FILE*,FILE*),locatero(char*,FILE*),
   locate2(char*,char*,FILE*),tobar(char*,int),findinline(char*),
   puttobar(char*,char*,int),locate1of2(char*,char*,FILE*);
int finished=0;
double mash2oend,duration;
char dummy[100],tdummy[100];
char froot[20],cname[20],fname[20];
FILE *fout,*fpick,*fotemp,*fptemp,*fstd,*foutout,*finin,
   *fttemp,*fs,*fin,*ferr;

void main()
{int i,j,k,flag;
fs=fopen("sfile","w");
ferr=fopen("junk.out","w");
fprintf(fs,"go\n");
flag=1;
fout=fopen("bldinput.out","w");/*file to be moved to input*/
infromlast();}

void infromlast()
{int i,j,k,dot;
char tempstr[30],carbstr[7],*cp,sstring[60],tempstr2[20];
double dmj13,msh2o,msh2ox,xx,yy,moles,dmoles,delmaxtime;
```

```
fin=fopen("bldinput.in","r");/*input parameters special to this case*/
fstd=fopen("input","r");/*template from last input file*/
fpick=fopen("pickup","r");/*old pickup file; extract section to bldinput.out*/
foutout=fopen("output","r");/*from last iteration to new input*/
finin=fopen("input","r");/*from last iteration to new input*/
fotemp=fopen("otemp","w");/*store intermediate segments from output*/
fptemp=fopen("ptemp","w");/*store intermediate segments from pickup*/
fgets(dummy,90,fin); /*readthrough labels*/
fscanf(fin,"%s %s %s %lf\n",
     tempstr,tempstr,tempstr,&delmaxtime);/*only 1 param used this prgrm*/
locatero("                    Moles of solvent H2O",foutout);
msh2ox=getfloat(dummy,44,12);  /*optional  parameter from the first block*/
foutout=freopen("output","r",foutout);
strcpy(sstring,"                          Reaction progress");
if(locatero(sstring,foutout)==-1)  /*find output block of interest*/
  {printf("bad output file\n");
  exit(0);}
fputs(dummy,fotemp);         /*and write it to temporary*/
while(fgets(dummy,90,foutout)!=NULL)
  {fputs(dummy,fotemp);
  if(strncmp(dummy,sstring,strlen(sstring))==0)
     {fotemp=freopen("otemp","w",fotemp);
     fputs(dummy,fotemp);}}
fotemp=freopen("otemp","r",fotemp);/* re-open to find water*/
strcpy(sstring,"Mass of solvent H2O");
if(locatero(sstring,fotemp)!=1)
  {printf("Can't find ending water\n");
  fs=fopen("sfile","w");
  fprintf(fs,"cant find ending water");
  exit(0);}/*ending water*/
mash2oend=getfloat(dummy,44,12);
fprintf(ferr,"mass of solvent = %lf\n",mash2oend);
fotemp=freopen("otemp","r",fotemp);/*now reopen for use*/
if(locatero("c pickup file",fpick)==-1)   /*start copying here*/
  {printf("bad pickup file\n");
  exit(0);}
fputs(dummy,fptemp);
for(i=0;i<2;i++)  /*readwrite through first "|EQ"*/
  {fgets(dummy,90,fpick);
  fputs(dummy,fptemp);}
while(fgets(dummy,90,fpick)!=NULL) /*pickup to ptemp*/
  {fputs(dummy,fptemp);
  if(strncmp(dummy,"|EQ",3)==0) /*read through without copying*/
    while(fgets(dummy,90,fpick)!=NULL)
      if(strncmp(dummy,"c pickup file",strlen("c pickup file"))==0)
        {fptemp=freopen("ptemp","w",fptemp);/*start copying over again*/
        fputs(dummy,fptemp);
        for(i=0;i<2;i++)
          {fgets(dummy,90,fpick);
          fputs(dummy,fptemp);}
        break;}}
fptemp=freopen("ptemp","r",fptemp); /*now reopen for use*/
if(locaterw("|EQ",fstd,fout)==-1)
  {printf("bad input file\n");
  exit(0);}
i=0;
```

```
while((i<strlen(dummy))&&(dummy[i]!='.'))i++;
dot=i;
i=0;
while((dummy[dot-i-1]<='9')&&(dummy[dot-i-1]>='0'))i++;
for(j=0;j<i;j++)tempstr[j]=dummy[dot-i+j];
tempstr[i]='\0';
k=atoi(tempstr);
sprintf(tempstr,"%u%s",k+1,".6i");
strinsert(dummy,tempstr,dot-i,strlen(tempstr));
fputs(dummy,fout);
fgets(dummy,90,fotemp);/*get ending value of zi from first line*/
xx=getfloat(dummy,48,22);
if(locaterw("| starting value of zi",fstd,fout)==-1)
  {printf("can't find starting zi in input file\n");
  exit(0);}
sprintf(tempstr,"%15.8lE",xx);
i=tobar(dummy,1);
strinsert(dummy,tempstr,i+1,strlen(tempstr));
fputs(dummy,fout); /*and put into input*/
fgets(dummy,90,fstd);
fputs(dummy,fout);
fgets(tdummy,90,fstd);/*this takes us to entry for starting time*/
if(locatero("       Time increased from",fotemp)==-1)
  {printf("can't find last ending time in output\n");
  exit(0);}
fgets(dummy,90,fotemp);/*this line will have end time of last run*/
xx=getfloat(dummy,31,12);
sprintf(tempstr,"%11.5lE",xx);
i=tobar(tdummy,1);
if(i==-1)
  {printf("cant find slot for starttime\n");
  exit(0);}
strinsert(tdummy,tempstr,i+1,strlen(tempstr));
i=tobar(tdummy,i+1);
i=tobar(tdummy,i+1);
if(i==-1)
  {fs=freopen("sfile","w",fs);
  printf("cant find slot for maxtime\n");
  exit(0);}
/*yy=gettobar(tdummy,i+1); */
sprintf(tempstr,"%12.4lE",xx+delmaxtime);
strinsert(tdummy,tempstr,i+1,strlen(tempstr));
fputs(tdummy,fout); /*and put into input*/
fotemp=freopen("otemp","r",fotemp);/*last read was beyond current interest*/
if(locatero("     Reactant                    Moles     Delta moles",fotemp)==-1)
  {printf("cant find values for reactants in the output file\n");
  exit(0);}
fgets(tdummy,90,fotemp);
fgets(tdummy,90,fotemp);/*get to first reactant in otemp*/
while((finished==0)&&(strncmp(tdummy,"\n",1)!=0))/*loop to do all reactants*/
  {moles=getfloat(tdummy,29,10);
  dmoles=getfloat(tdummy,42,10);
  locaterw("| moles remaining",fstd,fout);/*next reactant*/
  sprintf(tempstr,"%10.4lE",moles);
  strinsert(dummy,tempstr,20,strlen(tempstr));
  if(strncmp(tdummy,"  J-13 water",12)!=0)
```

```
    {sprintf(tempstr2,"%10.41E",dmoles);
    strinsert(dummy,tempstr2,58,strlen(tempstr2));}
  else
    {dmj13=dmoles;
    fprintf(ferr,"delt moles water = %lf   z=%lf\n",dmj13,dmj13/3);
    finished=1;}                          /*Water is the last reactant*/
  fputs(dummy,fout);
  fgets(tdummy,90,fotemp);}
if(locatero("                    Moles of solvent H2O",fotemp)==-1)
  {fprintf(fs,"cant find moles water in output\n");
  exit(0);}
msh2o=getfloat(dummy,44,12);
fprintf(ferr,"moles water (x) = %lf\n",msh2o);
k=locatero(" ---  The reaction path has terminated normally",fotemp);
if(k==-1)
  {fputs("abnormal reaction path termination\n",fs);
  exit(0);}
fotemp=freopen("otemp","r",fotemp);/*back to the top again*/
if((k=locate2(" CO3--"," HCO3-",fotemp))==1) strcpy(carbstr,"| CO3--");
else if (k==2) strcpy(carbstr,"| HCO3-");
fttemp=fopen("ttemp","w");/*will later attach to input*/
if(locate1of2("| CO3--","| HCO3-",fptemp)==-1)/*also copies ptemp to ttemp*/
  {fprintf(fs,"cant find line to insert carbonates in pickup\n");
  exit(0);}
strinsert(dummy,carbstr,0,strlen(carbstr));
fputs(dummy,fttemp);
while(fgets(dummy,90,fptemp)!=NULL)fputs(dummy,fttemp);/*rest of ptemp to ttemp*/
fttemp=freopen("ttemp","r",fttemp);
if(locaterw("c pickup file",fstd,fout)==-1)/*transfer the relevant remainder of
the template*/
  {fprintf(fs,"cant find start for pickup info\n");
  exit(0);}
convert(msh2o,dmj13/3,fstd,fttemp);}

int locate1of2(char sstring1[50],char sstring2[50],FILE *fp)
{int found1=0,found2=0;
while((found1==0)&&(found2==0))
  {if(fgets(dummy,90,fp)==NULL)return -1;
  if(found1==0)
     if(strncmp(dummy,sstring1,strlen(sstring1))==0)
       found1=1;
  if(found2==0)
     if(strncmp(dummy,sstring2,strlen(sstring2))==0)
       found2=1;
  if((found1==0)&&(found2==0))fputs(dummy,fttemp);}
if((found1==0)&&(found2==0))return -1;
else return 0;}

void strinsert(char inline[90],char insert[90],int start,int len)
{int i;
for(i=0;i<len;i++) inline[start+i]=insert[i];}

int locate2(char sstring1[50], char sstring2[50],FILE *fp)
{int i,found1=0,found2=0;
double x1=0,x2=0;
char buffer[100];
```

```
while((fgets(dummy,90,fp)!=NULL)&&((found1==0)||(found2==0)))
  {strcpy(buffer,dummy);
  if(found1==0)
     if(strncmp(dummy,sstring1,strlen(sstring1))==0)
       {found1=1;
       x1=getfloat(dummy,28,12);}
  if(found2==0)
     if(strncmp(dummy,sstring2,strlen(sstring2))==0)
       {found2=1;
       x2=getfloat(dummy,28,12);}}
if(x1<x2) return 2;
else return 1;}

int locatero(char sstring[60],FILE *fp)/*read only*/
{while(fgets(dummy,90,fp)!=NULL)
  if(findinline(sstring)==1)return 1;
return -1;}

int locaterw(char sstring[60],FILE *fpin,FILE *fpout)/*read&write*/
{while(fgets(dummy,90,fpin)!=NULL)
  {if(strncmp(dummy,sstring,strlen(sstring))==0)return 1;
  fputs(dummy,fpout);}
return -1;}

void convert(double x,double z,FILE *fins,FILE *finp)
{int i,count=0;
double u,v,w,r;
char buffer[100],temp[50],temp2[50];
r=x/(x+z);
if(mash2oend*r>1)     /* to bring the free water back to 1 kg */
  {r=1/mash2oend;
   printf("converted to %f\n",r);}
if(locaterw("| elements, moles",finp,fout)==-1)/*readwrite to this point*/
  {printf("cant locate place to put new values of reagents in input\n");
  exit(0);}
fputs(dummy,fout);
fgets(buffer,90,finp);
fputs(buffer,fout);
fgets(buffer,98,finp);
while(strncmp(buffer,"|--------",8)!=0)
  {w=getfloat(buffer,55,21);
  v=w*r;
  u=getfloat(buffer,30,21)-w*(1-r);
  sprintf(temp,"%22.15lE",u);
  strinsert(buffer,temp,29,strlen(temp));
  sprintf(temp,"%22.15lE",v);
  strinsert(buffer,temp,54,strlen(temp));
  fputs(buffer,fout);
  fgets(buffer,90,finp);
  count++;}
fputs(buffer,fout);
for(i=0;i<2;i++)
  {fgets(buffer,100,finp); /*readthrough to species table*/
  fputs(buffer,fout);}
for(i=0;i<count;i++)
  {fgets(buffer,100,finp);
```

```
  w=getfloat(buffer,56,22);
  sprintf(temp,"%+20.15lE",w+log10(r));
  strinsert(buffer,temp,56,strlen(temp));
  fputs(buffer,fout);}
while(fgets(buffer,100,finp)!=NULL) fputs(buffer,fout);}

double getfloat(string,start,len)
char string[100];
int start,len;
{char temp[30];
strncpy(temp,string+start,len);
temp[len]='\0';
return atof(temp);}

double gettobar(char line[100],int start)
{int i;
char temp[30];
i=start;
while((i<strlen(line))&&(line[i]!='|'))
  {temp[i-start]=line[i];
  i++;}
temp[i]='\0';
if(line[i]!='|')return -1;
return atof(temp);}

int puttobar(char line[100],char string[30],int start)
{int i,k;
i=start;
k=strlen(string);
while((i<strlen(line))&&(line[i]!='|')&&(i-start<k))
  {line[i]=string[i-start];
  i++;}
if(line[i]=='|')return i;
else return -1;}

int tobar(char line[100],int start)
{int i;
i=start;
while((i<strlen(line))&&(line[i]!='|'))i++;
if(line[i]=='|')return i;
else return -1;}

int findinline(char sstring[50])
{int i=0;
while(i<100)
  {if(strncmp(dummy+i,sstring,strlen(sstring))==0) return 1;
  else i++;}
return 0;}
```

	A	B	C	D	E	F	G	H
1	Grade 55 A-516 Carbon Steel for baskets, from Design Analysis report BBA000000-01717-0200-00002 REV 00							
2								
3	Element	At. Wt.	Wt %	G-Atoms	Atom fr.	Mol. Wt.		
4	Fe	55.847	98.535	1.7643741	9.7421E-01			
5	Mn	54.938	0.9	0.0163821	9.0455E-03			
6	S	32.064	0.035	0.0010916	6.0271E-04			
7	P	30.97376	0.035	0.00113	6.2393E-04			
8	Si	28.0855	0.275	0.0097915	5.4064E-03			
9	C	12.01	0.22	0.0183181	1.0114E-02			
10			100	1.8110874	1	55.21544832	= "mol. wt." (wgt of 1 "mole" of steel)	
11								
12	Borated Type 316 Steel for baskets, from Ref. 5.14							
13								
14	Element	At. Wt.	Wt %	G-Atoms	Atom fr.	Mol. Wt.		
15	B	10.811	1.2841	0.1187772	6.2404E-02			
16	C	12.01	0.0301	0.0025062	1.3167E-03			
17	N	14.0067	0.1003	0.0071609	3.7622E-03			
18	Si	28.0855	0.7524	0.0267896	1.4075E-02			
19	P	30.97376	0.0451	0.0014561	7.6500E-04			
20	S	32.064	0.0301	0.0009387	4.9320E-04			
21	Cr	51.996	19.061	0.3665859	1.9260E-01			
22	Mn	54.938	2.0064	0.0365212	1.9188E-02			
23	Fe	55.847	60.639	1.0858059	5.7047E-01			
24	Ni	58.71	13.5433	0.2306813	1.2120E-01			
25	Mo	95.94	2.508	0.0261413	1.3734E-02			
26			99.9998	1.9033643	1	52.53854992	= "mol. wt." (wgt of 1 "mole" of steel)	
27								
28								
29	304L Stainless Steel,taken from Ref. 5.14, p. I-4							
30								
31	C	12.01	0.03	0.0024979	0.001365509			
32	Mn	54.938	2	0.0364047	0.019900939			
33	P	30.97376	0.045	0.0014528	0.000794209			
34	S	32.064	0.03	0.0009356	0.00051147			
35	Si	28.0855	0.75	0.0267042	0.014598073			
36	Cr	51.996	19	0.3654127	0.199756114			
37	Ni	58.71	10	0.1703287	0.093111717			
38	N	14.0067	0.1	0.0071394	0.003902839			
39	Fe	55.847	68.045	1.2184182	0.666035913			
40				1.8292943		54.66588909	= "mol. wt." (wgt of 1 "mole" of steel)	

	A	B	C	D	E	F	G	H
41								
42	316L stainless steel, taken from Ref. 5.14, p. I-5							
43								
44	Element	At. Wt.	Wt %	G-Atoms	Atom fr.	Mol. Wt.		
45	C	12.01	0.03	0.0024979	1.3830E-03			
46	N	14.067	0.1	0.0071088	3.9359E-03			
47	Si	28.0855	0.75	0.0267042	1.4785E-02			
48	P	30.97376	0.045	0.0014528	8.0438E-04			
49	S	32.064	0.03	0.0009356	5.1802E-04			
50	Cr	51.996	17	0.3269482	1.8102E-01			
51	Mn	54.938	2	0.0364047	2.0156E-02			
52	Fe	55.847	65.545	1.1736453	6.4981E-01			
53	Ni	58.71	12	0.2043945	1.1317E-01			
54	Mo	95.94	2.5	0.026058	1.4427E-02			
55			100	1.8061577	1.0000E+00	55.36614953	= "mol. wt." (wgt of 1 "mole" of steel)	

	A	B	C	D	E	F
1	Grade 55 A-516 Carbon Steel for ba					
2						
3	Element	At. Wt.	Wt %	G-Atoms	Atom fr.	Mol. Wt.
4	Fe	55.847	98.535	=C4/B4	=D4/$D$10	
5	Mn	54.938	0.9	=C5/B5	=D5/$D$10	
6	S	32.064	0.035	=C6/B6	=D6/$D$10	
7	P	30.97376	0.035	=C7/B7	=D7/$D$10	
8	Si	28.0855	0.275	=C8/B8	=D8/$D$10	
9	C	12.01	0.22	=C9/B9	=D9/$D$10	
10			=SUM(C4:C9)	=SUM(D4:D9)	=SUM(E4:E9)	=100/D10
11						
12	Borated Type 316 Steel for baskets.					
13						
14	Element	At. Wt.	Wt %	G-Atoms	Atom fr.	Mol. Wt.
15	B	10.811	1.2841	=C15/B15	=D15/$D$26	
16	C	12.01	0.0301	=C16/B16	=D16/$D$26	
17	N	14.0067	0.1003	=C17/B17	=D17/$D$26	
18	Si	28.0855	0.7524	=C18/B18	=D18/$D$26	
19	P	30.97376	0.0451	=C19/B19	=D19/$D$26	
20	S	32.064	0.0301	=C20/B20	=D20/$D$26	
21	Cr	51.996	19.061	=C21/B21	=D21/$D$26	
22	Mn	54.938	2.0064	=C22/B22	=D22/$D$26	
23	Fe	55.847	60.639	=C23/B23	=D23/$D$26	
24	Ni	58.71	13.5433	=C24/B24	=D24/$D$26	
25	Mo	95.94	2.508	=C25/B25	=D25/$D$26	
26			=SUM(C15:C25)	=SUM(D15:D25)	=SUM(E15:E25)	=100/D26
27						
28						
29	304L Stainless Steel,taken from Ref					
30						
31	C	12.01	0.03	=C31/B31	=D31/D40	
32	Mn	54.938	2	=C32/B32	=D32/D40	
33	P	30.97376	0.045	=C33/B33	=D33/D40	
34	S	32.064	0.03	=C34/B34	=D34/D40	
35	Si	28.0855	0.75	=C35/B35	=D35/D40	
36	Cr	51.996	19	=C36/B36	=D36/D40	
37	Ni	58.71	10	=C37/B37	=D37/D40	
38	N	14.0067	0.1	=C38/B38	=D38/D40	
39	Fe	55.847	68.045	=C39/B39	=D39/D40	
40				=SUM(D31:D39)		=100/D40

	A	B	C	D	E	F
41						
42	316L stainless steel, taken from Ref.					
43						
44	Element	At. Wt.	Wt %	O-Atoms	Atom fr.	Mol. Wt.
45	C	12.01	0.03	=C45/B45	=D45/$D$55	
46	N	14.067	0.1	=C46/B46	=D46/$D$55	
47	Si	28.0855	0.75	=C47/B47	=D47/$D$55	
48	P	30.97376	0.045	=C48/B48	=D48/$D$55	
49	S	32.064	0.03	=C49/B49	=D49/$D$55	
50	Cr	51.996	17	=C50/B50	=D50/$D$55	
51	Mn	54.938	2	=C51/B51	=D51/$D$55	
52	Fe	55.847	65.545	=C52/B52	=D52/$D$55	
53	Ni	58.71	12	=C53/B53	=D53/$D$55	
54	Mo	95.94	2.5	=C54/B54	=D54/$D$55	
55			=SUM(C45:C54)	=SUM(D45:D54)	=SUM(E45:E54)	=100/D55

	G
1	
2	
3	
4	
5	
6	
7	
8	
9	
10	= "mol. wt." (wgt of 1 "mole" of steel)
11	
12	
13	
14	
15	
16	
17	
18	
19	
20	
21	
22	
23	
24	
25	
26	= "mol. wt." (wgt of 1 "mole" of steel)
27	
28	
29	
30	
31	
32	
33	
34	
35	
36	
37	
38	
39	
40	= "mol. wt." (wgt of 1 "mole" of steel)

	G
41	
42	
43	
44	
45	
46	
47	
48	
49	
50	
51	
52	
53	
54	
55	= "mol. wt." (wgt of 1 "mole" of steel)

	A	B	C	D	E	F	G	H
1	Normalization of data on preceding sheets to 1 kg water							
2	Item	Volume	Mass	Mol. Wt.	Moles	Surface	Nor. Mol	Nor. Area
3	316 SS	66799.65021	531257.6181	55.36614953	9595.350636	162131.968	3.288546057	55.56633252
4	XM-19	60532.15596	476993.389	54.79757212	8704.644577	70048.52414	2.983280725	24.00723086
5	B steel	13685.70686	105995.7997	52.53854992	2017.486204	67377.54331	0.691438651	23.09182465
6	Al	40448.78691	109292.6222	26.98	4050.875546	2200381.493	1.388327671	754.1210484
7	Fuel meat	23406.23345	51212.83878	70.1182928	730.3777193	622791.8125	0.250317144	213.4447198
8	Alloy 625	404678.9562	3415490.391	60.82368237	56973.79521	188269.2232	19.5262223	64.52416748
9	304L	91530.22265	723088.7589	54.66588909	52909.56143	454462.1679	18.13331646	155.754576
10	DHLW gls	2417135.114	6888892.076	21.11808343	326208.2044	5649024.481	111.7990103	1936.049852
11	A516	13685.70686	105995.7997	52.53854992	2017.486204	67377.54331	0.691438651	23.09182465
12	Gd*		1000	157.25	6.359300477	67377.54331	0.002179478	23.09182465
13	Water	2917809.412	2917809.412					
14								
15	* Assumed 1 kg of Gd per waste package, Ref. 5.35. Moles rounded to 6.5/package							
16	for EQ6 runs. Same surface area as for A516 steel.							
17								
18	Links to other spreadsheets in Attachment III. Cells shown as abbreviated name of							
19	sheet/cell. Some links via formulas used in this sheet. Many masses computed							
20	from volume and density in this sheet; no entry for these below.							
21								
22	Item		Volume	Mass	Surface			
23	316SS		Vol/F72	Vol/F75	Area/I29			
24	XM-19		Vol/F75		Area/I40			
25	B steel		Area/C54		Area/E57			
26	Al		Area/E69		Area/B69			
27	Fuel meat		Vol/E26		Sar/E14			
28	Alloy 625		WP e/I18	WP e/I8	Glpk/D8			
29	304L		Glpk/D31	Glpk/D33	Glpk/D30			
30	DHLW gls		WP e/D23	WP e/F23	WP e/F27			
31	A516		Area/C54		Area/E57			
32	Gd				Area/E57			
33	Water		WP e/E34	WP e/E34	N/A			

Normalization

	A	B	C	D	E	F	G	H
1	Normalization of da							
2	Item	Volume	Mass	Mol. Wt.	Moles	Surface	Nor. Mol	Nor. Area
3	316 SS	66799.650209819	531257.618118691	55.3661495284846	=C3/D3	162131.968	=E3/$C$13*1000	=F3/$C$13*1000
4	XM-19	60532.1559628681	=7.88*B4	54.79757211174971	=C4/D4	70048.5241438682	=E4/$C$13*1000	=F4/$C$13*1000
5	B steel	13683.7068626568	=7.745*B5	52.5385499204442	=C5/D5	67377.5433058878	=E5/$C$13*1000	=F5/$C$13*1000
6	Al	40448.7869118384	=2.702*B6	26.98	=C6/D6	2200381.49273403	=E6/$C$13*1000	=F6/$C$13*1000
7	Fuel meat	23406.233445504	=2.188*B7	70.1182928029386	=C7/D7	622791.01248	=E7/$C$13*1000	=F7/$C$13*1000
8	Alloy 625	404678.956234566	3415490.39061974	60.8236823729208	56973.7952059278	188269.22317266	=E8/$C$13*1000	=F8/$C$13*1000
9	304L	91530.2226464507	723088.75890696	54.6658890893323	52909.5614312365	=4*113615.54198357	=E9/$C$13*1000	=F9/$C$13*1000
10	DHLW gls	2417155.11440086	6888392.07604246	21.1180834311677	326208.204380672	5649024.48053958	=E10/$C$13*1000	=F10/$C$13*1000
11	A516	13683.7068626568	=7.745*B11	52.5385499204442	=C11/D11	67377.5433058878	=E11/$C$13*1000	=F11/$C$13*1000
12	Gd*		1000	157.25	=C12/D12	67377.5433058878	=E12/$C$13*1000	=F12/$C$13*1000
13	Water	2917809.41192746	2917809.41192746					
14								
15	* Assumed 1 kg of							
16	for EQ6 runs. San							
17								
18	Links to other sprea							
19	sheet/cell. Some l							
20	from volume and							
21								
22	Item		Volume	Mass	Surface			
23	316SS		Vol/F72	Vol/F75	Area/I29			
24	XM-19		Vol/F73		Area/I40			
25	B steel		Area/C54		Area/E57			
26	Al		Area/E69		Area/B69			
27	Fuel meat		Vol/E26		Surf/E14			
28	Alloy 625		WP e/H8	WP e/J8	Glpk/D8			
29	304L		Glpk/D31	Glpk/D33	Glpk/D30			
30	DHLW gls		WP e/D23	WP e/F23	WP e/F27			
31	A516		Area/C54		Area/E57			
32	Gd				Area/E57			
33	Water		WP e/E34	WP e/E34	N/A			

Alloy

	A	B	C	D	E	F	G	H	I
1	CALCULATION OF MOLES FOR SPECIAL REACTANTS								
2									
3	Alloy 625, taken from Ref. 5.49, p. 10 or Ref. 5.16								
4									
5	Element	At. Wt.	Wt %	G-Atoms	Atom fr.	Atom fr. less Nb		Mol. Wt.	Mol. Wt.-Nb
6	Fe	55.847	5	0.089530324	0.053001667	0.05445564			
7	Cr	51.996	21.5	0.413493346	0.244786744	0.251501879			
8	Mn	54.938	0.5	0.009101169	0.005387863	0.005535666			
9	Ni	58.71	58	0.98790666	0.584837597	0.600881209			
10	Mo	95.94	9	0.09380863	0.05553441	0.057037863			
11	Nb	92.91	1.8	0.019373587	0.011469102				
12	Ta	180.947	1.8	0.009947664	0.005888986				
13	S	32.06	0.015	0.000467873	0.000276979	0.000284577			
14	Si	28.0855	0.5	0.017802781	0.01053919	0.010828307			
15	P	30.97376	0.015	0.000484281	0.000286693	0.000294557			
16	C	12.011	0.1	0.008325701	0.004928789	0.005063998			
17	Co	58.9332	0.93	0.015780579	0.009342052				
18	Ti	47.9	0.4	0.008350731	0.004943606	0.005079222			
19	Al	26.98154	0.4	0.014824951	0.008776324	0.009017081			
20			99.96	1.689198276	1	1		59.19968155	
21				1.644096446					60.82368237
22									
23	Alloy XM-19 Data from Ref. 5.49								
24									
25	Element	At. Wt.*	Wt %**	G-Atoms	Atom fr.	Atom fr.*			
26	C	12.011	0.06	0.004995421	0.002728281	0.002737369			
27	Mn	54.938	5	0.091011686	0.04970662	0.049872194			
28	P	30.974	0.04	0.001291406	0.00070531	0.000707659			
29	S	32.06	0.03	0.000935745	0.000511063	0.000512766			
30	Si	28.086	1	0.035604928	0.019445861	0.019510636			
31	Cr	52	22	0.423076923	0.231066191	0.231835882			
32	Ni	58.71	12.5	0.212910918	0.116282672	0.116670014			
33	Mo	95.94	2.25	0.023452158	0.012808547	0.012851213			
34	N	14.01	0.3	0.021413276	0.011694999	0.011733955			
35	Nb	92.91	0.2	0.002152621	0.001175668				
36	V	50.94	0.2	0.003926188	0.002144313				
37	Total		43.58						
38	Fe by diff.	55.85	56.42	1.010205909	0.551730475	0.553568311			
39	Totals		100	1.830977178	1	1			
40	Total minus Nb and V			1.824898369					
41	"mol. wt." (wgt of 1 "mole" of metal), all elements				54.61564525				
42	"mol. wt." (wgt of 1 "mole" of metal), without Nb & V				54.79757212				
43									
44	* From inside front cover of 58th CRC Handbook of Chemistry and Physics, Ref. 5.39								

Alloy

	A	B	C	D	E	F	G	H	I
45	** Average or max								

Alloy

	J	K
1		
2		
3		
4		
5		
6		
7		
8		
9		
10		
11		
12		
13		
14		
15		
16		
17		
18		
19		
20	= "mol. wt." (wgt of 1 "mole" of metal)	
21	= "mol. wt." (wgt of 1 "mole" of metal)	
22		
23		
24		
25		
26		
27		
28		
29		
30		
31		
32		
33		
34		
35		
36		
37		
38		
39		
40		
41		
42		
43		
44		

Alloy

	J	K
45		

Alloy

	A	B	C	D
1	CALCULATION OF MOLES FOR SPE			
2				
3	Alloy 625, taken from Ref. 5.49, p. 10			
4				
5	Element	At. Wt.	Wt %	G-Atoms
6	Fe	55.847	=5	=C6/B6
7	Cr	51.996	21.5	=C7/B7
8	Mn	54.938	0.5	=C8/B8
9	Ni	58.71	58	=C9/B9
10	Mo	95.94	9	=C10/B10
11	Nb	92.91	1.8	=C11/B11
12	Ta	180.947	1.8	=C12/B12
13	S	32.06	0.015	=C13/B13
14	Si	28.0855	0.5	=C14/B14
15	P	30.97376	0.015	=C15/B15
16	C	12.011	0.1	=C16/B16
17	Co	58.9332	0.93	=C17/B17
18	Ti	47.9	0.4	=C18/B18
19	Al	26.98154	0.4	=C19/B19
20			=SUM(C6:C19)	=SUM(D6:D19)
21				=D20-D11-D12-D17
22				
23	Alloy XM-19 Data from Ref. 5.49			
24				
25	Element	At. Wt.*	Wt %**	G-Atoms
26	C	12.011	0.06	=C26/B26
27	Mn	54.938	5	=C27/B27
28	P	30.974	0.04	=C28/B28
29	S	32.06	0.03	=C29/B29
30	Si	28.086	1	=C30/B30
31	Cr	52	22	=C31/B31
32	Ni	58.71	12.5	=C32/B32
33	Mo	95.94	2.25	=C33/B33
34	N	14.01	0.3	=C34/B34
35	Nb	92.91	0.2	=C35/B35
36	V	50.94	0.2	=C36/B36
37	Total		=SUM(C26:C36)	
38	Fe by diff.	55.85	=100-C37	=C38/B38
39	Totals		=C37+C38	=SUM(D26:D36)+D38
40	Total minus Nb and V			=SUM(D26:D34)+D38
41	"mol. wt." (wgt of 1 "mole" of metal), a			
42	"mol. wt." (wgt of 1 "mole" of metal), v			
43				
44	* From inside front cover of 58th CRC			

	Alloy			
	A	B	C	D
45	** Average or max			

Alloy

	E	F	G	H	I
1					
2					
3					
4					
5	Atom fr.	Atom fr. less Nb		Mol. Wt.	Mol. Wt.-Nb
6	=D6/$D$20	=D6/$D$21			
7	=D7/$D$20	=D7/$D$21			
8	=D8/$D$20	=D8/$D$21			
9	=D9/$D$20	=D9/$D$21			
10	=D10/$D$20	=D10/$D$21			
11	=D11/$D$20				
12	=D12/$D$20				
13	=D13/$D$20	=D13/$D$21			
14	=D14/$D$20	=D14/$D$21			
15	=D15/$D$20	=D15/$D$21			
16	=D16/$D$20	=D16/$D$21			
17	=D17/$D$20				
18	=D18/$D$20	=D18/$D$21			
19	=D19/$D$20	=D19/$D$21			
20	=SUM(E6:E19)	=SUM(F6:F19)		=100/I20	
21					=100/I21
22					
23					
24					
25	Atom fr.	Atom fr.			
26	=D26/$D$39	=D26/$D$40			
27	=D27/$D$39	=D27/$D$40			
28	=D28/$D$39	=D28/$D$40			
29	=D29/$D$39	=D29/$D$40			
30	=D30/$D$39	=D30/$D$40			
31	=D31/$D$39	=D31/$D$40			
32	=D32/$D$39	=D32/$D$40			
33	=D33/$D$39	=D33/$D$40			
34	=D34/$D$39	=D34/$D$40			
35	=D35/$D$39				
36	=D36/$D$39				
37					
38	=D38/$D$39	=D38/$D$40			
39	=SUM(E26:E36)+E38	=SUM(F26:F34)+F38			
40					
41	=100/D39				
42	=100/D40				
43					
44					

Alloy

	E	F	G	H	I
45					

	J
1	
2	
3	
4	
5	
6	
7	
8	
9	
10	
11	
12	
13	
14	
15	
16	
17	
18	
19	
20	= "mol. wt." (wgt of 1 "mole" of metal)
21	= "mol. wt." (wgt of 1 "mole" of metal)
22	
23	
24	
25	
26	
27	
28	
29	
30	
31	
32	
33	
34	
35	
36	
37	
38	
39	
40	
41	
42	
43	
44	

Alloy

45	J

	A	B	C	D	E	F	G	H	I	J
1	Element	Atom Fr.	At. Wgt.	Wgt.						
2	O	6.7011E-01	15.9994	1.0721E+01						
3	Mo	4.0556E-04	95.94	3.8909E-02						
4	Tc	3.8958E-04	98.9062	3.8521E-02						
5	Ru	3.7123E-04	101.07	3.7520E-02						
6	Rh	2.4046E-04	102.9055	2.4745E-02						
7	Ag	3.4554E-05	107.868	3.7273E-03						
8	Nd	5.8416E-04	144.24	8.1374E-02						
9	Sm	2.4101E-04	150.4	3.6247E-02						
10	Eu	3.7410E-05	151.96	5.6847E-03						
11	Gd	3.5271E-06	157.25	5.5464E-04						
12	U	3.2487E-01	238.029	7.7327E+01						
13	Np	3.3127E-04	237.0482	7.8527E-02						
14	Pu	2.3242E-03	240	5.5780E-01						
15	Am	6.9007E-05	243	1.6769E-02						
16		1.00E+00		88.97021571	= "mol. wt." (wgt of 1 "mole" of fuel)					
17										
18										
19	Uranium aluminide fuel, fresh									
20										
21	Element	wt%	At. wt.*	g-at.	at. %					
22	U	69.5	235.04	0.29569435	0.20733583					
23	Al	30.5	26.98	1.130467013	0.79266417					
24				1.426161362	1	70.1182928	= "mol. wt." (wgt of 1 "mole" of fuel)			
25										
26										
27	Composition from Ref. 8. 48, II-1									
28	* Atomic mass of U-235 taken from Ref. 8.39, p. B-343 for									
29	U-235, which constitutes 93.5% of the U in this fuel. At. wt. of Al taken from same source, from inside front cover.									
30										
31	Uranium aluminide assembly, 5 year old fuel. Data are based on output file mitburn.output**									
32										
33	Element/Isotope	Grams	At. wt.*	g-at.	at. %					
34	U-234	9.92E+03	234.04	42.38591694	0.000458584					
35	U-235	9.24E+05	235.04	3931.245745	0.042533131					
36	U-236	1.69E+03	236.05	7.159500106	7.74604E-05					
37	U-238	5.56E+04	238.05	233.8643772	0.002526991					
38	Al	2.38E+06	26.98	88213.49148	0.954403833					
39		3.37E+06		92427.84701	1	36.47396438	= "mol. wt." (wgt of 1 "mole" of fuel)			
40										
41	* Atomic masses of U-234 to 238 taken from Ref. 8.39, pp. B-343 to B-345 for									

	A	B	C	D	E	F	G	H	I	J
42	U-235, which constitutes 93.5% of the U in this fuel. At. wt. of Al taken from same source, from inside front cover.									
43	** Only nuclides constituting > ca. 1% of total are included in this spreadsheet. The large differences compared to fresh fuel arise because of including the Al clad, etc.									
44	Comparison of the initial U-235 vs. that at 5 yrs in the assembly indicates only negligible difference. Consequently, data for fresh fuel used for EQ6 calculations.									
45	No significant amount of Pu-239 produced (0.004% of U-235)									

	A	B	C	D	E
1	Element	Atom Fr.	At. Wgt.	Wgt.	
2	O	0.67011	15.9994	=B2*C2	
3	Mo	0.00040556	95.94	=B3*C3	
4	Tc	0.00039958	98.9062	=B4*C4	
5	Ru	0.00037123	101.07	=B5*C5	
6	Rh	0.00024046	102.9055	=B6*C6	
7	Ag	0.000034554	107.868	=B7*C7	
8	Nd	=0.00032345+0.00024071	144.24	=B8*C8	
9	Sm	=0.00010491+0.0000016385+0.00009	150.4	=B9*C9	
10	Eu	=0.0000070705+0.000030339	151.96	=B10*C10	
11	Gd	0.0000035271	157.25	=B11*C11	
12	U	=0.000000078159+0.000081496+0.00	238.029	=B12*C12	
13	Np	0.00033127	237.0482	=B13*C13	
14	Pu	=0.0000000111044+0.0018402+0.0004	240	=B14*C14	
15	Am	=0.000062515+0.00000000225034+0.0	243	=B15*C15	
16		=SUM(B2:B15)		=SUM(D2:D15)	= "mol. wt." (wgt of 1 "mole" of fu
17					
18					
19	Uranium aluminide fuel, fresh				
20					
21	Element	wt%	At. wt.*	g-at.	at. %
22	U	69.5	235.04	=B22/C22	=D22/$D$24
23	Al	30.5	26.98	=B23/C23	=D23/$D$24
24				=SUM(D22:D23)	=SUM(E22:E23)
25					
26					
27	Composition from Ref. 5, 48, II-1				
28	* Atomic mass of U-235 taken fr				
29	U-235, which constitutes 93.5%				
30					
31	Uranium aluminide assembly, 5 y				
32					
33	Element/isotope	Grams	At. wt.*	g-at.	at. %
34	U-234	9920	234.04	=B34/C34	=D34/$D$39
35	U-235	924000	235.04	=B35/C35	=D35/$D$39
36	U-236	1690	236.05	=B36/C36	=D36/$D$39
37	U-238	55600	238.05	=B37/C37	=D37/$D$39
38	Al	2380000	26.98	=B38/C38	=D38/$D$39
39		=SUM(B34:B38)		=SUM(D34:D38)	=SUM(E34:E38)
40					
41	* Atomic masses of U-234 to 23				

	A	B	C	D	E
42	U-235, which constitutes 93.5%				
43	** Only nuclides constituting > c				
44	Comparison of the initial U-23				
45	No significant amount of Pu-2				

	F	G
1		
2		
3		
4		
5		
6		
7		
8		
9		
10		
11		
12		
13		
14		
15		
16		
17		
18		
19		
20		
21		
22		
23		
24	=100/D24	= "mol. wt." (wgt of 1 "mole" of fu
25		
26		
27		
28		
29		
30		
31		
32		
33		
34		
35		
36		
37		
38		
39	=B39/D39	= "mol. wt." (wgt of 1 "mole" of fu
40		
41		

	F	G
42		
43		
44		
45		

	A	B	C	D	E	F	G
1	J-13 Water						
2							
3	J-13 water. Col B & C: Adjusted for pH 7.6397 and log fO2 = -2.5390 to be consistent with thermodynamic data.						
4	Col. F & G correspond to original data, balanced on Cl- and for log fO2 = -3.500						
5	J-13 water	Molality	Mole Fr.		J-13 water	Molality	Mole Fr.
6	Na	1.9922E-03	1.1963E-05		Na	1.9922E-03	1.1963E-05
7	Si	1.0169E-03	6.1063E-06		Si	1.0169E-03	6.1064E-06
8	Ca	3.2437E-04	1.9478E-06		Ca	3.2437E-04	1.9478E-06
9	K	1.2891E-04	7.7409E-07		K	1.2891E-04	7.7410E-07
10	C	2.1797E-03	1.3089E-05		C	1.4474E-04	8.6916E-07
11	F	1.1475E-04	6.8906E-07		F	1.1475E-04	6.8907E-07
12	Cl	2.0140E-04	1.2094E-06		Cl	2.1533E-04	1.2930E-06
13	N	1.42E-04	8.5269E-07		N	1.42E-04	8.5270E-07
14	Mg	8.27E-05	4.9660E-07		Mg	8.27E-05	4.9660E-07
15	S	1.9154E-04	1.1502E-06		S	1.9154E-04	1.1502E-06
16	B	1.2388E-05	7.4388E-08		B	1.2388E-05	7.4389E-08
17	P	1.2711E-06	7.6328E-09		P	1.2711E-06	7.6329E-09
18	H	111.0167	6.6664E-01		H	111.0167	6.6665E-01
19	Al	1.48E-08	8.9022E-11		O	55.5084	3.3332E-01
20	Ba	1.00E-10	6.0049E-13			166.5294671	1
21	Ce	1.00E-24	6.0049E-27				
22	Cr	3.45E-07	2.0706E-09				
23	Cu	1.00E-10	6.0049E-13				
24	Cs	1.00E-10	6.0049E-13				
25	Fe	1.15E-04	6.8906E-07				
26	Gd	1.00E-14	6.0049E-17				
27	La	1.00E-14	6.0049E-17				
28	Li	1.00E-10	6.0049E-13				
29	Mn	7.28E-07	4.3721E-09				
30	Mo	1.00E-10	6.0049E-13				
31	Nd	1.00E-14	6.0049E-17				
32	Ni	1.00E-10	6.0049E-13				
33	Pb	1.00E-10	6.0049E-13				
34	Pu	1.00E-14	6.0049E-17				
35	Sm	1.00E-10	6.0049E-13				
36	Sr	1.00E-10	6.0049E-13				
37	Ti	1.00E-10	6.0049E-13				
38	U	1.00E-14	6.0049E-17				
39	Zn	1.00E-10	6.0049E-13				
40	Zr	1.00E-20	6.0049E-23				

Water

	A	B	C	D	E	F	G
41	O	85.8084	3.3332E-01				
42		166.531604	1				

	A	B	C	D
1	J-13 Water			
2				
3	J-13 water. Col B & C: Adjusted			
4	Col. F & G correspond to origin			
5	J-13 water	Molality	Mole Fr.	
6	Na	0.0019922	=B6/$B$42	
7	Si	0.0010169	=B7/$B$42	
8	Ca	0.00032437	=B8/$B$42	
9	K	0.00012691	=B9/$B$42	
10	C	0.0021797	=B10/$B$42	
11	F	0.00011475	=B11/$B$42	
12	Cl	0.0002014	=B12/$B$42	
13	N	0.000142	=B13/$B$42	
14	Mg	0.000082699	=B14/$B$42	
15	S	0.00019154	=B15/$B$42	
16	B	0.000012388	=B16/$B$42	
17	P	0.0000012711	=B17/$B$42	
18	H	111.0167	=B18/$B$42	
19	Al	0.000000014825	=B19/$B$42	
20	Ba	0.0000000001	=B20/$B$42	
21	Ce	1E-34	=B21/$B$42	
22	Cr	0.00000034485	=B22/$B$42	
23	Cu	0.0000000001	=B23/$B$42	
24	Cs	0.0000000001	=B24/$B$42	
25	Fe	0.00011475	=B25/$B$42	
26	Gd	0.00000000000001	=B26/$B$42	
27	La	0.00000000000001	=B27/$B$42	
28	Li	0.0000000001	=B28/$B$42	
29	Mn	0.00000072809	=B29/$B$42	
30	Mo	0.0000000001	=B30/$B$42	
31	Nd	0.00000000000001	=B31/$B$42	
32	Ni	0.0000000001	=B32/$B$42	
33	Pb	0.0000000001	=B33/$B$42	
34	Pu	0.00000000000001	=B34/$B$42	
35	Sm	0.0000000001	=B35/$B$42	
36	Sr	0.0000000001	=B36/$B$42	
37	Ti	0.0000000001	=B37/$B$42	
38	U	0.00000000000001	=B38/$B$42	
39	Zn	0.0000000001	=B39/$B$42	
40	Zr	1E-20	=B40/$B$42	

	A	B	C	D
41	0	55.8084	=B41/$B$42	
42		=SUM(B6:B41)	=SUM(C6:C41)	

	E	F	G
1			
2			
3			
4			
5	J-13 water	Molality	Mole Fr.
6	Na	0.0019922	=F6/$F$20
7	Si	0.0010169	=F7/$F$20
8	Ca	0.00032437	=F8/$F$20
9	K	0.00012891	=F9/$F$20
10	C	0.00014474	=F10/$F$20
11	F	0.00011475	=F11/$F$20
12	Cl	0.00021833	=F12/$F$20
13	N	0.000142	=F13/$F$20
14	Mg	0.000062699	=F14/$F$20
15	S	0.00019154	=F15/$F$20
16	B	0.000012388	=F16/$F$20
17	P	0.0000012711	=F17/$F$20
18	H	111.0167	=F18/$F$20
19	O	55.5084	=F19/$F$20
20		=SUM(F6:F19)	=SUM(G6:G19)
21			
22			
23			
24			
25			
26			
27			
28			
29			
30			
31			
32			
33			
34			
35			
36			
37			
38			
39			
40			

Water

	E	F	G
41			
42			

	A	B	C	D	E	F	G
1	DHLW Glass			DHLW Glass			
2							
3	Component	gms.	Mol. Wt.	G-Atoms, 1st elem.	G-Atoms, 2nd elem.	2nd elem.	G-Atoms, oxygen
4	Ag	0.05	107.868				
5	Al2O3	3.96	101.96	0.077677521			0.116516281
6	B2O3	10.28	69.62	0.295317436			0.442976156
7	BaSO4	0.14	233.4	0.000599829	0.000599829	S	0.002399314
8	Ca3(PO4)2	0.07	310.18	0.000677026	0.000451351	P	0.001805403
9	CaO	0.85	56.08	0.015156919			0.015156919
10	CaSO4	0.08	136.14	0.00058763	0.00058763	S	0.002350522
11	Cr2O3	0.12	151.99	0.001579051			0.002368577
12	Cs2O*						
13	CuO	0.19	79.54	0.002388735			0.002388735
14	Fe2O3	7.04	159.69	0.088170831			0.132256246
15	FeO	3.12	71.85	0.0434238			0.0434238
16	K2O	3.58	94.2	0.076008493			0.038004246
17	Li2O	3.16	29.88	0.211512718			0.105756359
18	MgO	1.36	40.31	0.033738526			0.033738526
19	MnO	2	70.94	0.028192839			0.028192839
20	Na2O	11	61.98	0.354953211			0.177476605
21	Na2SO4	0.36	142.04	0.005068995	0.002534497	S	0.010137989
22	NaCl	0.19	58.44	0.003251198	0.003251198	Cl	
23	NaF	0.07	41.99	0.001667064	0.001667064	F	
24	NiO	0.93	74.71	0.012448133			0.012448133
25	PbS	0.07	239.25	0.000292581	0.000292581	S	
26	SiO2	45.57	60.06	0.758741259			1.517482517
27	ThO2*	0.21	264.04	0.000795334			0.001590668
28	TiO2*	0.99	79.9	0.012390488			0.024780976
29	U3O8	2.2	842.09	0.007837842			0.020900379
30	Zeolite*						
31	ZnO*	0.08	81.37	0.000983163			0.000983163
32	Np	0.000751	237.048	3.16813E-06			
33	Pu	0.01234	239.052	5.16206E-05			
34	Am*						
35	Tc	0.010797	99.906	0.000108072			
36	Zr	0.026415	91.22	0.000289575			
37	Pd*						
38	Sn*						
39	Ce	0.023811	141.909	0.000167791			
40	Ba	0.034794	137.33	0.000253361			

	A	B	C	D	E	F	G
41	Nd	0.024435	143.9099	0.000169794			
42	Sm	0.00681	150.4	4.52793E-05			
43							2.705779548
44	* Not considered at this time in the interest of simplyfying the calculations						
45							
46	Element	g-at.	Atom fr.				
47	Al	0.077677521	0.016404004				
48	B	0.295317438	0.062385383				
49	Ba	0.000599829	0.000126672				
50	Ca	0.016421575	0.003467922				
51	Cr	0.001579051	0.000333465				
52	Cu	0.002388735	0.000504455				
53	Fe	0.131594631	0.027790264				
54	K	0.076008493	0.016051537				
55	Li	0.211512718	0.044667432				
56	Mg	0.033738526	0.00712493				
57	Mn	0.028192839	0.005953787				
58	Na	0.364940467	0.077068432				
59	Cl	0.003251198	0.000686591				
60	F	0.001667064	0.000352052				
61	Ni	0.012449135	0.002628807				
62	P	0.000451351	9.53166E-05				
63	Pb	0.000292581	6.17875E-05				
64	S	0.004014537	0.000847783				
65	Si	0.758741259	0.160231612				
66	U	0.007837642	0.00165516				
67	O	2.705779548	0.571408782				
68	Np	3.16813E-06	6.69049E-07				
69	Pu	5.16206E-05	1.09013E-05				
70	Tc	1.01E-04	2.13445E-05	Value from ORIGEN run used			
71	Zr	2.84E-04	6.00467E-05	Value from ORIGEN run used			
72	Ce	0.000167791	3.54342E-05				
73	Nd	0.000169794	3.58572E-05				
74	Sm	4.52793E-05	9.56211E-06				
75	Total	4.735278195	1	21.11808343	= "mol. wt." (wgt of 1 "mole" of glass)		
76							
77							
78	Pb-free LaBS glass						
79							
80	Oxide	Wt %	Mol. Wt.	G-Atoms, metal	G-Atoms, oxygen	At fr. Metal	At. fr. oxygen

Glass

	A	B	C	D	E	F	G
81	SiO2	25.8	60.08	0.42942743	0.85885486	0.119043075	
82	B2O3	10.4	69.62	0.298764723	0.448147084	0.082821611	
83	Al2O3	19.04	101.96	0.373479796	0.560219694	0.103533637	
84	ZrO2	1.15	123.22	0.009332901	0.018665801	0.002587206	
85	Gd2O3	7.61	362.5	0.041966207	0.06297931	0.011639143	
86	La2O3	11.01	325.82	0.067583328	0.101374992	0.01873501	
87	Nd2O3	11.37	336.48	0.067582026	0.101373039	0.018734649	
88	SrO	2.22	103.62	0.021424435	0.021424435	0.005939142	
89	PuO2	11.39	274	0.041569343	0.083138686	0.011523583	
90		99.99		1.351150189	2.256177902	0.374557056	0.625442944
91							
92	Check sum of st. fr.		1				
93			27.7185766	= "mol. wt." (wgt of 1 "mole" of glass)			

	A	B	C	D
1	DHLW Glass			DHLW Glass
2				
3	Component	gms.	Mol. Wt.	G-Atoms, 1st elem.
4	Ag	0.05	107.868	
5	Al2O3	3.96	101.96	=2*B5/C5
6	B2O3	10.28	69.62	=2*B6/C6
7	BaSO4	0.14	233.4	=B7/C7
8	Ca3(PO4)2	0.07	310.18	=3*B8/C8
9	CaO	0.85	56.08	=$B9/$C9
10	CaSO4	0.08	136.14	=$B10/$C10
11	Cr2O3	0.12	151.99	=2*$B11/$C11
12	Cs2O*			
13	CuO	0.19	79.54	=$B13/$C13
14	Fe2O3	7.04	159.69	=2*$B14/$C14
15	FeO	3.12	71.85	=$B15/$C15
16	K2O	3.58	94.2	=2*$B16/$C16
17	Li2O	3.16	29.88	=2*$B17/$C17
18	MgO	1.36	40.31	=$B18/$C18
19	MnO	2	70.94	=$B19/$C19
20	Na2O	11	61.96	=2*$B20/$C20
21	Na2SO4	0.36	142.04	=2*$B21/$C21
22	NaCl	0.19	58.44	=$B22/$C22
23	NaF	0.07	41.99	=$B23/$C23
24	NiO	0.93	74.71	=$B24/$C24
25	PbS	0.07	239.25	=$B25/$C25
26	SiO2	45.57	60.06	=$B26/$C26
27	ThO2*	0.21	264.04	=$B27/$C27
28	TiO2*	0.89	79.9	=$B28/$C28
29	U3O8	2.2	842.09	=3*$B29/$C29
30	Zeolite*			
31	ZnO*	0.08	81.37	=$B31/$C31
32	Np	0.000751	237.048	=B32/C32
33	Pu	0.01234	239.052	=B33/C33
34	Am*			
35	Tc	0.010797	99.906	=B35/C35
36	Zr	0.026415	91.22	=B36/C36
37	Pd*			
38	Sn*			
39	Ce	0.023811	141.909	=B39/C39
40	Ba	0.034794	137.33	=B40/C40

Glass

	A	B	C	D
41	Nd	0.024435	143.9099	=B41/C41
42	Sm	0.00681	150.4	=B42/C42
43				
44	* Not considered at this time in the			
45				
46	Element	g-at.	Atom fr.	
47	Al	0.0778775205963123	=B47/$B$75	
48	B	0.2953174437517955	=B48/$B$75	
49	Ba	0.000599828620394173	=B49/$B$75	
50	Ca	=SUM(D8:D10)	=B50/$B$75	
51	Cr	=D11	=B51/$B$75	
52	Cu	=D13	=B52/$B$75	
53	Fe	=D14+D15	=B53/$B$75	
54	K	0.0760084925690021	=B54/$B$75	
55	Li	0.211512717536814	=B55/$B$75	
56	Mg	0.0337385264202431	=B56/$B$75	
57	Mn	0.0281928390188892	=B57/$B$75	
58	Na	=SUM(D20:D23)	=B58/$B$75	
59	Cl	=E22	=B59/$B$75	
60	F	=E23	=B60/$B$75	
61	Ni	=D24	=B61/$B$75	
62	P	=E8	=B62/$B$75	
63	Pb	=D25	=B63/$B$75	
64	S	=E7+E10+E21+E25	=B64/$B$75	
65	Si	=D26	=B65/$B$75	
66	U	=D29	=B66/$B$75	
67	O	=G43	=B67/$B$75	
68	Np	=D32	=B68/$B$75	
69	Pu	=D33	=B69/$B$75	
70	Tc	0.000101072	=B70/$B$75	Value from ORIGEN run used
71	Zr	0.000284338	=B71/$B$75	Value from ORIGEN run used
72	Ce	=D39	=B72/$B$75	
73	Nd	=D41	=B73/$B$75	
74	Sm	=D42	=B74/$B$75	
75	Total	=SUM(B47:B74)	=SUM(C47:C74)	=100/B75
76				
77				
78	Pb-free LaBS glass			
79				
80	Oxide	Wt %	Mol. Wt.	G-Atoms, metal

Glass

	A	B	C	D
81	SiO2	25.8	60.08	=$B81/$C81
82	B2O3	10.4	69.62	=2*$B82/$C82
83	Al2O3	18.04	101.96	=2*$B83/$C83
84	ZrO2	1.15	123.22	=$B84/$C84
85	Gd2O3	7.61	362.5	=2*$B85/$C85
86	La2O3	11.01	325.82	=2*$B86/$C86
87	Nd2O3	11.37	336.48	=2*$B87/$C87
88	SrO	2.22	103.62	=$B88/$C88
89	PuO2	11.39	274	=$B89/$C89
90		=SUM(B81:B89)		=SUM(D81:D89)
91				
92	Check sum of at. fr.		=F90+G90	
93			=B90/(D90+E90)	= "mol. wt." (wgt of 1 "mole" of glass)

	E	F	G
1			
2			
3	G-Atoms, 2nd elem.	2nd elem.	G-Atoms, oxygen
4			
5			=3*B5/C5
6			=3*B6/C6
7	=B7/C7	S	=4*B7/C7
8	=2*B8/C8	P	=8*B8/C8
9			=$B9/$C9
10	=$B10/$C10	S	=4*$B10/$C10
11			=3*$B11/$C11
12			
13			=$B13/$C13
14			=3*$B14/$C14
15			=$B15/$C15
16			=$B16/$C16
17			=$B17/$C17
18			=$B18/$C18
19			=$B19/$C19
20			=$B20/$C20
21	=$B21/$C21	S	=4*$B21/$C21
22	=$B22/$C22	Cl	
23	=$B23/$C23	F	
24			=$B24/$C24
25	=$B25/$C25	S	
26			=2*$B26/$C26
27			=2*$B27/$C27
28			=2*$B28/$C28
29			=8*$B29/$C29
30			
31			=$B31/$C31
32			
33			
34			
35			
36			
37			
38			
39			
40			

	E	F	G
41			
42			
43			=SUM(G4:G26)+G29
44			
45			
46			
47			
48			
49			
50			
51			
52			
53			
54			
55			
56			
57			
58			
59			
60			
61			
62			
63			
64			
65			
66			
67			
68			
69			
70			
71			
72			
73			
74			
75	= "mol. wt." (wgt of 1 "mole" of glass)		
76			
77			
78			
79			
80	G-Atoms, oxygen	At fr. Metal	At. fr. oxygen

Glass

	E	F	G
81	=2*$B81/$C81	=D81/($D$90+$E$90)	
82	=3*$B82/$C82	=D82/($D$90+$E$90)	
83	=3*$B83/$C83	=D83/($D$90+$E$90)	
84	=2*$B84/$C84	=D84/($D$90+$E$90)	
85	=3*$B85/$C85	=D85/($D$90+$E$90)	
86	=3*$B86/$C86	=D86/($D$90+$E$90)	
87	=3*$B87/$C87	=D87/($D$90+$E$90)	
88	=$B88/$C88	=D88/($D$90+$E$90)	
89	=2*$B89/$C89	=D89/($D$90+$E$90)	
90	=SUM(E81:E89)	=SUM(F81:F89)	=E90/($D$90+$E$90)
91			
92			
93			

	A	B	C	D	E	F	G	H	I	J
1	Rates of reaction									
2	For 304L & Alloy 625, area is in cm**2, for HLW it is the conversion factor from m**2 to cm**2									
3	Rates in columns F & G are in volume (cm**3) for the metals, but in grams for glasses.									
4										
5	Mat'l	Rate, mm/yr	Rt,gm/m2/d	Area,cm^2	Rate/yr	Rate/sec	Density (gm/cm^3)	Rt,gms/sec	Rt,mols/sec	
6										
7	Alloy 625*	1.008E-02		1.000E+00	1.008E-06	3.196E-14	8.440E+00	2.698E-13	4.500E-15	
8	316L**	1.000E-01		1.000E+00	1.000E-05	3.171E-13	7.953E+00	2.522E-12	4.207E-14	
9	304L***	1.500E-01		1.000E+00	1.500E-05	4.756E-13	7.900E+00	3.758E-12	6.874E-14	
10	C-steel ****	3.000E+01		1.000E+00	3.000E-03	9.513E-11	7.832E+00	7.451E-10	1.371E-11	
11	A516*****	2.223E+01		1.000E+00	2.223E-03	7.050E-11	7.832E+00	5.522E-10	1.000E-11	
12	B-steel******	8.000E-01		1.000E+00	8.000E-05	2.537E-12	7.745E+00	1.965E-11	3.775E-13	
13	HLW*******		2.791E-02	1.000E-04	1.019E-03	3.230E-11		3.230E-11	1.529E-12	
14	HLW********		2.000E-04	1.000E-04	7.300E-06	2.315E-13		2.315E-13	1.096E-14	
15										
16	* Rate assumed to be approximately 1/10 of corrosion rate of corrosion of 316L stainless steel, specifically 4.5E-15 moles/cm2/sec. Assumption 4.3.10									
17	** Reference 5.16, p. 11									
18	*** Reference 5.16, p. 11									
19	**** Reference 5.36, p. 47, rate in water at 30 C at short times.									
20	***** Value for C-steel, Reference 5.36, p. 47, rounded to 1.0E-11 moles.cm2/sec									
21	****** Reference 5.16, p. 12. For conservatism, the rate was doubled (Assumption 4.3.27)									
22	Reference 5.9, p. 4. Used for runs with high degradation rates.									
23	Reference 5.36, Fig. 6.2-5, pH ca. 5.5-8.5, 25C, approximate average value. Used for runs with low degradation rates.									

	A	B	C	D	E	F	G
1	Rates of reaction						
2	For 304L & Alloy 625, area i						
3	Rates in columns F & G are i						
4							
5	Mat'l	Rate, mm/yr	Rt,gm/m2/d	Area,cm^2	Rate/yr	Rate/sec	Density
6							(gm/cm^3)
7	Alloy 625*	=0.01007925		1	=B7*D7*0.0001	=E7/(3600*24*365)	8.44
8	316L **	0.1		1	=B8*D8*0.0001	=E8/(3600*24*365)	7.953
9	304L***	0.15		1	=B9*D9*0.0001	=E9/(3600*24*365)	7.9
10	C-steel ****	30		1	=B10*D10*0.0001	=E10/(3600*24*365)	7.832
11	A516*****	22.233		1	=B11*D11*0.0001	=E11/(3600*24*365)	7.832
12	B-steel******	0.8		1	=B12*D12*0.0001	=E12/(3600*24*365)	7.745
13	HLW*******		0.027906976744186	0.0001	=C13*D13*365	=E13/(3600*24*365)	
14	HLW********		0.0002	0.0001	=C14*D14*365	=E14/(3600*24*365)	
15							
16	* Rate assumed to be approxi						
17	** Reference 5.16, p. 11						
18	*** Reference 5.16, p. 11						
19	**** Reference 5.36, p. 47, ta						
20	***** Value for C-steel, Refe						
21	****** Reference 5.16, p. 12.						
22	Reference 5.9, p. 4. Used for						
23	Reference 5.36, Fig. 6.2-5, pH						

	H	I
1		
2		
3		
4		
5	Rt,gms/sec	Rt,mols/sec
6		
7	=F7*G7	=H7/59.94478
8	=F8*G8	=H8/59.94478
9	=F9*G9	=H9/54.66589
10	=F10*G10	=H10/54.34
11	=F11*G11	=H11/55.21545
12	=F12*G12	=H12/52.048
13	=F13	=H13/21.11982
14	=F14	=H14/21.11982
15		
16		
17		
18		
19		
20		
21		
22		
23		

	A	B	C	D	E	F	G	H	I
1	Calculation of surface areas and otherwise unknown volumes and masses for MIT spent fuel canister								
2									
3	Area of surface of Al cladding around the U-Al "meat"								
4	See MIT drawing RJF-3-2, rev D, dtd. 5/18/70. (Ref. 5.4)								
5									
6	Ribs on plate, outside area:								
7	Height, in.	Width, in.	Space, in.	Contour length,	Ribs/side	End Len.	End thick.		Perimeter.
8				in.		in.	in.		in.
9	0.01	0.01	0.01	0.04	110	0.171	0.06		9.604
10									
11	Area adjacent to "meat":								
12	Thickness	Width, in.	Length, in.	Area/plate, in^2	Area/can (cm^2)				
13	in.								
14	0.03	2.18	22.75	100.555	622791.0125				
15									
16	Assumption: From BBA000000-01717-0200-00051 REV 00, p. 7, assume overall codisposal canister length of 272 cm. (Ref. 5.57)								
17									
18	Details of internal design for lengths of various components taken, in part, from: Evaluation of Codisposal Viability for Aluminum-Clad DOE-Owned, Spent Fuel: Phase I, Intact Codisposal Canister,								
19	Document Identifier BBA000000-01717-5705-00011 REV00. (Ref. 5.38)								
20									
21	316 Stainless steel								
22	Data for cross sectional area in the basket structure and volume/meter of length of basket of the steel taken from: Structural Evaluation of MIF-SNF Co-disposal Canister								
23	Document Identifier BBA000000-01717-0200-00051 REV 00, pp. 15-16. (Ref. 5.57)								
24	Inside radius of the codisposal canister taken from p. 25, Criticality Safety and Shielding Evaluations of the Codisposal Canister in the Five-Pack DHLW Waste Package								
25	Document Identifier BBA000000-1717-0200-00052 REV 00. (Ref. 5.48)								
26									
27	Length of steel in basket, ref. 00011, = 64 cm								
28									
29									
30	Basket.vol	Cross sectional Area,cm^2	Vol.per m of length, cm^3	Mass/m, g	Mass/bskt	Mass/pkg			
31		280	28000	222684	142517.76	570071.04			
32									
33	Basket.area								
34									
35									
36									
37	B stainless steel							Area/1 cm	Area/0.5 cm
38			Vol./3 center plates	Mass/plate	Mass/can	Circum.,cm.	Side area	thick plate	thick plate
39	Divider Plates	1315.749976	1315.749976	10190.48356	40761.93425	128.5853873	128.5853873	2760.085339	2695.792645

	J	K	L	M	N
1					
2					
3					
4					
5					
6					
7	Rib length	Area/plate	Area (cm^2)	Area/	Area (cm^2)/
8	in.	cm^2	assembly	qtr. can	canister
9	22.75	1409.616536	21144.24803	338307.9685	1353231.874
10					
11					
12					
13					
14					
15					
16					
17					
18					
19					
20					
21					
22					
23					
24					
25					
26					
27					
28					
29					
30					
31					
32					
33					
34					
35					
36					
37					
38	Area/pkg				
39	13671.84131				

	A	B	C
1	Calculation of surface areas and otherwise		
2			
3	Area of surface of Al cladding around the		
4	See MIT drawing 83F-3-2, rev D, dtd. 5/		
5			
6	Ribs on plate, outside area:		
7	Height, in.	Width, in.	Space, in.
8			
9	0.01	0.01	0.01
10			
11	Area adjacent to "meat":		
12	Thickness	Width, in.	Length, in.
13	in.		
14	0.03	=2.2-0.02	22.75
15			
16	Assumption: From BBA000000-01717-02		
17			
18	Details of internal design for lengths of var		
19	Document Identifier BBA000000-01717-		
20			
21	316 Stainless steel		
22	Data for cross sectional area in the basket		
23	Document Identifier BBA000000-01717		
24	Inside radius of the codisposal canister tal		
25	Document Identifier BBA000000-1717-(		
26			
27	Length of steel in basket, ref. 00011, = 64		
28			
29			
30	Basket,vol	Cross sectional Area,cm^2	Vol.per m of length, cm^3
31		=0.028*10000	=B31*100
32			
33	Basket,area		
34			
35			
36			
37	B stainless steel		
38			Vol./3 center plates
39	Divider Plates	=PI()*20.463^2	=B39

	D	E	F	G	H
1					
2					
3					
4					
5					
6					
7	Contour length,	Ribs/side	End Len,	End thick,	
8	in.		in.	in.	
9	=2*A9+B9+C9	110	0.171	0.06	
10					
11					
12	Area/plate, in^2	Area/can (cm^2)			
13					
14	=2*(A14+B14)*C14	=D14*15*16*2.54^2*4			
15					
16					
17					
18					
19					
20					
21					
22					
23					
24					
25					
26					
27					
28					
29					
30	Mass/m, g	Mass/bskt	Mass/pkg		
31	=C31*7.953	=D31*0.64	=E31*4		
32					
33					
34					
35					
36					
37					Area/1 cm
38	Mass/plate	Mass/can	Circum.,cm.	Side area	thick plate
39	=C39*7.745	=D39*4	=2*PI()*20.465	=F39	=G39+2*B39

	I	J	K	L	M	N
1						
2						
3						
4						
5						
6						
7	Perimeter,	Rib length	Area/plate	Area (cm^2)	Area/	Area (cm^2)/
8	in.	in.	cm^2	assembly	qtr. can	canister
9	=D9*E9*2+F9*4+G9*2	22.75	=I9*J9*2.54^2	=K9*15	=L9*16	=4*M9
10						
11						
12						
13						
14						
15						
16						
17						
18						
19						
20						
21						
22						
23						
24						
25						
26						
27						
28						
29						
30						
31						
32						
33						
34						
35						
36						
37	Area/0.5 cm					
38	thick plate	Area/pkg				
39	=G39/2+2*B39	=3*H39+2*I39				

	A	B	C	D	E	F	G	H	I
1	X stands for areas, or cross sectional								
2									
3	316 Stainless steel basket								
4									
5	Points are labeled from a to z and A to L on a copy of Fig. I-1 in ref. 5.57								
6	Lengths are derived from file mkt.xls, and measured using the AutoSketch software. They are either straight								
7	line distances between two points, perimeters of areas, or, for curved lines perimeters of an area minus the length of the chord,								
8	measured seperately.								
9									
10	The design for the combination of baskets is assumed to be: 1) An outer shell of XM-19 stainless steel of OD 43.93 cm and thickness								
11	1.5 cm; total length of 4*64 cm + 5*1 cm + 2*1.5 cm. See p. I-1 in Ref 5.57. Other data from Ref. 5.38.								
12	2) End plates of XM-19 for ends of the cylinder described in 1); OD 40.93 cm, 1.5 cm thick. 3) 1 cm thick plates of B-steel above								
13	and below the combination of baskets and between each pair of baskets; thus, 5 plates 1 cm thick and OD 40.93 cm.								
14	4) 4 baskets each 64 cm long as shown in cross section on p. I-1 of Ref 5.57.								
15									
16	Desc. of meas.	Value,cm	Chord desc.	Chord,cm	Element	X-sect. of surface,cm	Combined X-sect.	Area, cm^2 -per basket	Area/combo
17									
18	a-b	13.5			a-b	13.5	27		
19	c-h-g-c	22.83	c-g	8.1	c-h-g	14.73	58.92		
20	d-e-j-l-d	30.872			d-e-j-l-d	30.872	123.488		
21	f-l-k-f	13.84			f-l-k-f	13.84	55.36		
22	m-n-r-q-m	16.68	m-q	6.56	m-n-r-q	10.12	20.24		
23	o-p-t-s-o	78.67			o-p-t-s-o	78.67	157.34		
24	u-w-v-u	13.23			u-w-v-u	13.23	26.46		
25	x-z-y-x	15.47	x-z	6.34	x-y-z	9.13	18.26		
26	A-B-H-A	13.42			A-B-H-A	13.42	26.84		
27	C-D-J-I-C	46.43			C-D-J-I-C	46.43	92.86		
28	G-L-K-G	13.28			G-L-K-G	13.28	26.56		
29							633.328	40532.992	162131.968
30	XM-19 Stainless Steel, inside surface								
31	a-b+arc(a-b)	27.26	a-b	13.5	a-b arc	13.76	27.52		
32	g-c+arc(g-c)	21.39	g-c	8.1	g-c arc	13.29	53.16		
33	m-q+arc(m-q)	14.16	m-q	6.56	q-m arc	7.6	15.2		
34	x-z+arc(x-z)	13.54	x-z	6.34	x-z arc	7.2	14.4		
35							110.28	7057.92	28231.68
36	XM-19 plates at ends of cylinder								
37	Sides								257.1707746
38	Top and bottom								5262.999903
39	XM-19 SS, outside surface; diameter from p. I-1 in Ref. 5.57								36296.67347
40	Total surface of XM-19								70048.52414
41									

	A	B	C	D	E	F	G	H	I
42	B Stainless Steel								
43		X-Area	X-perimeter	Long side	Height	Volume/assembly*	Perimeter/asbly*	Axial length**	Vol./qtr cm*
44	Base plate	1.526	14.49	7.04	0.22	86.726395	7.45	56.8325	1040.71674
45	Divider	2.08	16.3						1064.96
46									
47	* Not all assemblies have associated B-steel								
48	** This is less than length of assembly. Assumed equal to length of cut fuel plates, 22.375in * 2.54; see Ref. 5.48, p. 7								
49	Length used in spreadsheet "axial homogenization" of file mixnum.xls is 23.0 in.								
50								Area/1 cm	Area/0.5 cm
51	Axial		Vol./plate	Mass/plate		Circum.,cm.	Side area	thick plate	thick plate
52	Divider Plates	1315.749976	1315.749976	10190.48356	40761.93425	128.5853873	128.5853873	2760.085339	2695.792645
53									
54	Total B steel		Vol	Mass	Area				
55	in asblies		8422.70696	65233.86541	53705.702				
56	in div. plates		5262.999903	40761.93425	13671.84131				
57	Total		13685.70686	105995.7997	67377.54331				
58									
59	Aluminum								
60		Assembly outside		Assembly inside					
61		X-Area	X-Perimeter	X-Area	X-Perimeter	Net X-area/assembly	Total X-perim/asbly	Vol./asbly.	Area/asbly
62	Bsk side plates	43.72	28.38	37.58	26.33	6.14	54.71	392.96	3501.44
63	Outside of cladding -- see surface sheet in this file								21144.24803
64	Inside of cladding -- see surface sheet in this file								
65	Combs -- 2 per assembly*								
66		X-Area	Thickness**	Vol./asbly	Fraction Al	Al area/asbly	Vol Al/asbly	Al area/can	
67		43.72	0.635	27.7622	0.345314	66.61151951	9.586676331	266.446078	
68	Al totals	Area	Vol.side+comb	Vol. clad	Total	Mass			
69		2200381.493	1610.185705	38338.60021	40448.78691				
70	*From file mixnum.xls, sheet "axial homogenization" one can deduce that the comb structure is 0. 635 cm thick, and consists of								
71	65.4686 % water and the remainder of Al. Area is assumed here to be the same as for outside of Al assembly.								
72	**For both combs together								

	J	K	L
1			
2			
3			
4			
5			
6			
7			
8			
9			
10			
11			
12			
13			
14			
15			
16			
17			
18			
19			
20			
21			
22			
23			
24			
25			
26			
27			
28			
29			
30			
31			
32			
33			
34			
35			
36			
37			
38			
39			
40			
41			

	J	K	L
42			
43	Area/qtr can*	Vol/canister	Area/canister
44	5080.8255	4162.86696	20323.302
45	8345.6	4259.84	33382.4
46		8422.70696	53705.702
47			
48			
49			
50			
51	Area/pkg		
52	13671.84131		
53			
54			
55			
56			
57			
58			
59			
60			
61	Area/qtr can	Area/canister	
62	56023.04	224092.16	
63	338307.9685	1353231.874	
64		622791.0125	
65			
66			
67			
68			
69			
70			
71			
72			

	A	B	C	D	E
1	X stands for cross, or cross sectional				
2					
3	316 Stainless steel basket				
4					
5	Points are labeled from a to z and A to L on a				
6	Lengths are derived from file mit.xls, and m				
7	line distances between two points, perimeters				
8	measured separately.				
9					
10	The design for the combination of baskets is				
11	1.5 cm; total length of 4*64 cm + 5*1 cm +				
12	2) End plates of XM-19 for ends of the cyl				
13	and below the combination of baskets and				
14	4) 4 baskets each 64 cm long as shown in c				
15					
16	Desc. of meas.	Value,cm	Chord desc.	Chord,cm	Element
17					
18	a-b	13.5			a-b
19	c-h-g-c	22.83	c-g	8.1	c-h-g
20	d-e-j-i-d	30.872			d-e-j-i-d
21	f-l-k-f	13.84			f-l-k-f
22	m-n-r-q-m	16.68	m-q	6.56	m-n-r-q
23	o-p-t-s-o	78.67			o-p-t-s-o
24	u-w-v-u	13.23			u-w-v-u
25	x-e-y-x	15.47	x-z	6.34	x-y-z
26	A-B-H-A	13.42			A-B-H-A
27	C-D-J-I-C	46.43			C-D-J-I-C
28	G-L-K-G	13.28			G-L-K-G
29					
30	XM-19 Stainless Steel, inside surface				
31	a-b+arc(a-b)	27.26	a-b	13.5	a-b arc
32	g-c+arc(g-c)	21.39	g-c	8.1	g-c arc
33	m-q+arc(m-q)	14.16	m-q	6.56	q-m arc
34	x-z+arc(x-z)	13.54	x-z	6.34	x-z arc
35					
36	XM-19 plates at ends of cylinder				
37	Sides				
38	Top and bottom				
39	XM-19 SS, outside surface; diameter from p				
40	Total surface of XM-19				
41					

	A	B	C	D	E
42	B Stainless Steel				
43		X-Area	X-perimeter	Long side	Height
44	Base plate	1.526	14.49	7.04	0.22
45	Divider	2.08	16.3		
46					
47	* Not all assemblies have associated B-steel				
48	** This is less than length of assembly. A				
49	Length used in spreadsheet "axial homog				
50					
51	Axial		Vol./plate	Mass/plate	
52	Divider Plates	=PI()*20.465^2	=B52	=C52*7.745	=D52*4
53					
54	Total B steel		Vol	Mass	Area
55	in assblies		=K46	=C55*7.745	=L46
56	in div. plates		=4*C52	=C56*7.745	=J52
57	Total		=SUM(C55:C56)	=SUM(D55:D56)	=SUM(E55:E56)
58					
59	Aluminum				
60		Assembly outside		Assembly inside	
61		X-Area	X-Perimeter	X-Area	X-Perimeter
62	Ext. side plates	43.72	28.38	37.58	26.33
63	Outside of cladding -- see surface sheet in th				
64	Inside of cladding -- see surface sheet in this				
65	Combs -- 2 per assembly*				
66		X-Area	Thickness**	Vol./assbly	Fraction Al
67		43.72	0.635	=B67*C67	=1-0.654686
68	Al totals	Area	Vol.side+comb	Vol. clad.	Total
69		=K62+K63+K64+H67	=(H62+G67)*4	38838.6002065152	=C69+D69
70	*From file mitnum.xls, sheet "axial homog				
71	65.4686 % water and the remainder of Al.				
72	**For both combs together				

	F	G	H	I
1				
2				
3				
4				
5				
6				
7				
8				
9				
10				
11				
12				
13				
14				
15				
16	X-sect. of surface,cm	Combined X-sect.	Area, cm^2	Area/combo
17			--per basket	
18	=B18-D18	=2*F18		
19	=B19-D19	=4*F19		
20	=B20-D20	=4*F20		
21	=B21-D21	=4*F21		
22	=B22-D22	=2*F22		
23	=B23-D23	=2*F23		
24	=B24-D24	=2*F24		
25	=B25-D25	=2*F25		
26	=B26-D26	=2*F26		
27	=B27-D27	=2*F27		
28	=B28-D28	=2*F28		
29		=SUM(G18:G28)	=64*G29	=4*H29
30				
31	=B31-D31	=2*F31		
32	=B32-D32	=4*F32		
33	=B33-D33	=2*F33		
34	=B34-D34	=2*F34		
35		=SUM(G31:G34)	=64*G35	=4*H35
36				
37				=PI()*40.93*2
38				=PI()*(40.93/2)^2*2*2
39				=PI()*(43.93)*(64*4+1.5*2+1*4)
40				=I35+SUM(I37:I39)
41				

	F	G	H	I
42				
43	Volume/assembly*	Perimeter/asbly*	Axial length**	Vol./qtr can*
44	=H44*B44	=C44-D44	=22.375*2.54	=12*F44
45				=B45*8*64
46				
47				
48				
49				
50			Area/1 cm	Area/0.5 cm
51	Circum.,cm.	Side area	thick plate	thick plate
52	=2*PI()*20.465	=F52	=G52+2*B52	=G52/2+2*B52
53				
54				
55				
56				
57				
58				
59				
60				
61	Net X-area/assembly	Total X-perim/asbly	Vol./asbly	Area/asbly
62	=B62-D62	=C62+E62	=64*F62	=64*Q62
63				21144.348034
64				
65				
66	Al area/asbly	Vol Al/asbly	Al area/can	
67	=(4*B62+C87*C62)*E67	=D67*E67	=4*F67	
68	Mass			
69				
70				
71				
72				

	J	K	L
1			
2			
3			
4			
5			
6			
7			
8			
9			
10			
11			
12			
13			
14			
15			
16			
17			
18			
19			
20			
21			
22			
23			
24			
25			
26			
27			
28			
29			
30			
31			
32			
33			
34			
35			
36			
37			
38			
39			
40			
41			

	J	K	L
42			
43	Area/qtr can*	Vol/canister	Area/canister
44	=12*G44*H44	=I44*4	=J44*4
45	=G45*I*64	=I45*4	=J45*4
46		=SUM(K44:K45)	=SUM(L44:L45)
47			
48			
49			
50			
51	Area/pkg		
52	=3*H52+2*I52		
53			
54			
55			
56			
57			
58			
59			
60			
61	Area/qtr can	Area/canister	
62	=16*I62	=4*I62	
63	338307.968544	1353231.874176	
64		622791.01248	
65			
66			
67			
68			
69			
70			
71			
72			

	A	B	C	D	E	F	G	H	I
1	Calculation of volumes and masses for MIT spent fuel canister								
2									
3	Area of surface of Al cladding around the U-Al "meat"								
4	See MIT drawing R3F-3-2, rev D, dtd. 5/18/70. Records Batch # MOY-970605-02 (Ref. 5.4)								
5									
6	Ribs on plate								
7	Height, in.	Width, in.	Space, in.	Length,	Ribs/side	X-sect ribs/side	Rib length	Rib vol/plate	Rib vol/assbly
8				in.			in.	in.^3	in.^3
9	0.01	0.01	0.01	2.18	110	0.011	22.75	0.5005	120.12
10									
11	Ends of plates								
12	End Len,	End thick,	End area/plate	End vol	End vol/pkg				
13	in.	in.	in^2	in^3	cm^3				
14	0.171	0.06	0.02052	0.46683	7343.974164				
15									
16	Al clad between ribs and fuel								
17	Len	Thick	Area/plate	Vol/plate	Vol/pkg				
18	in.	in.	in^2	in^3	cm^3				
19	2.2	0.015	0.066	1.5015	23620.96953				
20									
21	Total Al volume in fuel plates			38838.60021					
22									
23	Fuel								
24	Thickness	Width, in.	Length, in.	Vol/plate	Vol/pkg	Area			
25	in.			in^3	cm^3				
26	0.03	2.18	22.75	1.48785	23406.23345	622791.0125			
27									
28	Assumption: From BBA000000-01717-0200-00051 REV 00A, p. 7, assume overall codisposal canister length of 272 cm.								
29									
30	Details of internal design for lengths of various components taken, in part, from: Evaluation of Codisposal Viability for Aluminum-Clad DOE-Owned, Spent Fuel: Phase I, Intact								
31	Document Identifier BBA000000-01717-5705-00011 REV00. (Ref. 5.38)								
32									
33									
34	Water volume #								
35	This is estimated by combining the various entries in spreadsheets in mtmum.xls. In many of the individual spreadsheets the volume								
36	of water in individual components, e.g. the fuel itself, is determined and expressed as a volume fraction of that item. Later, these								
37	numbers are combined into the fractions in another item. Multiplication of the volume fraction of water in an item by the volume								
38	fraction of the item in a subsequent spreadsheet, i.e. a combination of items, and addition of any new volume fraction of water								
39	yields the volume fraction of water in the new combination of items. Upon completion, the volume fraction of water in the entire								
40	canister is obtained.								
41									

	A	B	C	D	E	F	G	H	I
42	Item	spreadsheet	Vol. fr. water	Fr. of asby	Fr. of cell	Fr. water in cell	Fr. of cell2	Fr.water in cell2	Fr of cell+div
43									
44	Fuel "cell"*	Intact sides	0.654686073	0.910575391	0.84844054	0.505845761			
45	Side plates	MIT Asby	0	0.089324609					
46	Side water	MIT cell	0.15155946		0.15155946	0.15155946			
47	Total fraction in fuel cell + side water					0.657405221	0.61553809	0.404657955	
48	Water cells	MIT cell 2	0.164814691				0.164814691	0.164814691	
49	Total fraction in cell2							0.569472645	0.964196901
50									
51	Item	spreadsheet	Fr. of cyl. ten.	Water fr. in item					
52	Cell 2 tot	N/A	0.889	0.54908376					
53	Divider	Cell+divider	0	0					
54	Combs	Axial homog.	0.009769231	0.654686073					
55	Water	Axial homog.	0.085846154	1					
56									
57	Overall water fraction in cylinder			0.580377395					
58	Water volume in cylinder			225197.0735					
59									
60	* Called "plate array" in Homog. MIT Asby								
61	** Combined water fr. is the fraction of the total water in the entire canister that comes from the item in column A.								
62	# The set of spreadsheets in file mitnum.xls combines components axially before the final homogenization to a cylinder.								
63	In the homogenization to a cylinder the cross-sectional areas of water cells, fuel cells, and stainless steel are normalized and								
64	multiplied by the corresponding compositions of the cells and steel. However, the contribution of the water cells was already								
65	taken into account in spreadsheet, "Homog. MIT cell (2)". Doing so for a second time is a mistake. So far as the water content is								
66	concerned, the homogenization should stop at the spreadsheet, "Axial homogenization". The 316 SS is added in for the								
67	homogenized cylinder spreadsheet, but it should have been incorported before axial homogenization.								
68									
69	Data from file mitnum.xls, sheet basket vol.:				tube radius	20.465	tube area	1315.749976	
70									
71			X-section	length	volume/qtr	vol/can	density	mass	
72	316 Stainless steel		289.0008229	57.785	16699.91253	66799.65021	7.953	531257.6181	
73	XM-19, tube		199.9466644	64	13996.26651	55985.06604			
74	XM-19, ends		1513.69664	3		4547.08992			
75	XM-19, total					60532.15596			

	J
1	
2	
3	
4	
5	
6	
7	Rib vol/pkg
8	cm^3
9	7873.656511
10	
11	
12	
13	
14	
15	
16	
17	
18	
19	
20	
21	
22	
23	
24	
25	
26	
27	
28	
29	
30	codisposal Canister.
31	
32	
33	
34	
35	
36	
37	
38	
39	
40	
41	

	J
42	Fr. water in cell + div.
43	
44	
45	
46	
47	
48	
49	0.54908376
50	
51	
52	
53	
54	
55	
56	
57	
58	
59	
60	
61	
62	
63	
64	
65	
66	
67	
68	
69	
70	
71	
72	
73	
74	
75	

	A	B	C	D	E
1	Calculation of volumes and mas				
2					
3	Area of surface of Al cladding				
4	See MIT drawing R3F-3-2, re				
5					
6	Ribs on plate				
7	Height, in.	Width, in.	Space, in.	Length,	Ribs/side
8				in.	
9	0.01	0.01	0.01	=2.2-0.02	110
10					
11	Ends of plates				
12	End Len,	End thick,	End area/plate	End vol	End vol/pkg
13	in.	in.	in^2	in^3	cm^3
14	0.171	0.06	=A14*B14*2	=C14*O9	=D14*2.54^3*15*16*4
15					
16	Al clad between ribs and fuel				
17	Len	Thick	Area/plate	Vol/plate	Vol/pkg
18	in.	in.	in^2	in^3	cm^3
19	2.2	0.015	=A19*B19*2	=C19*O9	=D19*2.54^3*15*16*4
20					
21	Total Al volume in fuel plates			=J9+E14+E19	
22					
23	Fuel				
24	Thickness	Width, in.	Length, in.	Vol/plate	Vol/pkg
25	in.			in^3	cm^3.
26	0.03	=2.2-0.02	22.75	=A26*B26*C26	=D26*2.54^3*15*16*4
27					
28	Assumption: From BBA00000				
29					
30	Details of internal design for le				
31	Document Identifier BBA000				
32					
33					
34	Water volume #				
35	This is estimated by combinin				
36	of water in individual compor				
37	numbers are combined into th				
38	fraction of the item in a subse				
39	yields the volume fraction of				
40	canister is obtained.				
41					

	A	B	C	D	E
42	Item	spreadsheet	Vol. fr. water	Fr. of assy	Fr. of cell
43					
44	Fuel "cell"*	Intact sides	0.654686073174539	0.910675391290359	=1-C46
45	Side plates	MIT Assy	0	=1-D44	
46	Side water	MIT cell	0.151559460348061		0.151559460348061
47	Total fraction in fuel cell + side				
48	Water cells	MIT cell 2	0.164814690676691		
49	Total fraction in cell2				
50					
51	Item	spreadsheet	Fr. of cyl. len.	Water fr. in item	
52	Cell 2 tot	N/A	0.889	=J49	
53	Divider	Cell+divider	0	0	
54	Combs	Axial homog.	0.00976923076923085	0.654686073174539	
55	Water	Axial homog.	0.0858461538461538	1	
56					
57	Overall water fraction in cylind			=C52*D52+C54*D54+C55*D55	
58	Water volume in cylinder			=PI()*(43.93/2)^2*64*4*D57	
59					
60	* Called "plate array" in Homog				
61	** Combined water fr. is the fr				
62	# The set of spreadsheets in fil				
63	- hi the homogenization to a cy				
64	multiplied by the correspond				
65	taken into account in spreads				
66	concerned, the homogenizati				
67	homogenized cylinder spread				
68					
69	Data from file mitnum.xls, shee				tube radius
70					
71			X-section	length	volume/qtr
72	316 Stainless steel		=0.219647218898483*H69	57.785	=C72*D72
73	XM-19, tube		=PI()*((43.93/2)^2-((43.93-3)/2)^2)	64	=C73*(D73+3+1.5*2)
74	XM-19, ends		=PI()*(43.93/2)^2	=1.5*2	
75	XM-19, total				

	F	G	H	I
1				
2				
3				
4				
5				
6				
7	X-sect ribs/side	Rib length	Rib vol/plate	Rib vol/asbly
8		in.	in.^3	in.^3
9	=A9*B9*E9	22.75	=F9*O9*2	=H9*15*16
10				
11				
12				
13				
14				
15				
16				
17				
18				
19				
20				
21				
22				
23				
24	Area			
25				
26	=(2*(A26+B26)*C26)*2.54^2*16*15*4			
27				
28				
29				
30				
31				
32				
33				
34				
35				
36				
37				
38				
39				
40				
41				

	F	G	H	I
42	Fr. water in cell	Fr. of cell2	Fr.water in cell2	Fr of cell+div
43				
44	=C44*D44*E44			
45				
46	0.151559460348061			
47	=F44+F46	0.615538090424826	=F47*G47	
48		0.164814690676691	0.164814690676691	
49			=H47+H48	0.964196900661083
50				
51				
52				
53				
54				
55				
56				
57				
58				
59				
60				
61				
62				
63				
64				
65				
66				
67				
68				
69	20.465	tube area	=PI()*F69^2	
70				
71	vol/can	density	mass	
72	=E72*4	7.953	=F72*G72	
73	=E73*4			
74	=C74*D74			
75	=SUM(F73:F74)			

	J
1	
2	
3	
4	
5	
6	
7	Rib vol/pkg
8	cm^3
9	=I9*2.54^3*4
10	
11	
12	
13	
14	
15	
16	
17	
18	
19	
20	
21	
22	
23	
24	
25	
26	
27	
28	
29	
30	
31	
32	
33	
34	
35	
36	
37	
38	
39	
40	
41	

	J
42	Pr. water in cell + div.
43	
44	
45	
46	
47	
48	
49	=H49*I49
50	
51	
52	
53	
54	
55	
56	
57	
58	
59	
60	
61	
62	
63	
64	
65	
66	
67	
68	
69	
70	
71	
72	
73	
74	
75	

	A	B	C	D	E	F	G	H	I	J
1	Container									
2	Internal volume									
3		ID, cm	Hgt. inside	Vol						
4		156.9	303.5	5868058.894						
5										
6	Alloy 625 inner barrier									
7		OD	ID	Hgt	Cyl. vol	End thick	End vol.	Tot vol	Density	Mass
8		160.9	156.9	303.5	303013.8371	2.5	101665.1191	404678.9562	8.44	3415490.391
9										
10	304L shell for DHLW glass -- 4 canisters									
11	Calculations per canister									
12		OD	ID	Overall hgt	Cyl hgt outside	End thick	Cyl hgt inside	Cyl. vol inside*	Cyl. vol outside	End vol
13		60.96	57.785	299.64	274.26	1.5875	271.085	710927.9748	800464.8569	8326.526071
14										
15	* Assumes that ends fit inside the cylinder									
16										
17	Combination of 4 canisters									
18		Vol	Mass	Moles						
19		399426.9949	3155473.259	57722.75679						
20										
21	DHLW glass									
22		Vol. inside 304L	Vol.gls/can	vol gls/pkg	Density	Mass/pkg	Mol. Wt.	Moles/pkg		
23		710927.9748	604288.7786	2417155.114	2.85	6888392.076	21.11808343	326208.2044		
24										
25		Outside surface area, 4 canisters; ef. file glpckdim.xls:				188300.816				
26		Fracture factor				30				
27		Surface area, 4 canisters				5649024.481				
28										
29	Total water in package									
30		Volume of Al fuel canister			400143.913					
31		Between inner barrier and canisters			2266055.554	Does not subtract volume of neck on canisters				
32		Void volume in 4 DHLW canisters			426556.7849	See file glpkgdim.xls, sheet area&vol				
33		Void volume in Al fuel canister			225197.0735					
34		Water volume/pkg			2917809.412					

	K	L	M	N	O	P	Q	R
1								
2								
3								
4								
5								
6								
7	"Mol. Wt."	Moles						
8	59.94844434	56973.79521						
9								
10								
11								
12	Vol ends + cyl	Neck OD	Neck vol	Tot vol	Density	Mass	"Mol. Wt."	Moles
13	97863.40818	10	1993.340539	99856.74872	7.9	788868.3149	54.66601796	14430.6892
14								
15								
16								
17								
18								
19								
20								
21								
22								
23								
24								
25								
26								
27								
28								
29								
30								
31								
32								
33								
34								

	A	B	C	D	E
1	Container				
2	Internal volume				
3		ID, cm	Hgt. inside	Vol	
4		156.9	303.5	=PI()*(B4/2)^2*C4	
5					
6	Alloy 625 inner barrier				
7		OD	ID	Hgt	Cyl. vol
8		160.9	156.9	303.5	=PI()*(160.9/2)^2*D8-D4
9					
10	304L shell for DHLW glass -				
11	Calculations per canister				
12		OD	ID	Overall hgt	Cyl hgt outside
13		60.96	=B13-2*1.5875	299.64	=D13-25.38
14					
15	* Assumes that ends fit insi				
16					
17	Combination of 4 canisters				
18		Vol	Mass	Moles	
19		=4*N13	=4*P13	=4*R13	
20					
21	DHLW glass				
22		Vol. inside 304L	Vol.gls/can	vol gls/pkg	Density
23		=PI()*(C13/2)^2*G13	=B23*0.85	=C23*4	2.85
24					
25		Outside surface area, 4 canisters; cf. file glpck			
26		Fracture factor			
27		Surface area, 4 canisters			
28					
29	Total water in package				
30		Volume of Al fuel canister			400143.91298691
31		Between inner barrier and canisters			=D4-4*I13-E30
32		Void volume in 4 DHLW canisters			426556.78439427
33		Void volume in Al fuel canister			225197.073491509
34		Water volume/pkg			=SUM(E31:E33)

	F	G	H	I	J
1					
2					
3					
4					
5					
6					
7	End thick	End vol.	Tot vol	Density	Mass
8	2.5	=PI()*(B8/2)^2*2*F8	=E8+G8	8.44	=H8*I8
9					
10					
11					
12	End thick	Cyl hgt inside	Cyl. vol inside*	Cyl. vol outside	End vol
13	1.5875	=E13-2*1.5875	=PI()*(C13/2)^2*G13	=PI()*(B13/2)^2*E13	=PI()*(C13/2)^2*F13*2
14					
15					
16					
17					
18					
19					
20					
21					
22	Mass/pkg	Mol. Wt.	Moles/pkg		
23	=D23*E23	21.1180834311677	=F23/G23		
24					
25	188300.816017986				
26	30				
27	=F25*F26				
28					
29					
30					
31	Does not subtract volume of				
32	See file gipkgdim.xls, sheet a				
33					
34					

	K	L	M	N	O	P
1						
2						
3						
4						
5						
6						
7	"Mol. Wt."	Moles				
8	=100/1.6681	=J8/K8				
9						
10						
11						
12	Vol ends + cyl	Neck OD	Neck vol	Tot vol	Density	Mass
13	=I13-H13+J13	10	=PI()*(L13/2)^2*(D13-E13)	=K13+M13	7.9	=N13*O13
14						
15						
16						
17						
18						
19						
20						
21						
22						
23						
24						
25						
26						
27						
28						
29						
30						
31						
32						
33						
34						

	Q	R
1		
2		
3		
4		
5		
6		
7		
8		
9		
10		
11		
12	"Mol. Wt."	Moles
13	=100/1.82929	=P13/Q13
14		
15		
16		
17		
18		
19		
20		
21		
22		
23		
24		
25		
26		
27		
28		
29		
30		
31		
32		
33		
34		

	A	B	C	D	E	F	G	H	I	J	K	L
1	Calculation of volumes and other physical characteristics for a codisposal waste package											
2												
3	Inner barrier -- alloy 625											
4	OD, cm			160.9								
5	ID, cm			156.9								
6	Height, inside lid to inside lid			303.5								
7	Height, outside lid to outside lid			312								
8	Area of inside of inner barrier			188269.223								
9	Area of outside of inner barrier			198376.512								
10	Volume			475844.54	404678.956							
11	Density			8.44	8.44							
12	Mass			4016127.91	3415490.39							
13	Mol. Wt. without Nb			61.3904937	61.3904937							
14	Moles			65419.378	55635.4931							
15												
16	Volume inside inner barrier			5868058.89								
17												
18	Filler glass canister											
19	Overall outside height			299.64								
20	OD, cm			60.96								
21	ID, cm			57.785								
22	Height, inside lid to inside lid			271.085								
23	Height, outside lid to outside lid			274.26								
24	Area of inside of canister			54456.9949								
25	Area of outside of canister			58361.2109								
26	Volume			89536.8821								
27	Neck, est. -- OD			10								
28	Neck, hgt			25.38								
29	Neck, vol			1993.34054								
30	Total metal area			113615.542		Area at top of neck effectively already included above						
31	Total metal volume			91530.2226								
32	Density of 304L steel			7.9								
33	Mass			723088.759								
34	Mol. Wt. of 304L steel			54.6658891								
35	Moles of 304L steel			13227.4215		Moles in 4 canisters		52909.6862				
36	Total metal area, w/o neck			112818.206		Area for 4 canisters		451272.823				
37	Total volume of canister			802438.197		Vol for 4 canisters		3209832.79				
38	Interior volume			710927.975		Vol for 4 canisters		2843711.9				
39	Glass volume			604288.779		Vol for 4 canisters		2417155.11				
40	Glass density			2.85								

	A	B	C	D	E	F	G	H	I	J	K	L
41	Glass mass			1722223.02		Vol for 4 canisters		6888892.08				
42	Glass mol. wt.			21.1180834								
43	Glass moles			81552.0511		Vol for 4 canisters		326208.204				
44	Glass surface area, outside			47075.204		Area for 4 canisters		188300.816	For fracture factor of 100			18830081.6
45	Void volume			106639.196		Vol for 4 canisters		426556.785				
46	Void inside barrier & outside											
47	4 canisters			2658226.1								

	A	B	C	D
1	Calculation of volumes and			
2				
3	Inner barrier – alloy 825			
4	OD, cm			160.9
5	ID, cm			156.9
6	Height, inside lid to inside bi			303.5
7	Height, outside lid to outside			312
8	Area of inside of inner barrie			=PI()*D5*D6+PI()*(D5/2)^2*2
9	Area of outside of inner barr			=PI()*D4*D7+PI()*(D4/2)^2*2
10	Volume			=PI()*((D4/2)^2-(D5/2)^2)*D6+2*PI()*(D4/2)^2*((D7-D6)/2)
11	Density			8.44
12	Mass			=D10*D11
13	Mol. Wt. without Nb			61.3904937337781
14	Moles			=D12/D13
15				
16	Volume inside inner barrier			=PI()*(D5/2)^2*D6
17				
18	Filler glass canister			
19	Overall outside height			299.64
20	OD, cm			60.96
21	ID, cm			=D20-2*1.5875
22	Height, inside lid to inside bi			=D23-2*1.5875
23	Height, outside lid to outside			=299.64-25.38
24	Area of inside of canister			=PI()*D21*D22+PI()*(D21/2)^2*2
25	Area of outside of canister			=PI()*D20*D23+PI()*(D20/2)^2*2
26	Volume			=PI()*((D20/2)^2-(D21/2)^2)*D22+2*PI()*(D20/2)^2*((D23-D22)/2)
27	Neck, est. – OD			10
28	Neck, hgt			=D19-D23
29	Neck, vol			=PI()*(D27/2)^2*D28
30	Total metal area			=D24+D25+PI()*D27*D28
31	Total metal volume			=D26+D29
32	Density of 304L steel			7.9
33	Mass			=D31*D32
34	Mol. Wt. of 304L steel			54.6658890893323
35	Moles of 304L steel			=D33/D34
36	Total metal area, w/o neck			=D24+D25
37	Total volume of canister			=PI()*(D20/2)^2*D23+D29
38	Interior volume			=PI()*(D21/2)^2*D22
39	Glass volume			=0.85*D38
40	Glass density			2.85

	A	B	C	D
41	Glass mass			=D39*D40
42	Glass mol. wt.			23.1180834311677
43	Glass moles			=D41/D42
44	Glass surface area, outside			=PI()*D21*D22*0.85+2*PI()*(D21/2)^2
45	Void volume			=0.15*D38
46	Void inside barrier & outsid			
47	4 canisters			=D16-H37

	E	F	G	H	I
1					
2					
3					
4					
5					
6					
7					
8					
9					
10	=PI()*((D4/2)^2-(D5/2)^2)*D6+2*PI()*(D4/2)^2*2.5				
11	8.44				
12	=E10*E11				
13	61.3904937337781				
14	=E12/E13				
15					
16					
17					
18					
19					
20					
21					
22					
23					
24					
25					
26					
27					
28					
29					
30		Area at top of neck effective			
31					
32					
33					
34					
35		Moles in 4 canisters		=4*D35	
36		Area for 4 canisters		=4*D36	
37		Vol for 4 canisters		=4*D37	
38		Vol for 4 canisters		=4*D38	
39		Vol for 4 canisters		=4*D39	
40					

	E	F	G	H	I
41		Vol for 4 canisters		=4*D41	
42					
43		Vol for 4 canisters		=4*D43	
44		Area for 4 canisters		=4*D44	Per fracture factor of 100
45		Vol for 4 canisters		=4*D45	
46					
47					

	J	K	L
1			
2			
3			
4			
5			
6			
7			
8			
9			
10			
11			
12			
13			
14			
15			
16			
17			
18			
19			
20			
21			
22			
23			
24			
25			
26			
27			
28			
29			
30			
31			
32			
33			
34			
35			
36			
37			
38			
39			
40			

	J	K	L
41			
42			
43			
44			=100*H44
45			
46			
47			

	A	B	C	D	E	F	G	H	I	J
1	Calculations for uranium and boron in the MIT fuel waste package during a simulated degradation and flushing									
2	Source files are UAIIIb5mm. Doesn't include HLW. MIT fuel & B-steel are included									
3	Data in columns including "moles" in the heading have been normalized to 1 kg of initial water in the waste package									
4		Multipliers for moles in solids--multiply moles of solid by these factors to get moles of element								
5		Borated steel		6.24E-02		Mole fraction of B in the steel				
6		Atomic weight of B		10.81						
7		Atomic weight of U-235		235						
8		Normalizing factor		2917.8	Used to convert output values, which were normalized to 1 kg water initially, back to an					
9					entire waste package					
10										
11	Time, yrs	pH	Moles U in soln	kg U in soln	Moles B in soln	kg B in soln	Moles U-235, fuel	Moles U, soddyite	Tot moles U	Tot kg U
12	5756	7.7523	8.69E-18	5.96E-15	1.30E-05	4.09E-04	0.051825	0	5.18E-02	3.55E+01
13	5813	7.1168	2.36E-08	1.62E-05	7.75E-04	2.45E-02	0	5.18E-02	5.18E-02	3.55E+01
14	6531	6.9036	1.35E-08	9.29E-06	2.08E-03	6.57E-02	0	5.18E-02	5.18E-02	3.55E+01

	K	L	M
1			
2			
3			
4			
5			
6			
7			
8			
9			
10			
11	Moles B in reactants	Tot moles B	Tot kg B
12	4.36E-02	4.36E-02	1.37E+00
13	4.26E-02	4.33E-02	1.37E+00
14	3.03E-02	3.24E-02	1.02E+00

	A	B	C	D	E
1	Calculations for uranium an				
2	Source files are UAIIIb5mm				
3	Data in columns including				
4		Multipliers for moles in solic			
5		Borated steel		0.062404	
6		Atomic weight of B		10.81	
7		Atomic weight of U-235		235	
8		Normalizing factor		2917.8	Used to convert output values, which were i
9					entire waste package
10					
11	Time, yrs	pH	Moles U in soln	kg U in soln	Moles B in soln
12	5756	7.7523	8.691006E-18	=C12*$D$7*$D$8/1000	0.00001298074
13	5813	7.1168	0.00000002356641	=C13*$D$7*$D$8/1000	0.0007751749
14	6531	6.9036	0.00000001354551	=C14*$D$7*$D$8/1000	0.002083993

	F	G	H	I
1				
2				
3				
4				
5	Molc fraction of B in the steel			
6				
7				
8				
9				
10				
11	kg B in soln	Moles U-235, fuel	Moles U, soddyite	Tot moles U
12	=E12*$D$6*$D$8/1000	=0.25*0.2073	=0*2	=C12+G12
13	=E13*$D$6*$D$8/1000	0	=0.025912*2	=C13+G13+H13
14	=E14*$D$6*$D$8/1000	0	=0.025912*2	=C14+G14+H14

	J	K	L	M
1				
2				
3				
4				
5				
6				
7				
8				
9				
10				
11	Tot kg U	Moles B in reactants	Tot moles B	Tot kg B
12	=I12*$D$7*$D$8/1000	=0.698*$D$5	=E12+K12	=L12*$D$6*$D$8/1000
13	=I13*$D$7*$D$8/1000	=0.6822*$D$5	=E13+K13	=L13*$D$6*$D$8/1000
14	=I14*$D$7*$D$8/1000	=0.48517*$D$5	=E14+K14	=L14*$D$6*$D$8/1000

	A	B	C	D	E	F	G	H	I
1	Calculations for uranium and boron in the MIT fuel waste package during a simulated degradation and flushing								
2	Source files are UAIIaSenmr, UAIIIaSenmr, and UAIIIaSenmr. Includes HLW and MIT fuel, B-steel								
3	Data in columns including "moles" in the heading have been normalized to 1 kg of initial water in the waste package								
4		Multipliers for moles in solids--multiply moles of solid by these factors to get moles of element							
5		Borated steel		6.18E-02		Mole fraction of B in the steel			
6		DHLW Glass		6.24E-02		Mole fraction of B in the glass			
7		Borax		4		Gram atoms of B in borax			
8		DHLW Glass		1.66E-03		Mole fraction of U-238 in glass			
9		Atomic weight of B		10.81					
10		Atomic weight of U-235		235					
11		Normalizing factor		2917.8	Used to convert output values, which were normalized to 1 kg water initially, back to an				
12					entire waste package				
13									
14	Time, yrs	pH	Moles U in soln	kg U in soln	Moles B in soln	kg B in soln	Moles U-235, fuel	Moles U, soddyite	Mol U in DHLW
15	0	8.4953	0	0.00E+00		0.00E+00	0.051825	0	1.85E-01
16	12.6	9.2229	3.88E-03	2.66E+00	7.21E-02	2.27E+00	0	4.98E-02	1.83E-01
17	369	9.1344	8.17E-02	5.60E+01	1.13E-01	3.58E+00	0	0	1.28E-01
18	1001	9.8818	2.18E-02	1.50E+01	2.32E-01	7.33E+00	0		3.23E-02
19	1206	9.8868	1.80E-02	1.23E+01	2.11E-01	6.65E+00	0		0.00E+00
20	1999	8.8418	3.74E-05	2.56E-02	2.15E-01	6.79E+00	0		0.00E+00
21	2996	8.7543	1.62E-08	1.11E-05	2.28E-01	7.19E+00	0		0.00E+00
22	4008	8.847	6.21E-12	4.25E-09	2.15E-01	6.77E+00	0		0.00E+00
23	5006	8.2409	2.79E-15	1.91E-12	1.09E-04	3.43E-03	0		0.00E+00
24	6002	7.8536	1.27E-18	8.69E-16	1.24E-05	3.92E-04	0		0.00E+00
25	7104	7.6437	2.54E-22	1.74E-19	1.24E-05	3.91E-04	0		0.00E+00
26				0.00E+00		0.00E+00	0		0.00E+00
27				0.00E+00		0.00E+00	0		0.00E+00
28									
29	* Includes B in unreacted solids, but mostly the B is simulated to be in borax								
30									
31									
32		Computation of U-235 in solution							
33									
34	Stage*	pH	Time,yrs	Moles U in soln	U from fuel	U from DHLW	U ppt'd, moles	U-235 fraction	U-235 ppt'd,moles
35	1		0	0	0	0			
36	1	9.1944	9.99E+00	3.42E-03	0.051825	1.95E-03	0.049952	9.64E-01	4.81E-02
37	1	9.2229	1.26E+01	3.96E-03	0.051825	1.95E-03	0.049816	9.64E-01	4.80E-02
38	2	9.2229	1.26E+01	3.88E-03			0.049816	0.963682655	4.80E-02
39	2	9.1828	2.80E+01	7.97E-03	0.051825	4.34E-03	0.048114	9.23E-01	4.44E-02

5mm+HLW

	A	B	C	D	E	F	G	H	I
40	3	9.1828	2.80E+01	7.78E-03			0.048114	0.922785297	4.44E-02
41	3	9.1771	4.08E+01	1.19E-02	0.051825	6.31E-03	0.046014	8.92E-01	4.10E-02
42	4	9.1771	4.08E+01	1.16E-02			0.046014	8.92E-01	4.10E-02
43									
44	Approximation to be used after this step is that the ratio of U-235 to total U is about the ratio of U from the fuel to total U released to solution.								
45									
46		9.1344	369	8.17E-02	0.051825	5.71E-02		4.76E-01	0.00E+00
47		9.8818	1001	2.18E-02	0.051825	1.53E-01		2.53E-01	0.00E+00
48		9.8868	1206	1.80E-02	0.051825	1.85E-01		2.19E-01	0.00E+00
49		8.8418	1999	3.74E-05	0.051825	1.85E-01		2.19E-01	0.00E+00
50		8.7543	2996	1.62E-08	0.051825	1.85E-01		2.19E-01	0.00E+00
51		8.847	4008	6.21E-12	0.051825	1.85E-01		2.19E-01	0.00E+00
52		8.2409	5006	2.79E-15	0.051825	1.85E-01		2.19E-01	0.00E+00
53		7.8536	6002	1.27E-18	0.051825	1.85E-01		2.19E-01	0.00E+00
54		7.6437	7104	2.54E-22	0.051825	1.85E-01		2.19E-01	0.00E+00

	J	K	L	M	N	O	P	Q	R	S
1										
2										
3										
4										
5										
6										
7										
8										
9										
10										
11										
12										
13										
14	Tot moles U	Tot kg U-235	Tot kg U	Moles B in ppt*	Moles B in reactants	Tot moles B	Tot kg B			
15	2.37E-01	3.55E+01	1.62E+02	0.00E+00	7.02E+00	7.02E+00	2.21E+02			
16	2.37E-01	3.55E+01	1.62E+02	0.00E+00	6.94E+00	7.01E+00	2.21E+02			
17	2.10E-01	2.67E+01	1.44E+02	4.91E-01	4.86E+00	5.46E+00	1.72E+02	Last point taken from run UAlla5mmr.slio		
18	5.42E-02	3.79E+00	3.71E+01	4.16E+00	1.25E+00	5.64E+00	1.78E+02			
19	1.80E-02	2.69E+00	1.23E+01	5.02E+00	2.56E-02	5.25E+00	1.66E+02			
20	3.74E-05	5.61E-03	2.56E-02	3.70E+00	1.43E-02	3.92E+00	1.24E+02			
21	1.62E-08	2.42E-06	1.11E-05	1.85E+00	7.31E-05	2.08E+00	6.57E+01			
22	6.21E-12	9.31E-10	4.25E-09	0.00E+00	0.00E+00	2.15E-01	6.77E+00			
23	2.79E-15	4.18E-13	1.91E-12	0.00E+00	0.00E+00	1.09E-04	3.43E-03			
24	1.27E-18	1.90E-16	8.69E-16	0.00E+00	0.00E+00	1.24E-05	3.92E-04			
25	2.54E-22	3.80E-20	1.74E-19	0.00E+00	0.00E+00	1.24E-05	3.91E-04			
26	0.00E+00	0.00E+00	0.00E+00	0.00E+00	0.00E+00	0.00E+00	0.00E+00			
27	0.00E+00	0.00E+00	0.00E+00	0.00E+00	0.00E+00	0.00E+00	0.00E+00			
28										
29										
30										
31										
32										
33										
34	Moles U-235 in soln	Tot U-235, moles; soln + ppt.	Kg U-235 in solution							
35	0									
36	3.30E-03	5.14E-02	2.26E+00							
37	3.81E-03	5.18E-02	2.61E+00							
38	3.74E-03	5.17E-02	2.56E+00							
39	7.36E-03	5.18E-02	5.04E+00							

5mm+HLW

	J	K	L	M	N	O	P	Q	R	S
40	7.17E-03	5.16E-02	4.92E+00							
41	1.06E-02	5.16E-02	7.24E+00							
42	1.03E-02	5.14E-02	7.10E+00							
43										
44										
45										
46	3.89E-02	3.89E-02	2.67E+01							
47	5.53E-03	5.53E-03	3.79E+00							
48	3.93E-03	3.93E-03	2.69E+00							
49	8.18E-06	8.18E-06	5.61E-03							
50	3.53E-09	3.53E-09	2.42E-06							
51	1.36E-12	1.36E-12	9.31E-10							
52	6.10E-16	6.10E-16	4.18E-13							
53	2.77E-19	2.77E-19	1.90E-16							
54	5.55E-23	5.55E-23	3.80E-20							

	T
1	
2	
3	
4	
5	
6	
7	
8	
9	
10	
11	
12	
13	
14	
15	
16	
17	
18	
19	
20	
21	
22	
23	
24	
25	
26	
27	
28	
29	
30	
31	
32	
33	
34	
35	
36	
37	
38	
39	

	T
40	
41	
42	
43	
44	
45	
46	
47	
48	
49	
50	
51	
52	
53	
54	

	A	B	C	D	E
1	Calculations for uranium ma				
2	Source files are UAlla5mmr.				
3	Data in columns including				
4		Multipliers for moles in solic			
5		Borated steel		0.061821	
6		DHLW Glass		0.062365	
7		Borax		4	
8		DHLW Glass		0.00165515	
9		Atomic weight of B		10.81	
10		Atomic weight of U-235		235	
11		Normalizing factor		2917.8	Used to convert output values, which were
12					entire waste package
13					
14	Time, yrs	pH	Moles U in soln	kg U in soln	Moles B in soln
15	0	8.4953	0	=C15*$D$10*$D$11/1000	
16	12.6	9.2229	0.003876157	=C16*$D$10*$D$11/1000	0.0720734
17	369	9.1344	0.08169775	=C17*$D$10*$D$11/1000	0.113436
18	1001	9.8818	0.02183792	=C18*$D$10*$D$11/1000	0.2323445
19	1206	9.8868	0.01795413	=C19*$D$10*$D$11/1000	0.2107885
20	1999	8.8418	0.00003739604	=C20*$D$10*$D$11/1000	0.2151748
21	2996	8.7543	0.000000016615246	=C21*$D$10*$D$11/1000	0.2280385
22	4008	8.847	0.000000000006205423	=C22*$D$10*$D$11/1000	0.2147411
23	5006	8.2409	2.786924E-15	=C23*$D$10*$D$11/1000	0.0001088248
24	6002	7.8536	1.267016E-18	=C24*$D$10*$D$11/1000	0.0000124313
25	7104	7.6437	2.535799E-22	=C25*$D$10*$D$11/1000	0.000001238694
26				=C26*$D$10*$D$11/1000	
27				=C27*$D$10*$D$11/1000	
28					
29	* Includes B in sorbated sp				
30					
31					
32		Computation of U-235 in so			
33					
34	Stage*	pH	Time,yrs	Moles U in soln	U from fuel
35	1		0	0	0
36	1	9.1944	9.994	0.003419818	=G15-G16
37	1	9.2229	12.58	0.003955716	0.051825
38	2	9.2229	12.58	0.003876157	
39	2	9.1828	28.04	0.007970465	0.051825

5mm+HLW

	A	B	C	D	E
40	3	9.1828	28.04	0.007775029	
41	3	9.1771	40.82	0.01185095	0.051825
42	4	9.1771	40.82	0.01160795	
43					
44	Approximation to be used at				
45					
46		9.1344	369	0.08169775	0.051825
47		9.8818	1001	0.02183792	0.051825
48		9.8868	1206	0.01795413	0.051825
49		8.8418	1999	0.00003738907	0.051825
50		8.7543	2996	0.00000001615246	0.051825
51		8.847	4008	0.000000000006205423	0.051825
52		8.2409	5006	2.7869245-15	0.051825
53		7.8536	6002	1.267016E-18	0.051825
54		7.6437	7104	2.535799E-22	0.051825

	F	G	H	I
1				
2				
3				
4				
5	Mole fraction of B in the steel			
6	Mole fraction of B in the glass			
7	Gram atoms of B in borax			
8	Mole fraction of U-238 in glass			
9				
10				
11				
12				
13				
14	kg B in soln	Moles U-235, fuel	Moles U, soddyite	Mol U in DHLW
15	=E15*$D$9*$D$11/1000	=0.25*0.2073	0	=111.8*$D$8
16	=E16*$D$9*$D$11/1000	0	=0.024908*2	=110.62*$D$8
17	=E17*$D$9*$D$11/1000	0	=0*2	=77.304*$D$8
18	=E18*$D$9*$D$11/1000	0		=19.535*$D$8
19	=E19*$D$9*$D$11/1000	0		=0*$D$8
20	=E20*$D$9*$D$11/1000	0		=0*$D$8
21	=E21*$D$9*$D$11/1000	0		=0*$D$8
22	=E22*$D$9*$D$11/1000	0		=0*$D$8
23	=E23*$D$9*$D$11/1000	0		=0*$D$8
24	=E24*$D$9*$D$11/1000	0		=0*$D$8
25	=E25*$D$9*$D$11/1000	0		=0*$D$8
26	=E26*$D$9*$D$11/1000	0		=0*$D$8
27	=E27*$D$9*$D$11/1000	0		=0*$D$8
28				
29				
30				
31				
32				
33				
34	U from DHLW	U ppt'd, moles	U-235 fraction	U-235 ppt'd,moles
35	0			
36	=$I$15-I16	=0.024976*2	=E36/(E36+F36)	=G36*H36
37	=$I$15-110.62*$D$8	=0.024908*2	=E37/(E37+F37)	=G37*H37
38		=0.024908*2	0.96368265455085	=G38*H38
39	=$I$15-109.18*$D$8	=0.024057*2	=E39/(E39+F39)	=G39*H39

5mm+HLW

	F	G	H	I
40		=0.024057*2	0.922785297036174	=G40*H40
41	=SIS15-107.99*SDS8	=0.023007*2	=E41/(E41+F41)	=G41*H41
42		=0.023007*2	0.891519011894515	=G42*H42
43				
44				
45				
46	=SIS15-77.304*SDS8		=E46/(E46+F46)	=G46*H46
47	=SIS15-19.535*SDS8		=E47/(E47+F47)	=G47*H47
48	=SIS15-0*SDS8		=E48/(E48+F48)	=G48*H48
49	=SIS15-0*SDS8		=E49/(E49+F49)	=G49*H49
50	=SIS15-0*SDS8		=E50/(E50+F50)	=G50*H50
51	=SIS15-0*SDS8		=E51/(E51+F51)	=G51*H51
52	=SIS15-0*SDS8		=E52/(E52+F52)	=G52*H52
53	=SIS15-0*SDS8		=E53/(E53+F53)	=G53*H53
54	=SIS15-0*SDS8		=E54/(E54+F54)	=G54*H54

	J	K	L	M
1				
2				
3				
4				
5				
6				
7				
8				
9				
10				
11				
12				
13				
14	Tot moles U	Tot kg U-235	Tot kg U	Moles B in ppt*
15	=C15+G15+I15	=(C15+G15)*$D$10*$D$11/1000	=J15*$D$10*$D$11/1000	=0*4
16	=C16+G16+H16+I16	=(J38+G16+H16*H38)*$D$10*$D$11/1000	=J16*$D$10*$D$11/1000	=0*4
17	=C17+G17+H17+I17	=(J46+G17+H17*H46)*$D$10*$D$11/1000	=J17*$D$10*$D$11/1000	0.4912
18	=C18+G18+H18+I18	=(J47+G18+H18*H47)*$D$10*$D$11/1000	=J18*$D$10*$D$11/1000	=1.0404*4
19	=C19+G19+H19+I19	=(J48+G19+H19*H48)*$D$10*$D$11/1000	=J19*$D$10*$D$11/1000	=1.2538*4
20	=C20+G20+H20+I20	=(J49+G20+H20*H49)*$D$10*$D$11/1000	=J20*$D$10*$D$11/1000	=0.92377*4
21	=C21+G21+H21+I21	=(J50+G21+H21*H50)*$D$10*$D$11/1000	=J21*$D$10*$D$11/1000	=0.46344*4
22	=C22+G22+H22+I22	=(J51+G22+H22*H51)*$D$10*$D$11/1000	=J22*$D$10*$D$11/1000	=0*4
23	=C23+G23+H23+I23	=(J52+G23+H23*H52)*$D$10*$D$11/1000	=J23*$D$10*$D$11/1000	=0*4
24	=C24+G24+H24+I24	=(J53+G24+H24*H53)*$D$10*$D$11/1000	=J24*$D$10*$D$11/1000	=0*4
25	=C25+G25+H25+I25	=(J54+G25+H25*H54)*$D$10*$D$11/1000	=J25*$D$10*$D$11/1000	=0*4
26	=C26+G26+H26+I26	=(J55+G26+H26*H55)*$D$10*$D$11/1000	=J26*$D$10*$D$11/1000	=0*4
27	=C27+G27+H27+I27	=(J56+G27+H27*H56)*$D$10*$D$11/1000	=J27*$D$10*$D$11/1000	=0*4
28				
29				
30				
31				
32				
33				
34	Moles U-235 in soln	Tot U-235, moles; sol'n + ppt.	Kg U-235 in solution	
35	0			
36	=D36*H36	=I36+J36	=J36*$D$10*$D$11/1000	
37	=D37*H37	=I37+J37	=J37*$D$10*$D$11/1000	
38	=D38*H38	=I38+J38	=J38*$D$10*$D$11/1000	
39	=D39*H39	=I39+J39	=J39*$D$10*$D$11/1000	

	J	K	L	M
40	=D40*H40	=I40+J40	=J40*$D$10*$D$11/1000	
41	=D41*H41	=I41+J41	=J41*$D$10*$D$11/1000	
42	=D42*H42	=I42+J42	=J42*$D$10*$D$11/1000	
43				
44				
45				
46	=D46*H46	=I46+J46	=J46*$D$10*$D$11/1000	
47	=D47*H47	=I47+J47	=J47*$D$10*$D$11/1000	
48	=D48*H48	=I48+J48	=J48*$D$10*$D$11/1000	
49	=D49*H49	=I49+J49	=J49*$D$10*$D$11/1000	
50	=D50*H50	=I50+J50	=J50*$D$10*$D$11/1000	
51	=D51*H51	=I51+J51	=J51*$D$10*$D$11/1000	
52	=D52*H52	=I52+J52	=J52*$D$10*$D$11/1000	
53	=D53*H53	=I53+J53	=J53*$D$10*$D$11/1000	
54	=D54*H54	=I54+J54	=J54*$D$10*$D$11/1000	

	N	O	P	Q
1				
2				
3				
4				
5				
6				
7				
8				
9				
10				
11				
12				
13				
14	Moles B in reactants	Tot moles B	Tot kg B	
15	=(6.254*$D$5*0.691439/6.254+111.8*$D$6)	=E15+M15+N15	=O15*$D$9*$D$11/1000	
16	=(0.6885*$D$5+110.62*$D$6)	=E16+M16+N16	=O16*$D$9*$D$11/1000	
17	=0.60644*$D$5+77.304*$D$6	=E17+M17+N17	=O17*$D$9*$D$11/1000	Last point taken from run U.
18	=0.46414*$D$5+19.535*$D$6	=E18+M18+N18	=O18*$D$9*$D$11/1000	
19	=(0.41355*$D$5+0*$D$6)	=E19+M19+N19	=O19*$D$9*$D$11/1000	
20	=(0.23093*$D$5+0*$D$6)	=E20+M20+N20	=O20*$D$9*$D$11/1000	
21	=(0.0011825*$D$5+0*$D$6)	=E21+M21+N21	=O21*$D$9*$D$11/1000	
22	=(0*$D$5+0*$D$6)	=E22+M22+N22	=O22*$D$9*$D$11/1000	
23	=(0*$D$5+0*$D$6)	=E23+M23+N23	=O23*$D$9*$D$11/1000	
24	=(0*$D$5+0*$D$6)	=E24+M24+N24	=O24*$D$9*$D$11/1000	
25	=(0*$D$5+0*$D$6)	=E25+M25+N25	=O25*$D$9*$D$11/1000	
26	=(0*$D$5+0*$D$6)	=E26+M26+N26	=O26*$D$9*$D$11/1000	
27	=(0*$D$5+0*$D$6)	=E27+M27+N27	=O27*$D$9*$D$11/1000	
28				
29				
30				
31				
32				
33				
34				
35				
36				
37				
38				
39				

5mm+HLW

	N	O	P	Q
40				
41				
42				
43				
44				
45				
46				
47				
48				
49				
50				
51				
52				
53				
54				

Hindered Settling Particle Diameter Ratios

	A	B	C	D	E	F	G	H
1	Estimation of Differential Settling Rates Degraded Material inside DHWL WP (Note: 304L SS is outside the WP)							
2	Calculate diameter ratios for two situations: (1) without FEOOH, (2) include FEOOH							
3	Content: Soddyite, FeOOH, $Al(OH)_3$, H_2O							
4	Mixture Density = $UM [f(I)*rho(I)] where f(I) = volume fraction of I-th component, rho(I) = density of I-th component							
5	Material densities from Ref. 5.45, density of water = 1.0 g/cm^3							
6	The settling rate depends upon the media density which must be determined. Given the water volume fraction, the total volume can be calculated.							
7	Component volume fractions are calculated as f(I) = m(I)/(rho(I)*volume) where volume = total volume.							
8	Total volume is unknown but can be obtained from the closure equation sum [f(I)] = 1.0							
9	Material mass from Summary Spreadsheet, Attachment III, Compositions from Ref. 5.13, 5.14, and 5.15							
10								
11	Volume fraction of water - 0.6 - 0.9 Ref. 5.55, Calculate bounding values - use 0.6 and 0.9							
12	Structural materials					degraded materials		
13	material	mass, kg	Fe fraction	Elemental mass, kg		material	molecular wt	composition
14	316L stainless steel	531.3	0.6554	348.21402		soddyite	668.169	$(UO_2)_2*SiO_4*2$
15	carbon steel	106	0.9954	105.5124				U
16	XM-19	477	0.5737	273.6549				O
17								Si
18	U	35.2		35.2				H
19	Al	125.3		125.3		iron oxide	88.854	FeOOH
20								Fe
21								O
22								H
23						aluminum hyd	78.004	$Al(OH)_3$
24								Al
25								O
26								H
27	Ratio of Particle Diameters which have equal settling rates for the 4 cases							
28								
29	Case 1a. 0.6 volume fraction water, without FeOOH	1.969317909						
30	Ratio (Aluminum hydroxide/Soddyite)							
31	Case 1b. 0.9 volume fraction water, without FeOOH	1.674863914						
32	Ratio (Aluminum hydroxide/Soddyite)							
33	Case 2a. 0.6 volume fraction water, with FeOOH	1.095162933						
34	Ratio (Iron hydroxide/Soddyite)							
35	Case 2b. 0.9 volume fraction water, with FeOOH	1.07090052						
36	Ratio (Iron hydroxide/Soddyite)							
37	Case 2c. 0.6 volume fraction water, with FeOOH	2.686181323						
38	Ratio (Aluminum hydroxide/Soddyite)							
39	Case 2d. 0.9 volume fraction water, with FeOOH	1.723692524						
40	Ratio (Aluminum hydroxide/Soddyite)							

Hindered Settling Particle Diameter Ratios

	I	J	K	L	M	N	O	P
1								
2								
3								
4								
5								
6								
7								
8								
9								
10								
11							without Fe	without Fe
12							$f(H_2O) = 0.6$	$f(H_2O) = 0.9$
13	moles comp/mole mat	gm at wt	moles available	moles - degraded matl	mass, g - degraded matl	density g/cm³	Total Volume cm³	Total Volume cm³
14	H_2O			73.94025963	49404.58934	4.7	400497.2216	1601988.886
15	2	238.03	147.8805193					
16	10	15.9994						
17	1	28.0855					mixture density g/cm³	mixture density g/cm³
18	4	1.00794					1.627841817	1.156960454
19				13024.53704	1157282.214	4.26		
20	1	55.847	13024.53704					
21	2	15.9994						
22	1	1.00794						
23				4643.905476	362243.2028	2.42		
24	1	26.9816	4643.905476					
25	3	15.9994						
26	3	1.00794						
27								
28								
29								
30								
31								
32								
33								
34								
35								
36								
37								
38								
39								
40								

	Q	R
1		
2		
3		
4		
5		
6		
7		
8		
9		
10		
11	with Fe	with Fe
12	$f(H_2O) = 0.6$	$f(H_2O) = 0.9$
13	Total Volume cm^3	Total Volume cm^3
14	1079653.45	4318613.802
15		
16		
17	mixture density g/cm^3	mixture density g/cm^3
18	2.053179264	1.263294816
19		
20		
21		
22		
23		
24		
25		
26		
27		
28		
29		
30		
31		
32		
33		
34		
35		
36		
37		
38		
39		
40		

Hindered Settling Particle Diameter Ratios

	A	B	C
1	Estimation of Differential Settling Rates Degraded Material inside DHWL WP (Note: 304L SS is outside the WP)		
2	Calculate diameter ratios for two situations: (1) without FEOOH, (2) include FEOOH		
3	Content: Soddyite, FeOOH, $Al(OH)_3$, H_2O		
4	Mixture Density = SUM {[(I)*rho(I)] where f(I) = volume fraction of I-th component, rho(I) = density of I-th component		
5	Material densities from Ref. 5.45, density of water = 1.0 g/cm^3		
6	The settling rate depends upon the media density which must be determined. Given the water volume fraction, the total v		
7	Component volume fractions are calculated as f(I) = m(I)/(rho(I)*volume) where volume = total volume.		
8	Total volume is unknown but can be obtained from the closure equation sum [f(I)] = 1.0		
9	Material mass from Summary Spreadsheet, Attachment III, Compositions from Ref. 5.13, 5.14, and 5.15		
10			
11	Volume fraction of water - 0.6 - 0.9 Ref. 5.55, Calculate bounding values - use 0.6 and 0.9		
12	Structural materials		
13	material	mass, kg	Fe fraction
14	316L stainless steel	531.3	0.6554
15	carbon steel	106	0.9954
16	XM-19	477	0.5737
17			
18	U	35.2	
19	Al	125.3	
20			
21			
22			
23			
24			
25			
26			
27	Particle Diameter Ratio d(1)/d(2) = SQRT(rho(2) - rho(slurry))/SQRT(rho(1) - rho(slurry))		
28	Ratio of Particle Diameters which have equal settling rates for the 4 cases		
29			
30	Case 1a. 0.6 volume fraction water, without FeOOH	=(SQRT(N14-O18)/SQRT(N23-O18))	
31	Ratio (Aluminum hydroxide/Soddyite)		
32	Case 1b. 0.9 volume fraction water, without FeOOH	=(SQRT(N14-P18)/SQRT(N23-P18))	
33	Ratio (Aluminum hydroxide/Soddyite)		
34	Case 2a. 0.6 volume fraction water, with FeOOH	=(SQRT(N14-Q18)/SQRT(N19-Q18))	
35	Ratio (Iron hydroxide/Soddyite)		
36	Case 2b. 0.9 volume fraction water, with FeOOH	=(SQRT(N14-R18)/SQRT(N19-R18))	
37	Ratio (Iron hydroxide/Soddyite)		
38	Case 2c. 0.6 volume fraction water, with FeOOH	=SQRT(N14-Q18)/SQRT(N23-Q18)	
39	Ratio (Aluminum hydroxide/Soddyite)		
40	Case 2d. 0.9 volume fraction water, with FeOOH	=SQRT(N14-R18)/SQRT(N23-R18)	
41	Ratio (Aluminum hydroxide/Soddyite)		

	D	E	F	G	H
1					
2					
3					
4					
5					
6					
7					
8					
9					
10					
11					
12			degraded materials		
13	Elemental mass, kg		material	molecular wt	composition
14	=B14*C14		soddyite	668.169	$(UO_2)_2*SiO_4*2H_2O$
15	=B15*C15				U
16	=B16*C16				O
17					Si
18	=B18				H
19	=B19		iron oxide	88.854	FeOOH
20					Fe
21					O
22					H
23			aluminum hydroxide	78.004	$Al(OH)_3$
24					Al
25					O
26					H
27					
28					
29					
30					
31					
32					
33					
34					
35					
36					
37					
38					
39					
40					
41					

	I	J	K
1			
2			
3			
4			
5			
6			
7			
8			
9			
10			
11			
12			
13	moles comp/mole mat	gm at wt	moles available
14			
15	2	238.03	=$D$18*1000/J15
16	10	15.9994	
17	1	28.0855	
18	4	1.00794	
19			
20	1	55.847	=(D14+D15+D16)*1000/J20
21	2	15.9994	
22	1	1.00794	
23			
24	1	26.9816	=D19*1000/J24
25	3	15.9994	
26	3	1.00794	
27			
28			
29			
30			
31			
32			
33			
34			
35			
36			
37			
38			
39			
40			
41			

Hindered Settling Particle Diameter Ratios

	L	M	N	O
1				
2				
3				
4				
5				
6				
7				
8				
9				
10				
11				without Fe
12				$\phi(H_2O) \approx 0.6$
13	moles - degraded matl	mass, g - degraded matl	density g/cm³	Total Volume cm³
14	=K15/2	=L14*G14	4.7	=($M14/$N14 + $M23/$N23)/0.4
15				
16				
17				mixture density g/cm³
18				=0.6 + $M14/O14 + $M23/O14
19	=K20	=L19*G19	4.26	
20				
21				
22				
23	=K24	=L23*G23	2.42	
24				
25				
26				
27				
28				
29				
30				
31				
32				
33				
34				
35				
36				
37				
38				
39				
40				
41				

Hindered Settling Particle Diameter Ratios

	P	Q	R
1			
2			
3			
4			
5			
6			
7			
8			
9			
10			
11	without Fe	with Fe	with Fe
12	f(H_2O) = 0.9	f(H_2O) = 0.6	f(H_2O) = 0.9
13	Total Volume cm^3	Total Volume cm^3	Total Volume cm^3
14	=($M14/$N14 + $M23/$N23)/0.1	=($M14/$N14 + $M23/$N23 + $M19/$N19)/0.4	=($M14/$N14 + $M19/$N19 + $M23/$N23)/0.1
15			
16			
17	mixture density g/cm^3	mixture density g/cm^3	mixture density g/cm^3
18	=0.9 + $M14/P14 + $M23/P14	=0.6 + $M14/Q14 + $M19/Q14 + $M23/Q14	=0.9 + $M14/R14 +$M19/R14 + $M23/R14
19			
20			
21			
22			
23			
24			
25			
26			
27			
28			
29			
30			
31			
32			
33			
34			
35			
36			
37			
38			
39			
40			
41			

Attachment V. Listing of pitgen.c, program to generate pit locations and analyse them for occurrence of cutouts

```
/*pitgen.c  This program generates pits over randomly selected locations
on a rectangular grid, to simulate pitting corrosion in a rectangular plate.
The pits locations are generated sequentially up to some limit (maxpits,
currently specified as 80% of the number of grid cells); the sequence is
divided into intervals (nspits) at which the program analyses the pit
locations to identify cutouts (collections of non-pitted, contiguous cells
which are completely surrounded by pits).  The program can be repeated a
specified number of times (specified by the parameter "realize") to
generate statistics on cutout areas.  For demonstration and verification
purposes the program can also plot the cutout locations (printsw=1).


A cutout is defined as an region containing contiguous un-pitted cells,
and completely surrounded by pits.  Contiguous means adjacent in the
horizontal or vertical direction; cells linked only by a diagonal are not
considered contiguous.  The basic cutout algorithm processes each non-pitted
cell to trace connections with previously analysed locations.  The
bookkeeping for this analysis uses the 2 dimensional integer array
"status", in which the values identify the cells as belonging to specific
cutouts, and the parameter "color" is used to refer to this id while a
cutout analysis is in progress. To display a map of cutouts, the "colors"
are mapped into printing ASCII characters.  The basic cutout identification
algorithm leaves gaps in the color sequence which are eliminated by shifting
the colors into the gaps prior to printing.  In this manner the re-use of
printing ASCII characters can be minimized.  At the end of each cutout
analysis the non-pit locations are all reset to color=0.

The algorithm for cutout analysis described in the previous paragraph
requires further specification for cutouts which intersect the grid/plate
boundary.  According to the rule requiring complete enclosure by pits,
an intersection with the boundary would preclude classification as a
cutout.  The physical interpretation is that as long as a plate fragment
can be supported at at least 1 location (pit-sized cell) it will not be
able to fall like a cutout.  In actual fact, a plate fragment extending
sufficiently far from a single point of support will overstress (and
rupture) the attachment and fall.  Hence, the model is not conservative
with respect to the possibility of cutouts breaking off the basket and
falling.  A comprehensive analysis of this possibility would require an
understanding of the distribution of length and width for such
attachments, which is beyond the scope of the study to which this code
is applied.  Instead, this limitation of cantilever capability is
approximated by implementing it on the top and left boundaries of the
grid (plate) and permitting the designation of cutout when the
collection of unpitted cells intersects the lower or right border. A
cantilever which connects opposite borders (thereby becomming a bridge)
will not be counted as a cutout, in keeping with the additional
support supplied by the connection to the opposite side.

For controlling the cutout plotting mode, use the following values of
printsw:
   0.  No plotting of cutouts
   1.  Unique ASCII character symbols for each cutout (with re-use if there
```

```
    are more than 94 cutouts)
2.  Same symbol (.) for all cutouts, with 'o' for cantilever locations
3.  Combined 1 and 2
Note that '+' is always used to designate a pit location; a cutout
location is indicated by a '.' or a general printing ascii character
other than '+' (options 2 and 1, respectively); a cantilever location is
indicated by a space (' ') or a 'o' (options 1 and 2, respectively).
Using plotting option 1 or 3, it is straightforward to verify the correct
functioning of the cutout analysis algorithm (by visual inspection); it can
easily be seen that each location identified as belonging to a cutout is
adjacent (contiguous, vertically or horizontally) with at least one other
location also having the same symbol.  Furthermore, using options 2 or 3,
it can be easily verified that each cutout is completely surrounded by pits
(with the exception that cutouts within one cell of the bottom or right
border may be bounded by an unpitted border cell, which could have served
as the base of a cantilever if it had occurred at the upper or left
borders, as discussed above).

For additional verification, the program has three different variables which
calculate the cutout area (number of locations within the cutout border) in
three different ways: totalarea,checkcheck, and checkarea.  In this version
of the program only the first of these variables is printed,  because the
program has been amply verified by the writer; the review may, however, wish
to print them.  */

#include <stdlib.h>
#include <stdio.h>
#include <math.h>

#include <time.h>
#include <malloc.h>
int **status, //Array to keep the status of each cell (including cutout ID)
    nrows=190,ncols=750,  //number of rows and columns in the grid.
    bcolor,  //keeps track of the highest cutout index (color)
    maxpits, //maximum number of pits to be placed
    *narea, //array to bookkeep number of pits in each cutout
    *transfer, //Identification of transfers in downshifting before cutout
plotting
    firstslot; //bookkeep gaps in downshifting; ends as number of cutouts
void cutouts(),testhigher(int,int,int,int);
FILE *fout;
int checkup(int r,int c,int color),
    printsw=0; //no plots of cutouts
long int count, //Number of pit locations
    tcells, //total number of cells nrows*ncols
    totalarea,//number of pits in cutouts before downshifting (each cut anlyss)
    checkcheck,//check by summing array of indices (narea)
    checkarea;//check with num pits in cutouts after downshifting

void main()
{int i,ii,j,k,
    nspits=10000,//pit accumulation interval between cutout analyses
    realize=100, //number of realizations (Monte Carlo iterations)
    steps;  //number of cutout evaluations for each realization
long int tcount; //total number of random locations tried
float grandarea[20]={0}, //accumulates cutout area, successive realizations
```

```
   grandareasq[20]={0},  //accumulates sum of squares for SD calc
    grandcutouts[20]={0}, //number of cutouts, for successive realizations
   grandcutoutsq[20]={0};//sum of squares for num cutout SD calculation
fout=fopen("crsnstats.out","w");//output file
tcells=nrows*ncols;   //total number of cells in the grid
maxpits=(int)(0.8*tcells); //no point in pitting all the cells
steps=maxpits/nspits;   //number of intervals at which cutouts analyzed
narea=(int*)malloc(maxpits*sizeof(int));//for totaling locs by cutout
transfer=(int*)malloc(maxpits*sizeof(int));//for downshifting cutout ID's
srand((unsigned)time(NULL));   //random seed for the random number generator
status=(int**)malloc(nrows*sizeof(int));//allocate basic pit location array
for(i=0;i<nrows;i++) status[i]=(int*)malloc(ncols*sizeof(int));
for(ii=0;ii<realize;ii++) //basic loop for each Monte Carlo realization
 {for(i=0;i<nrows;i++)   //initialize for each realization
   for(j=0;j<ncols;j++) status[i][j]=0;
 count=0;
 tcount=0;
 while(count<maxpits) //generate pits up to the maximum allowed
  {bcolor=0;
  i=(int)((float)rand()*nrows/RAND_MAX); //generate coordinates randomly
  j=(int)((float)rand()*ncols/RAND_MAX);
  if(i==nrows)i--;        //don't hit the limit
  if(j==ncols)j--;
  tcount++;           //increment total number of tries
  if(status[i][j]==0) status[i][j]=-1; //mark pit at this location
  else continue;   //location already pitted, try again
  count++;          //increment count of pits placed
  if(count%nspits==0) //if we have reached the specified analysis interval
    {cutouts();       //analyse the pits generated thus far for cutouts
    k=count/nspits;   //pitting count (fraction) index
    grandarea[k]+=(float)totalarea;//cumulate cutout statistics by pitting
    grandareasq[k]+=(float)totalarea*totalarea;//by pitting count index
    grandcutouts[k]+=(float)firstslot-1;
    grandcutoutsq[k]+=(float)(firstslot-1)*(firstslot-1);}}
 printf("realization %d\n",ii);}//print to monitor program execution
fprintf(fout,"%8s%10s%10s%10s%10s%10s\n","Pitfrac","Cutfrac","SDcutfrac",
        "NumCutout","SDCutout","Avarea");
for(k=1;k<=steps;k++)//print grand summary statistics (all realizations)
  fprintf(fout,"%8.3f%10.3f%10.3f%10.0f%10.3f%10.3f\n",
    (float)k*nspits/tcells,grandarea[k]/realize/tcells,//avg cutout frac
    pow((grandareasq[k]-pow(grandarea[k],2)/realize)/realize,.5)/tcells,
    grandcutouts[k]/realize,                          //avg cutout num
    pow((grandcutoutsq[k]-pow(grandcutouts[k],2)/realize)/realize,.5),
    (grandcutouts[k]>0?grandarea[k]/grandcutouts[k]:0));//avg area
printf("counts= %ld  total counts= %ld\n",count,tcount);}

void cutouts()
{int i,j,k,kk,lastslot,//upper bound of slot for downshifting
    gap,               //equals 1 if downshifting slot exists
    cantarea;//accumulate cantilevered area for checking, not printed now
char c;
for(i=0;i<maxpits;i++)  //initialize arrays for cutout tabulation
  {transfer[i]=0;
  narea[i]=0;}
totalarea=0;
checkarea=0;
```

```
checkcheck=0;
cantarea=0;
for(j=0;j<ncols;j++)
  {if(status[0][j]==0)status[0][j]=-9; //Label unpitted border locations
  if(status[nrows-1][j]==0)status[nrows-1][j]=-9;}//for attaching cantilever,
for(i=0;i<nrows;i++)                    //but only 2 borders will be used
  {if(status[i][0]==0)status[i][0]=-9; //for this purpose.
  if(status[i][ncols-1]==0)status[i][ncols-1]=-9;}
for(i=1;i<nrows-1;i++)      //now process non-border cells
  for(j=1;j<ncols-1;j++)
   if(status[i][j]!=-1)  //only process for non-pit location
    {if((k=status[i][j-1])==-9)
       {status[i][j]=-9;//continue cantilever to left border
      testhigher(i-1,j,-9,1);} //attach prior cutouts to this cantilever
     else if(k==-1) //going from pit to non-pit location
      {bcolor++;      //index for new cutout
      status[i][j]=bcolor;
       if((kk=status[i-1][j])==-9)//adjacent to cantilever from upper border?
        {status[i][j]=-9; //attach this cell to cantilever to upper border
        testhigher(i,j-1,-9,-1);         //attach prior cutouts to too
        if(bcolor>0) bcolor--;}         //reset base color for next new cutout
      else if((kk<bcolor)&&(kk!=-1))  //continue existing cutout
        {status[i][j]=kk;
        if(bcolor>0) bcolor--;}} //give back the unneeded new color
    else                    //continue previous color in this line
      {status[i][j]=k;
      if((kk=checkup(i-1,j,k))!=0)//This routine will attach to cutouts
        {status[i][j]=kk;          //so only cantilever is processed here
        if(kk==-9) testhigher(i,j-1,-9,-1);}}}//end loop to mark cutouts
for(i=0;i<nrows;i++)
  for(j=0;j<ncols;j++)
    {if((k=status[i][j])>0)
       {narea[k]++;       //accumulate area by cutout index
      totalarea++;}       //accumulate total cutout area
     else if(k==-9)cantarea++;}//accumulate cantilever area (check only)
for(i=0;i<maxpits;i++)checkcheck+=narea[i];//to check area
i=1;
firstslot=1;
lastslot=1;
gap=0;
while(i<bcolor)//loop to identify downshift source-destination pairs
  {if((k=narea[i])>0)  //any cutout for this index?
    {if(gap==1)         //is there a lower index to move it to
       {narea[firstslot]=k;//move the total area for this cutout
      transfer[i]=firstslot++;//setup to-from to transfer color index
      lastslot=i;} //mark end of gap (not used)
     else transfer[i]=i;}//otherwise no transfer
  else
    {lastslot++;//no area so increment upper end of gap
     gap=1;}      //now there is certainly a gap
  i++;}          //next index (or color)
for(i=0;i<nrows;i++)
  for(j=0;j<ncols;j++)
    if((k=status[i][j])>0)
       {status[i][j]=transfer[k];//now downshift the status values (colors)
      checkarea++;}  //another check of total (this analysis) cutout area
```

```
if((printsw==1)||(printsw==3))    //picture of pits and cutouts
  {for(i=0;i<nrows;i++)
   {for(j=0;j<ncols;j++)
    {switch(k=status[i][j])
       {case -9: c=' ';break; //space for cantilever or border non-pit
      case -1: c='+';break;  //symbol for pit
      default:
        if(k%94!=10)c=(char)(k%94+33);//assign unique symbols, with reuse
        else c='~';     //alternative for '+'}
    fprintf(fout,"%c",c);}//now print the map (picture) symbol
  fprintf(fout,"\n");}}
if((printsw==2)||(printsw==3)) //Picture with same symbol for all cutouts
  {for(i=0;i<nrows;i++)
   {for(j=0;j<ncols;j++)
    {switch(k=status[i][j])
       {case -9: c='o';break;
      case -1: c='+';break;
      default: c='.';}
    fprintf(fout,"%c",c);}
  fprintf(fout,"\n");}}
for(i=0;i<nrows;i++)      //reset colors and cantilevers to spaces
  for(j=0;j<ncols;j++) if(status[i][j]!=-1)status[i][j]=0;
fprintf(fout,"pit frctn=%.3f cutout frctn=%.3f num cuts=%d avg cut=%.3f\n",
        (float)count/tcells,(float)totalarea/tcells,firstslot-1,
        (firstslot>1?(float)totalarea/(firstslot-1):0));
if(printsw==1)        //same symbol for all pits (used only for check)
  {for(i=0;i<nrows;i++)
   {for(j=0;j<ncols;j++)
     fprintf(fout,"%c",(status[i][j]==0?'.':'+'));
   fprintf(fout,"\n");}
  fprintf(fout,"\n");}}

int checkup(int r,int c,int color)//Check upper neighbor and reset
{int k;                                //backward or forward, to lowest color
if((k=status[r][c])==-9) return (-9);//return for attachment to leak
else if((k==-1)||(k==color)) return (0);//no further processing of this cell
else if(k<color) //backtrack to attach to existing cutout
  {r++;          //backup to original location (cell)
  status[r][c]=k;//attach this cell to the existing cutout
  c--;           //backup to previous cell location
  status[r][c]=k; //attach but don't test; must have had pit above
  testhigher(r,c-1,k,-1);//back one more; now test above and back
  return(0);}
else           //forward to attach (reset) encountered area (cutout)
  {status[r][c]=color; //attach (reset) this cell (location)
  testhigher(r-1,c,color,0);//move up one row and test back, forward and up
  testhigher(r,c+1,color,1);//move forward one cell and test forward and up
  return(0);}}

void testhigher(int r, int c, int color, int nums)//recursively attaches
{int k;                                          //existing cutout cells
if(((k=status[r][c])>color)&&(k!=-1))//only continue if cell is non-pit
  {status[r][c]=color;              //attach this cell
  if(nums<=0) testhigher(r,c-1,color,-1);//back one column and back and up
  testhigher(r-1,c,color,0);        //up one row and test back, up, frwrd
  if(nums>=0)testhigher(r,c+1,color,1);}}//frwrd one col and test ftwrd,up
```

Calculation of the conditional probability of Gd being contacted by acidified water

As explained in Section 7.4.4.1, the conditional probability of Gd being contacted by acidified water, given that water is penetrating the DOE SNF canister, is equal to the probability that the corroding stainless steel lies above the DOE SNF canister. This, in turn, is equal to the average depth of the DOE SNF canister below the surface of the clay which contains the corroding stainless steel (remnants of the canisters for the HLW glass. To determine this average depth we use the joint probability density function (pdf) for the height of the clay surface above the canister bottom (H) and the depth of the DOE SNF canister top below the clay surface (h). This joint pdf is approximated by the product of a uniform pdf for H, between 0 and the DOE SNF canister diamenter (D), and the conditional pdf for h, given H, which is uniform between 0 and H-d (the diameter of the DOE SNF canister). These pdf's are 1/D and 1/(H-d), respectively, so that the average of h over this distribution is given by

$$\frac{1}{D}\int_d^D dH \int_0^{H-d} \frac{h\,dh}{H-d}$$

where the lower limit of the first integral is set equal to d because any clay (or water) level below the top of the DOE SNF canister cannot get the acidified water into the canister. The value of this integral is (D-d)/(4D), which is slightly less than 1/4.

Calculation of fractions/probabilities with respect to insoluble elements (U, Gd) segregating at the canister bottom

The probability of an insoluble element, or particulate, falling through corroded steel plates is proportional to the fraction of the plate area corroded. This, in turn, is equal to the sum of the pitting fraction and the cutout fraction. The average probability of falling through 0, 1, or 2 plates is thus

$$(1+f+f^2)/3.$$

For stainless steel and carbon steel the maximum cutout fractions are 0.49 and 0.32, respectively, so the f=0.42+0.49=0.91 and f=0.56 + 0.32=0.88, respectively. With these values for f, the formula then gives the values 0.78 and 0.83 for the probability that any given particle of insoluble element will fall to the bottom of the canister or for the fraction of such an element uniformly distributed throughout the package which could fall to the bottom of the package. This calculation could apply to uranium or gadolinium.

Calculation of probabilities of criticality

The conditions necessary to have criticality within the waste package all include water dripping on the waste package and have sufficient water remaining in the waste package to provide the necessary moderator, either as standing water or as water attached to clay. A previous criticality evaluation developed estimates for the probability of enhanced dripping over an individual waste package (0.07), and the probability of ponding water in the waste package given that there is enhanced dripping (0.01), Ref. 5.52, p. 20. The probility of the occurrence of these preconditions for criticality is then the product of the individual probabilities, 0.0007.

The nominal environmental parameters and corrosion models have changed somewhat since the analysis of Ref. 5.52. Furthermore, the previous analysis considered the possibility of ponding only by an intact waste package bottom, while the codisposal package may degrade into an amount of clay sufficient to retain water for moderation even in the presence of a significant amount of penetration of the waste package bottom. Nevertheless, the previous estimates still fall within the current range of uncertainty so it is not appropriate to do a comprehensive re-assessment at this time.

Check of Flushing Routine for case Uall5mmr Stage 1 to 2

End of Stage 1, mole solvent = 55.7212 = y
mass solvent = 1.00383

Al moles aqueous = 4.053240E-07
B moles aqueous = 7.355274E-02
Ca moles aqueous = 1.376098E-08

Delta moles J-13 water (added)/3 = 1.144 = z
Initial moles solvent = 55.5088 = x

x/(x+z) = 0.979812

Start of Stage 2, mass solvent = 0.983643,
therefore, reduction factor should be x/(x+z)

Element	Hand calc. of new moles aqueous	Flushing routine calc.
Al	3.971413E-07	3.9717878E-07
B	7.206786E-02	7.207341E-02
Ca	1.348317E-08	1.348421E-08

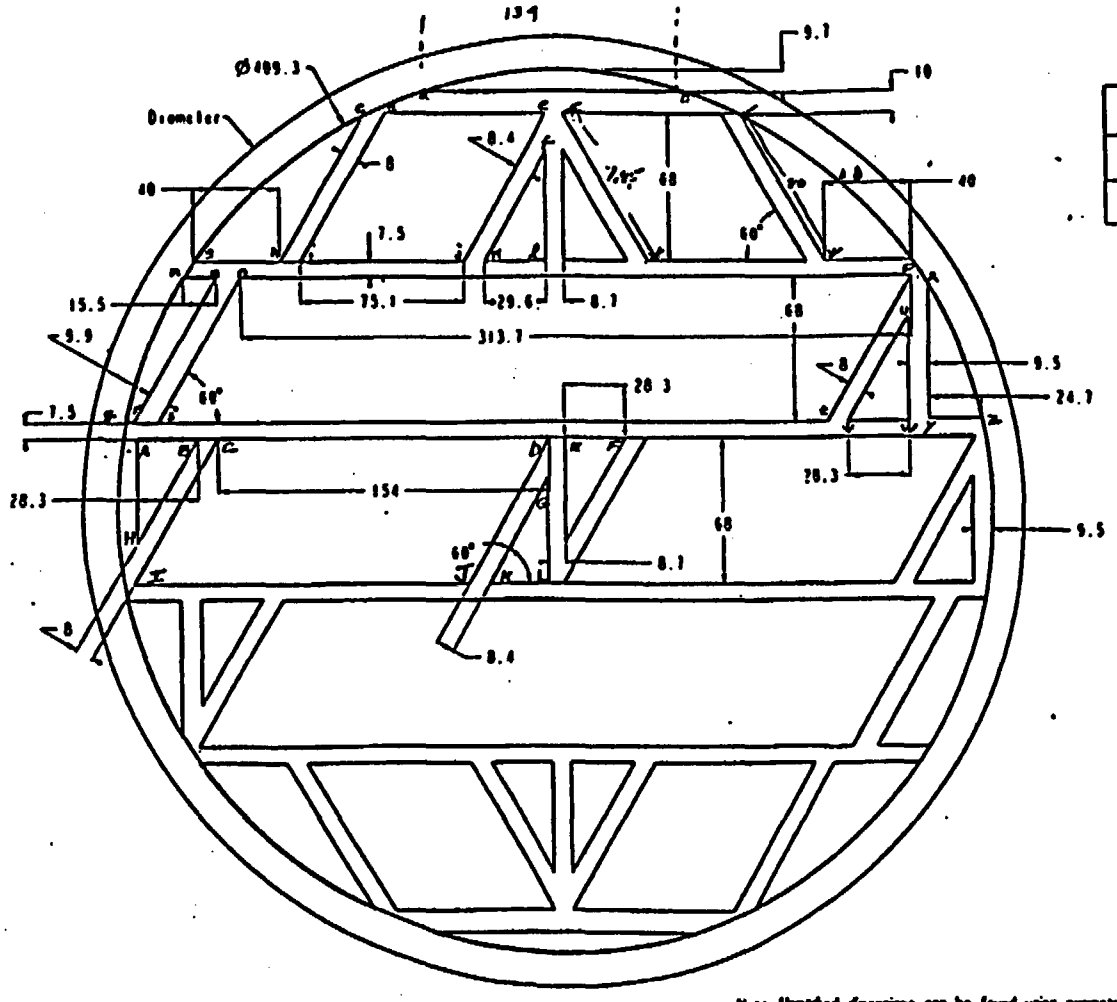

Diameter	Material	Thickness
489.3	316. Stainless Steel	20
439.3	EN-19	15

Note: Unmarked dimensions can be found using symmetry.

Note: Do Not Scale From Sketch

"For Information Only"

Units: cm

MT-SNF Canister

Sketch Number: SK0060 Rev 00
Sketched by: Zeke Ceylan
Date: 5/14/97
File: /users/ceylan/sk0060-0.dwg

R.C. 5/14/97
S=B ability
T=D 5-14-97